VOCALS Telecon on POCs, May 13th

Agenda

1. Discussion of POCs cases – Ron Brown, C-130, BAe-146, other?
2. Materials from contributors:

3. Future foci?

Current mailing list for VOCALS telecons

Display Name	Primary Email
Robert Wood	robwood@atmos.washington.edu
Chris Bretherton	breth@washington.edu
Carlos R Mechoso	mechoso@atmos.ucla.edu
David Leon	leon@uwyo.edu
Tony Clarke	tclarke@soest.hawaii.edu
Brown, Phil	phil.brown@metoffice.gov.uk
Abel, Steven	steven.abel@metoffice.gov.uk
hugh.coe@manchester.ac.uk	hugh.coe@manchester.ac.uk
Dr. Keith N. Bower	k.bower@manchester.ac.uk
Grant Allen	Grant.Allen@manchester.ac.uk
Geraint Vaughan	Geraint.Vaughan@manchester.ac.uk
Jose Meitin	meitin@ucar.edu
Vidal Salazar	vidal@ucar.edu
Thomas Toniazzo	t.toniazzo@reading.ac.uk
Jefferson R. Snider	JSnider@uwyo.edu
balbrecht@rsmas.miami.edu	balbrecht@rsmas.miami.edu
Peter Daum	phdaum@bnl.gov
Chris Fairall	Chris.Fairall@noaa.gov
David Covert	dcovert@u.washington.edu
Lelia N Hawkins	lnahid@ucsd.edu
Sara Tucker	Sara.Tucker@noaa.gov
Al Schanot	schanot@ucar.edu
Alan Brewer	alan.brewer@noaa.gov
Jim McQuaid	J.B.McQuaid@leeds.ac.uk
Stephen R. Springston	srs@bnl.gov
Alan Gadian	alan@env.leeds.ac.uk
Jim Anderson	janderson@asu.edu
Cynthia Twohy	twohy@coas.oregonstate.edu
Byron Blomquist	blomquis@hawaii.edu
Sandra E. Yuter	sandra_yuter@ncsu.edu
Miroslaw Andrejczuk	M.Andrejczuk@leeds.ac.uk
Jorgen Jensen	jbj@ucar.edu

RF06 POC Sequence

(Dave Leon & Jeff Snider -- UWYO)

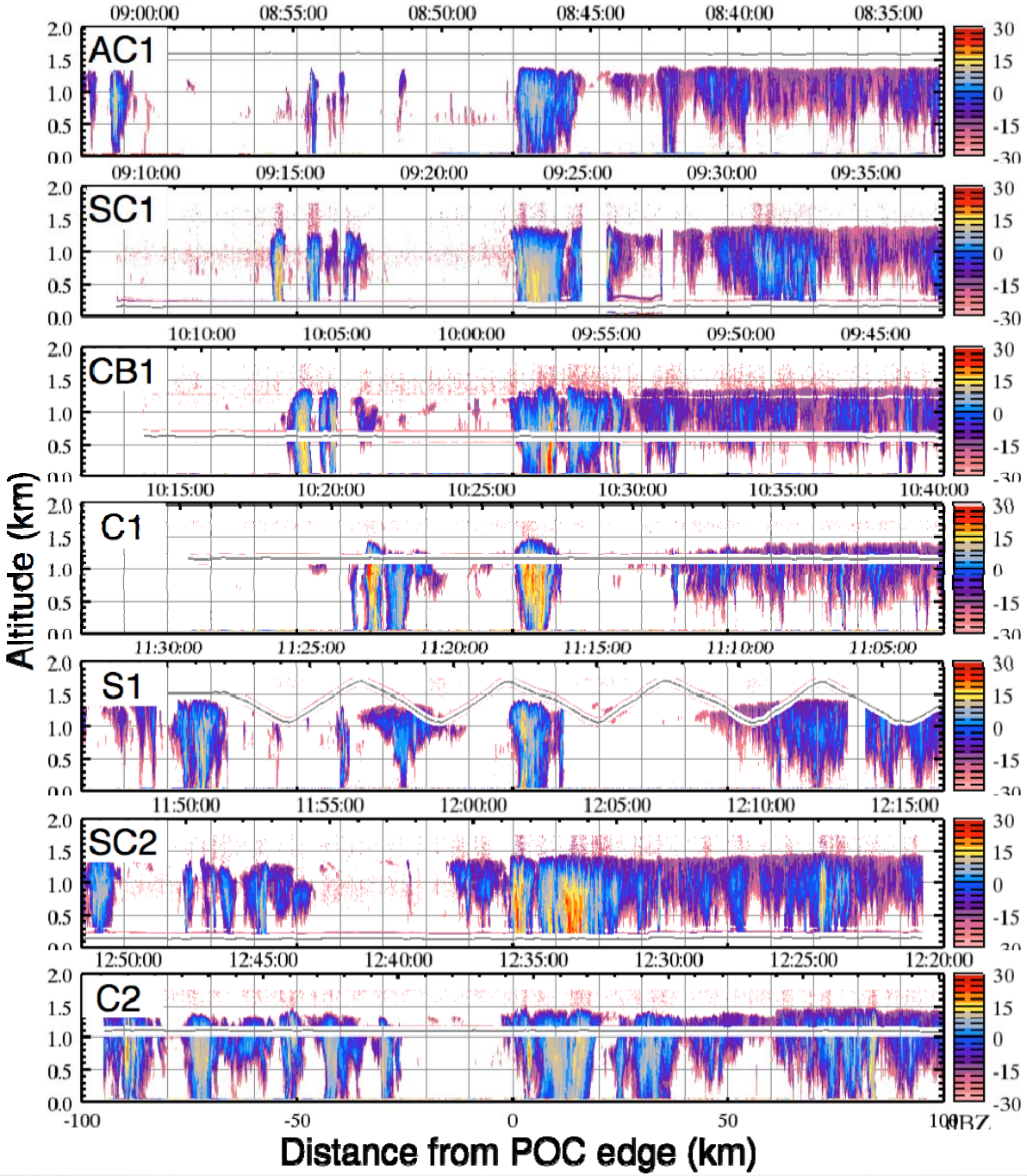

RF06 SC2

Transition Region

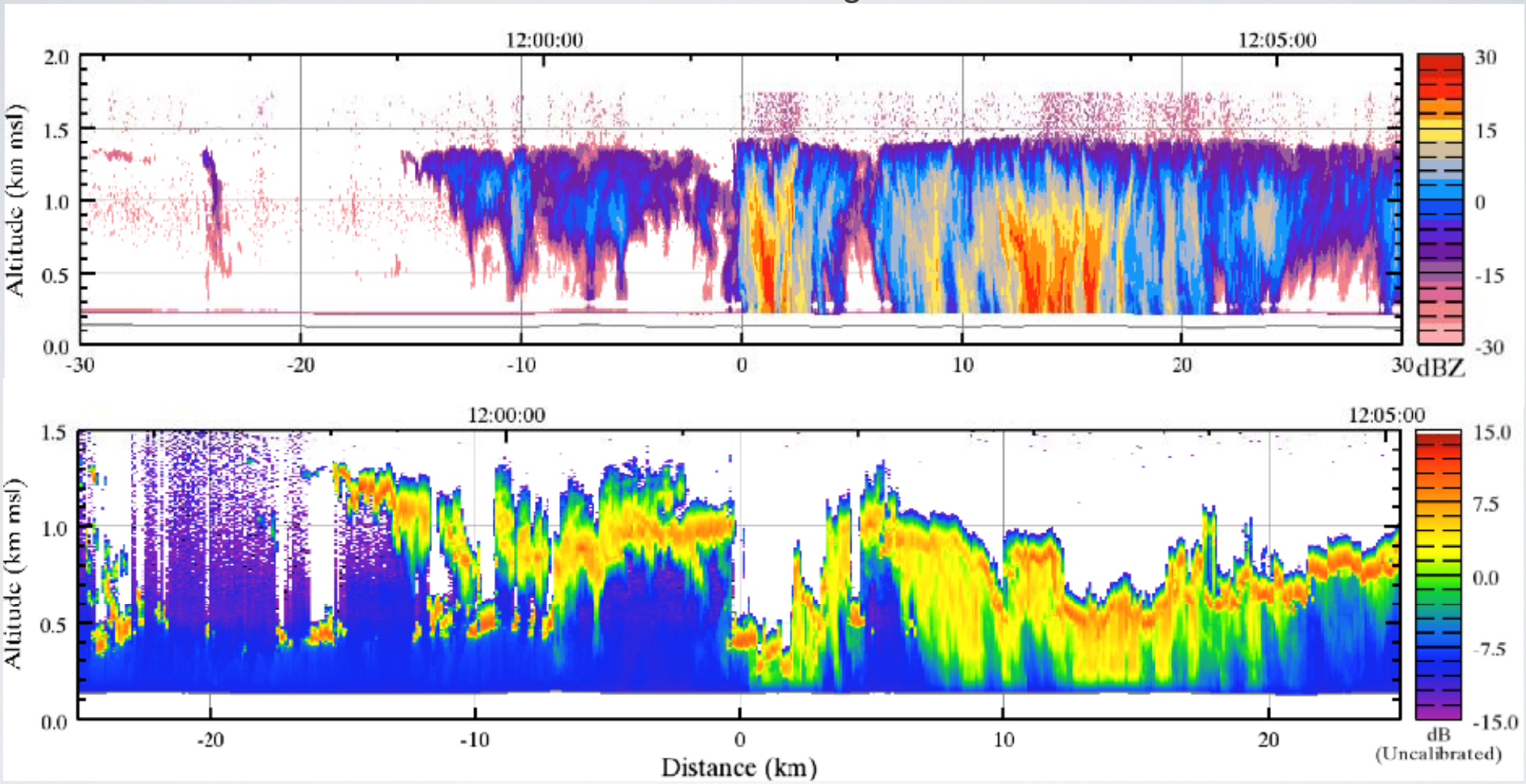

Attenuated Backscatter

(molecular signal crudely removed to show enhanced scattering near surface)

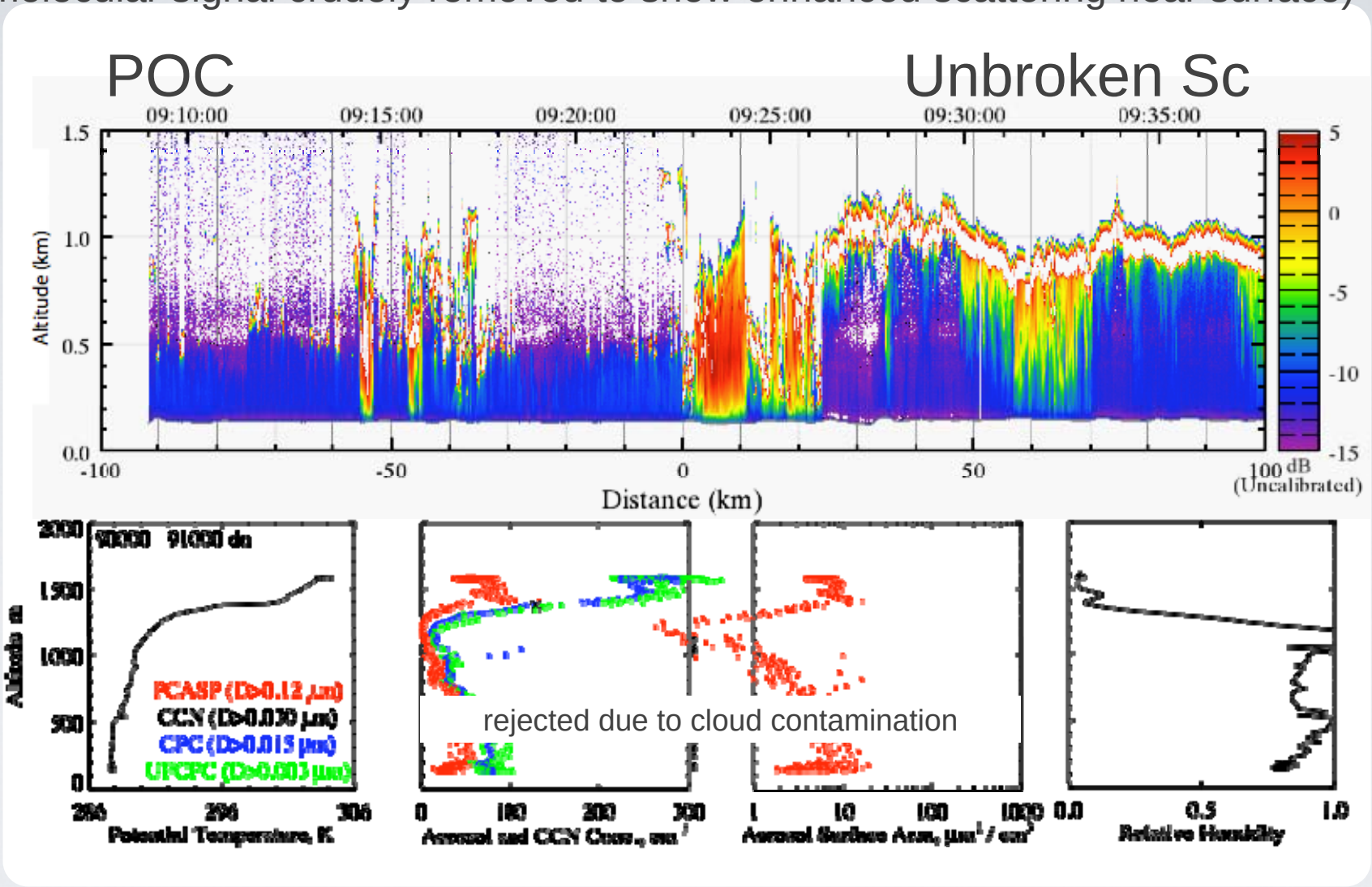

PCASP concentrations increase at ~500m consistent with height of plumes. Descent located to left of plot region (in POC). Suggests that the aerosol population within the POC is maintained by fluxes from the surface.

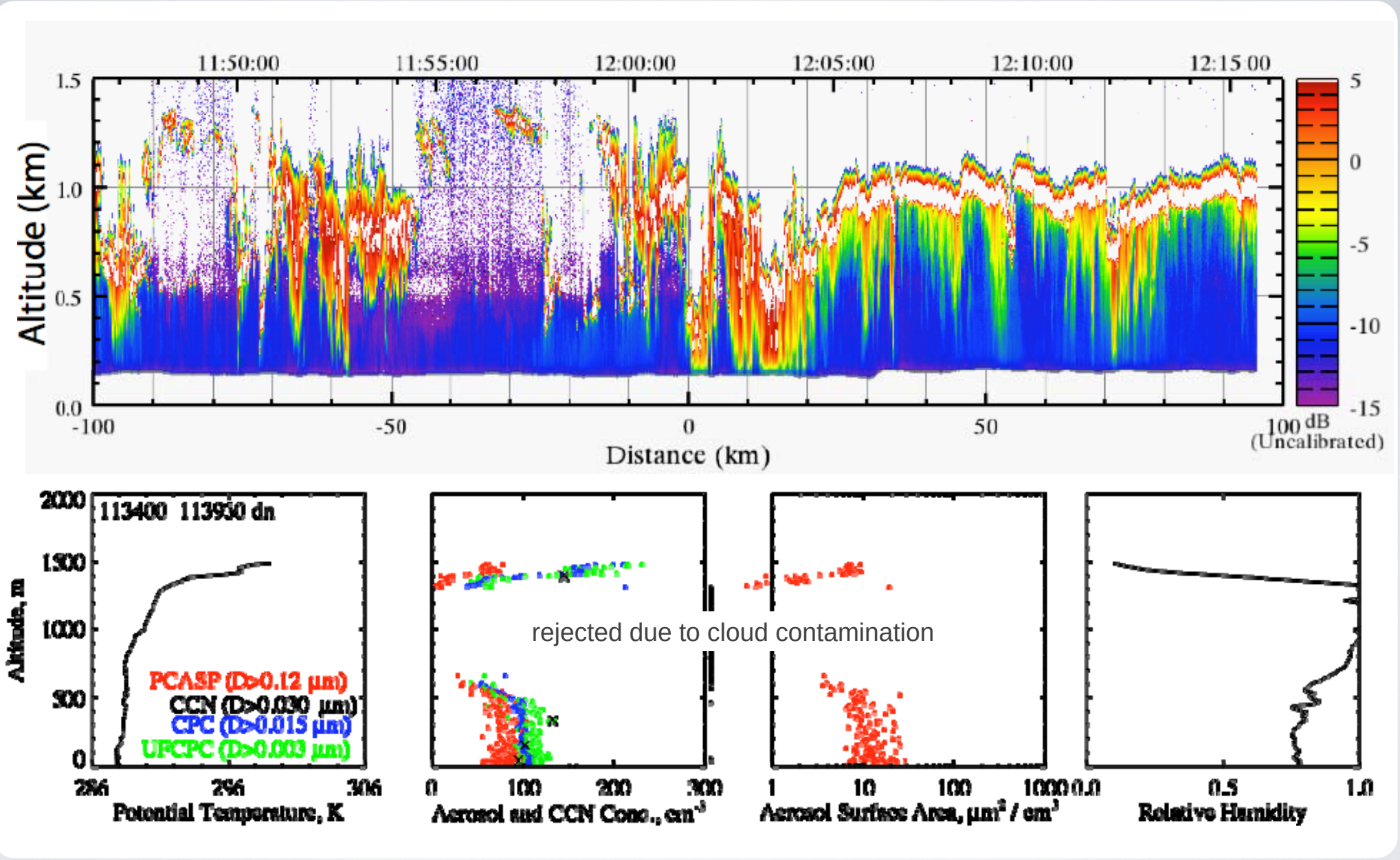

Same as previous figure for descent prior to SC2 (to left of plotted region)

DMS Emissions are the *Dominant* Sulfur Source in the VOCALS region

along 20°S, project-average

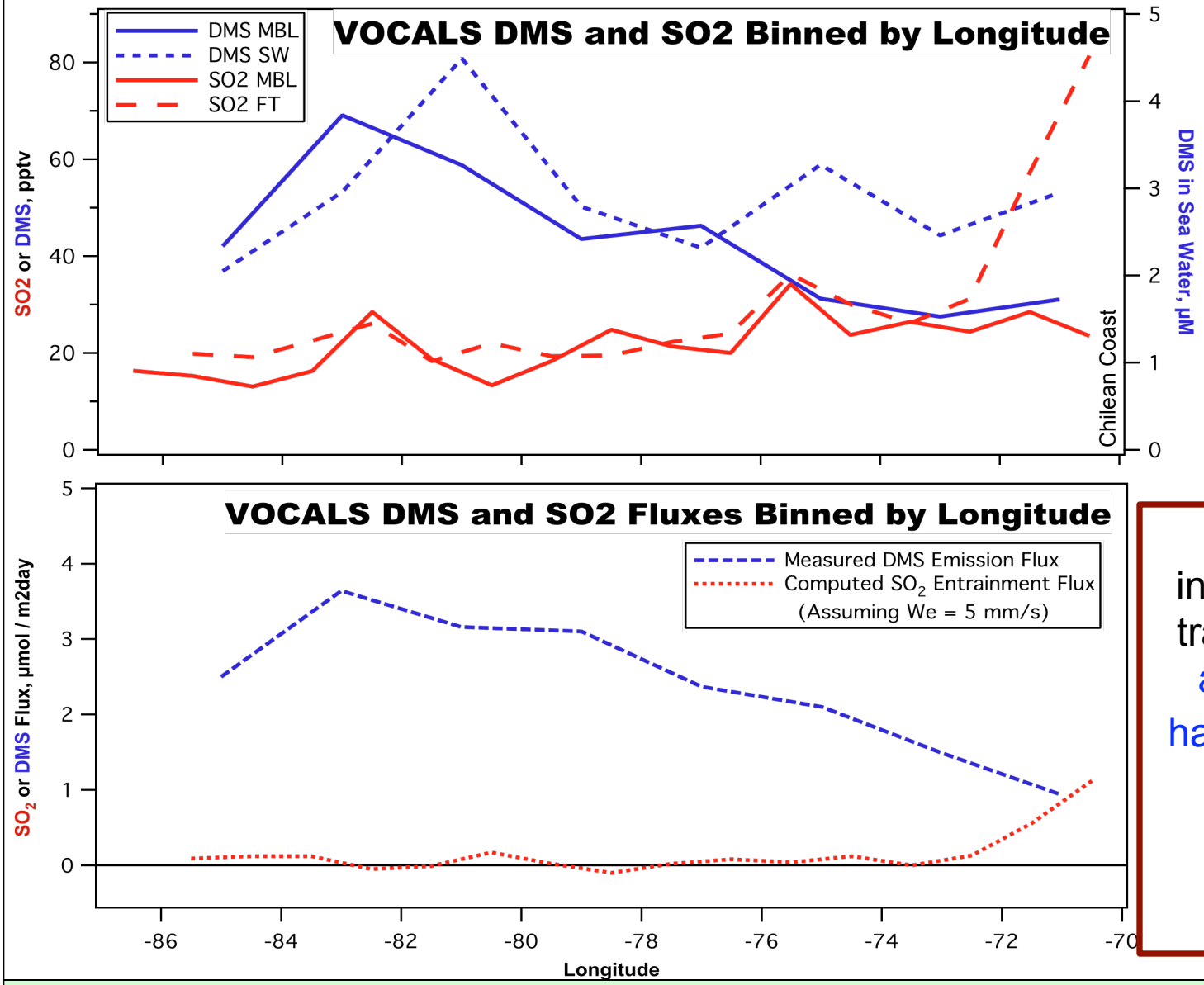

While there were instances of off-shore transport, on average anthropogenic SO_2 had virtually no impact on VOCALS MBL Sulfur (nor on CCN formation)

Preliminary data: post-cals still underway.

Huebert et al., Univ. Hawaii

VOCALS REx, C-130 Research Flight RF06

Data analysis notes, by Robert Wood, University of Washington

1. Determination of the leading and back edges of the strongly drizzling boundary cell.

A combination of in-situ C-130 data (primarily temperature and dewpoint) and radar reflectivity quicklooks (available in the VOCALS field catalog[1]), was used to determine subjectively the location of the leading and back edges of the strongly drizzling boundary cell. Figure 1 shows WCR reflectivity profiles for the two subcloud runs in RF06.

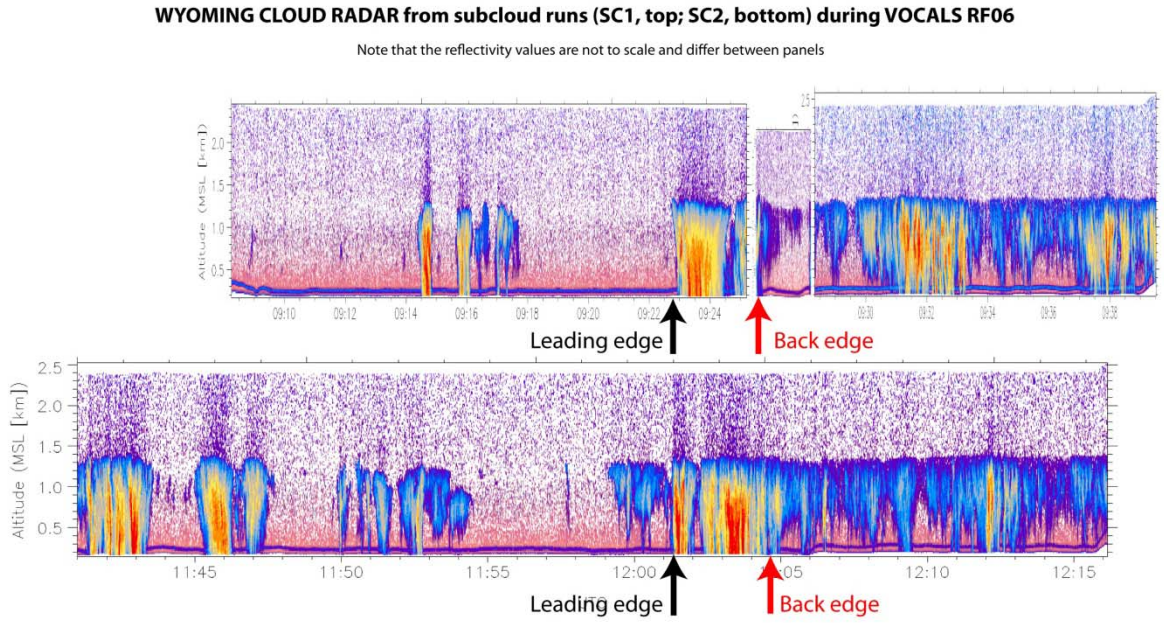

Figure 1: Quick-look Wyoming Cloud Radar (WCR) profiles composited for the two subcloud runs in RF06. Note that the reflectivity color scale is not consistent among the plots, and that these plots are simply designed to give a sense of the key features. [From WCR_SC1_SC2_Composite_lowres.jpg]

Although the structures of the boundary cell in run SC1 and SC2 is qualitatively similar in the WCR data, the thermodynamic data from the two runs show quite different structures (Fig. 2). Thus, I have used a somewhat subjective combination of the temperature, relative humidity, and WCR reflectivity data to determine the leading and back edges of the boundary cell.

[1] *http://catalog.eol.ucar.edu/cgi-bin/vocals/research/prod_browse?platform=WCR_Reflectivity_and_Velocity&prod=up_and_or_down&howmany=Use+Start%2FEnd+Dates+-%3E&start=20081028&end=20081028&submit=retrieve+products*

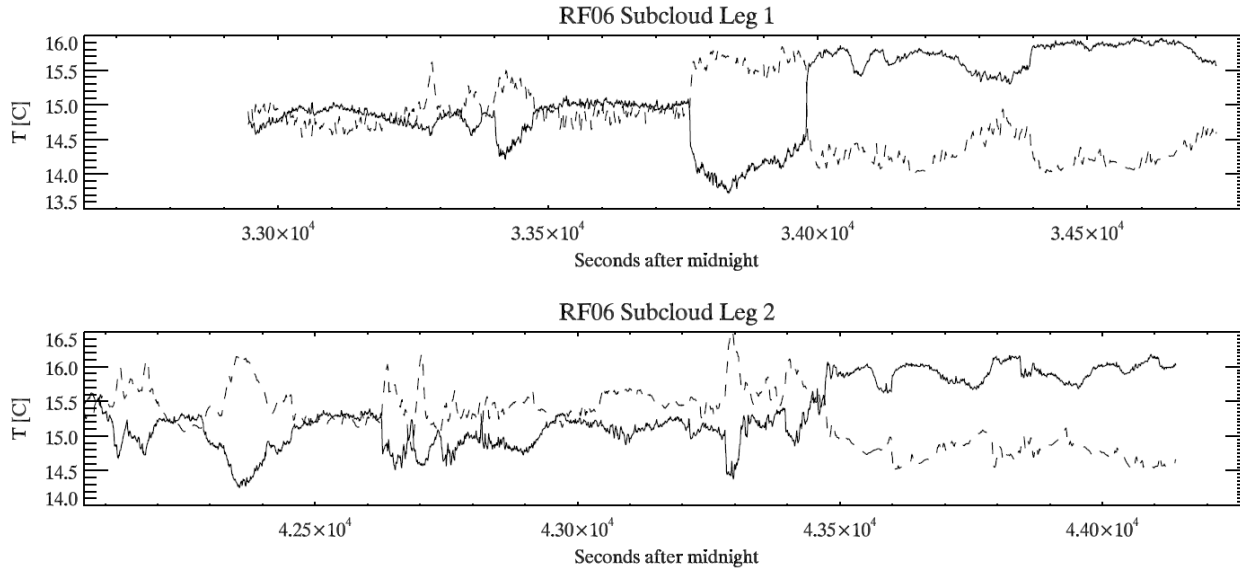

Figure 2: Temperature (solid) and relative humidity (dashed, right axis runs from 0.5 to 1.0) for runs SC1 and SC2 in RF06. While the location of the cold pool in SC1 delineates the boundary cell very clearly as a large drop in temperature of 1 K and a rise in RH, no such clearly defined boundary cell signature is evident in the thermodynamic signature in SC2.[From RF06.20081028.061800_151200.PNI.nc.sav_subcloud.ps]

Table 1: Times (in seconds after midnight), latitudes and longitudes of the leading edge and back edge of the boundary cell during RF06

Run	*Leading Edge*			*Back Edge*		
	Time [SAM]	*Latitude*	*Longitude*	*Time [SAM]*	*Latitude*	*Longitude*
AC1	31665	18.352	79.612	31530	18.233	79.528
SC1	33765	18.233	79.710	33978	18.034	79.623
CB1	35910	18.134	79.814	35675	17.945	79.682
C1	37560	18.184	79.968	37800	17.947	79.865
S1	40680	17.994	80.131	40300	17.669	79.908
SC2	43280	17.651	80.151	43472	17.472	80.072
C2	45340	17.719	80.347	45160	17.575	80.246

Table 1 shows the locations and times of the leading and back edges for the 7 runs across the POC boundary performed in RF06. Figure 3 shows the flight track with the leading and back edges marked with solid and open circles respectively. The lower panel shows the advected flight track using the mean boundary layer wind ($z < 1300$ m) vector determined from the entire POC-stack section of the mission ($u = -6.86$ m s^{-1}, $v = 8.36$ m s^{-1}, or equivalently a mean wind speed of 10.82 m s^{-1}, and a direction of 141° clockwise from N).

The alternation of left and right handed turns led to a net upwind advection of the pattern relative to the mean wind.

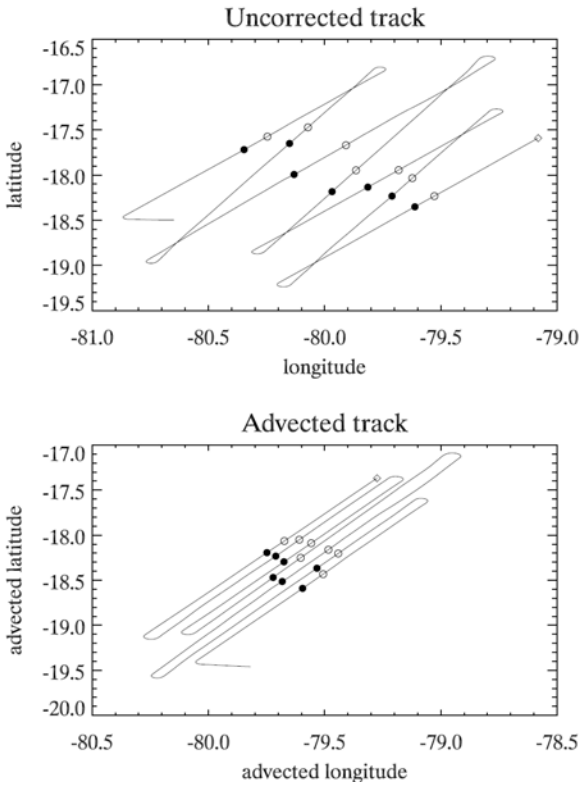

Figure 3. Top: basic flight track in RF06 during POC stacks. The start of the POC stack is marked by a diamond at 79.1W, 17.6S. The leading edge is shown as a filled circle, with the back edge shown as an open circle. The variability in these locations with time reflects both the mean advection of the POC-overcast boundary, plus the undulations in the boundary itself. Bottom: the flight track is now shown after the mean wind below 1300 m is used to advect the flight track back to the starting position. Alternating the turns from a left hand to a right hand turn after each run resulted in a net upwind advection of the pattern with respect to the mean wind.[From rf06_advect_track.ps]

2. Satellite imagery from GOES (IR and VIS)

During POC-drift mission

Figures 4a and 4b show satellite images from GOES-10 for the duration of the POC-drift legs in RF06. The undulating POC-overcast boundary can quite clearly be seen in both infrared (Fig. 4a) and visible (last 8 images in Fig 4b) imagery. The movement of the POC-overcast boundary is clearly seen in the progression of the images. The orientation of the boundary is derived from the images to be $\phi = 27 \pm 2°$ with respect to the E-W direction, and does not change systematically over the course of the measurements.

Motion of the POC-overcast boundary

Calculations show that the boundary is advecting in a direction perpendicular to its orientation at a rate of 4.85 ± 0.5 m s^{-1}. If the boundary were advecting with the mean wind in the MBL, $\underline{u} = [u,v] = [-6.86,8.36]$ m s^{-1}, then the edge would advect at a speed of $\underline{u} \cdot [\sin\phi , \cos\phi] = u \sin\phi + v \cos\phi = 4.3 \pm 0.6$ m s^{-1}. Errors stem from the uncertainty in the wind components (0.3 m s^{-1}) and from the error in the orientation angle of the edge. Thus, we cannot rule out the hypothesis that the edge is simply being advected with the mean wind in the MBL. Note, however, that these observations do not (cannot) rule out the possibility of advection at a different velocity because we only have one piece of information to constrain two independent wind components. We do not have information on the speed of advection of the edge in a direction parallel to its orientation because features on the edge are constantly changing on timescales shorter than the duration of the measurements. Thus, the advection velocity components need to satisfy $u \sin(27°) + v \cos(27°) = 4.3$. This defines a line of possibilities in u,v space.

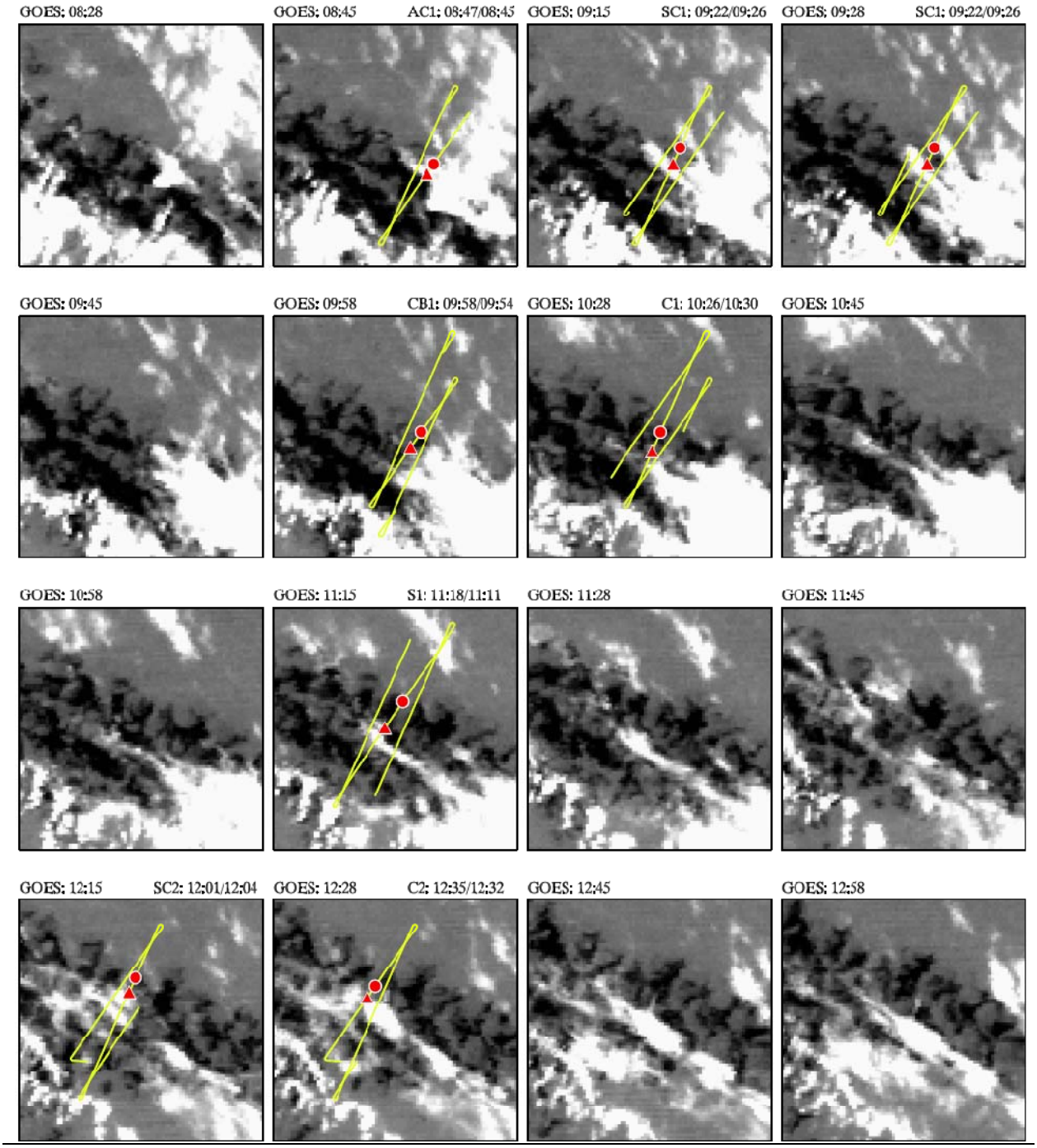

Figure 4a. GOES IR satellite imagery (GOES-10 Channel 5) showing low clouds (gray) and high clouds (white). The images span 16.5-19.5 °S and 81.5-78.5 °W, and are therefore approximately 300 km square. Overlaid are aircraft tracks (yellow) for those images with a POC boundary traverse within 15 minutes of the image time. Tracks are shown for one hour before to one hour after the time of the image, the time (UTC) of which is shown in the top left of the panel. Also shown are the locations of the leading edge (triangle) and back edge (circle) for each of the aircraft passes through the boundary.[from goes_rf06_ir.ps]

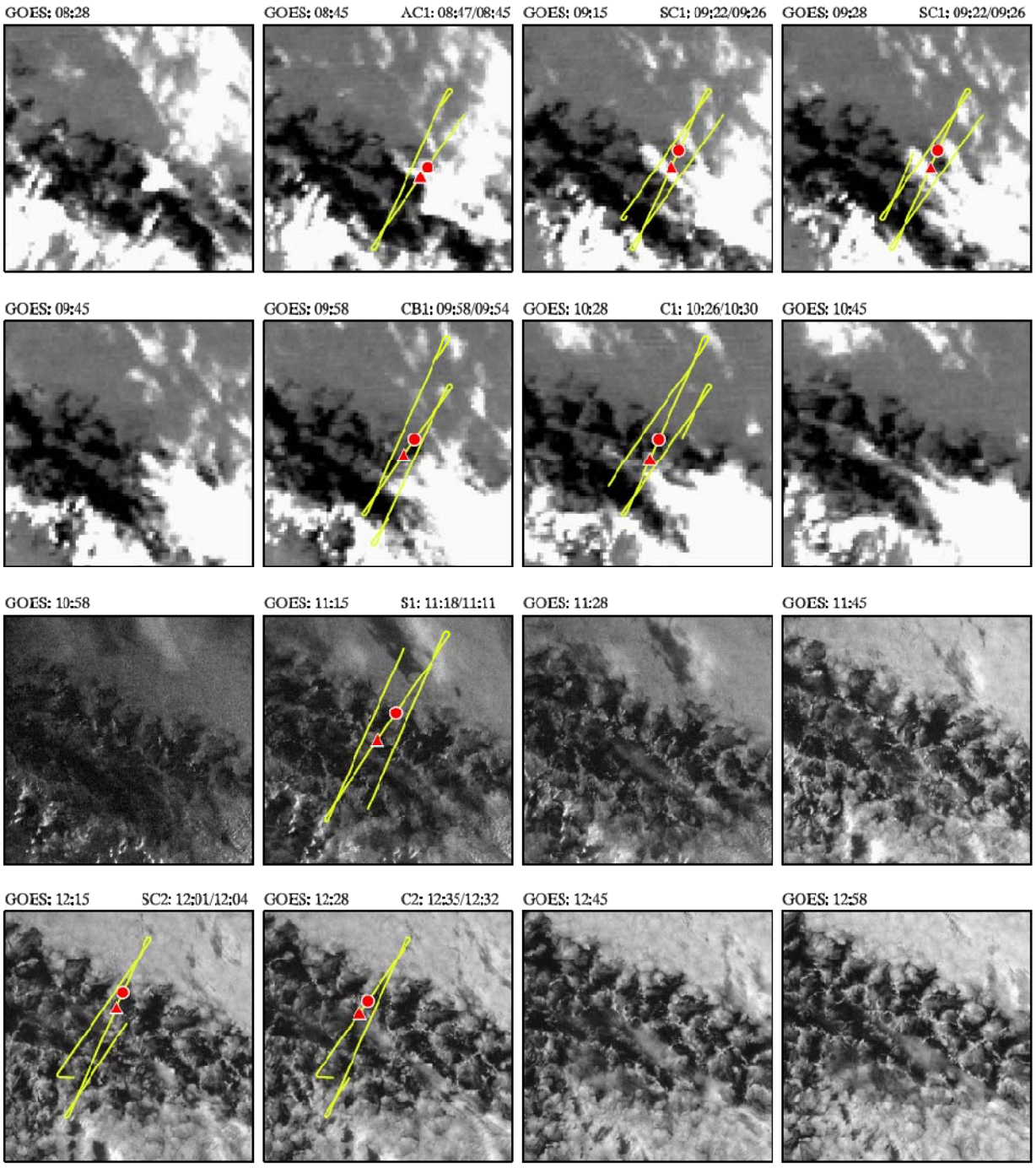

Figure 4b: As for Fig 4a but with the lower 8 panels showing visible imagery at 1km resolution rather than infrared imagery. Shadows of the high clouds on the lower cloud deck are clearly seen. The aircraft tracks are for Fig. 4a. [from goes_rf06_ir.ps]

Days before and after RF06

Figure 5 shows the time evolution of the

3. Aerosol concentrations in clear air relative to the leading edge

Figure 6 shows, for all straight and level runs in the MBL, CN concentrations and refractory fraction of CN for regions clear of cloud and/or drizzle, as a function of distance from the leading edge. Positive distances reflect overcast regions, and negative distances are inside the POC. A 1 Hz sample is designated as containing cloud/drizzle if ANY of the following conditions are satisfied:

1. The PVM liquid water content (LWC) exceeds 0.004 g m^{-3}
2. The CDP LWC exceeds 0.01 g m^{-3}
3. Smoothed 2DC drizzle LWC, using 10 second running mean filter exceeds 10^{-5} g m^{-3}
4. The 2DC drop concentration exceed 1 $liter^{-1}$

In addition, we assume a 10 second lag in the CN measurements (made inside the cabin) an apply the cloud/drizzle criteria for this lag.

Figure 7 shows the same plot but for the accumulation mode aerosol concentration measured with the PCASP. The same cloud/drizzle screening described above has been applied to the PCASP data.

The interesting features in Fig. 6 and 7 are:

- On the overcast side of the CN concentrations gradually increase from less than 100 cm^{-3} near the back edge of the boundary cell, to over 200 cm^{-3} around 100 km from the back edge. Refractory fractions are more or less constant in the overcast region at around 0.75-0.8
- A broad maximum in CN concentration is observed inside the POC at a distance of some 10-60 km in from the leading edge. The maximum concentrations in this region vary from 200-400 cm^{-3}. Coincident with the increases in CN in this region, the refractory fraction minimizes at very low values of 0.1-0.2.
- Further into the POC region, the CN concentration falls to very low values (50-100 cm^{-3}) with coincident rises in refractory fraction to values comparable with, or slightly lower than those in the overcast region.
- Accumulation mode aerosol concentration (N_{acc}) decreases markedly with height in the POC region, with values of 10-60 cm^{-3} in the surface layer, 5-20 cm^{-3} at the cloud base level, and extremely low values of 0.5-5~cm^{-3} are present throughout the cloud layer.
- Inside the POC in the surface layer, N_{acc} decreases with distance away from the boundary cell, from values close to 60 cm^{-3} near the cell, to values of 10-30 cm^{-3} between 40 and 70 km inside the POC. Further into the POC, values rise again to ~50 cm^{-3}.
- Outside the POC, the cloud-base and surface layer N_{acc} values are similar and reach ~100 cm^{-3} around 50 km into the overcast cloud. There is a marked gradient as the boundary cell is approached, at which point values are around 50 cm^{-3}.
- Cloud droplet concentrations are consistent with N_{acc} in adjacent regions inside the POC and are very low. Outside the POC, the cloud droplet concentration falls at a faster rate towards the back edge than the subcloud N_{acc}.

The results are consistent with a refractory CN concentration that does not vary strongly inside the POC, but a non-refractory CN concentration elevation in the 10-60 km immediately inside the POC.

In the free-troposphere the refractory fraction is 0.4-0.5 (not shown), and the mean CN concentration is 275-300 cm^{-3}, so it is difficult to envisage how entrainment can be the cause of the elevated values in the MBL inside the POC.

The extremely depleted accumulation mode aerosol concentrations in the cloud layer are consistent with near-complete removal of CCN from air parcels transported there. This is almost certainly the result of precipitation. The elevated values of N_{acc} at cloud base inside the POC adjacent to the leading edge of the boundary cell are similar to those at the surface at the same location suggesting coupling between the subcloud and cloud layers at this location.

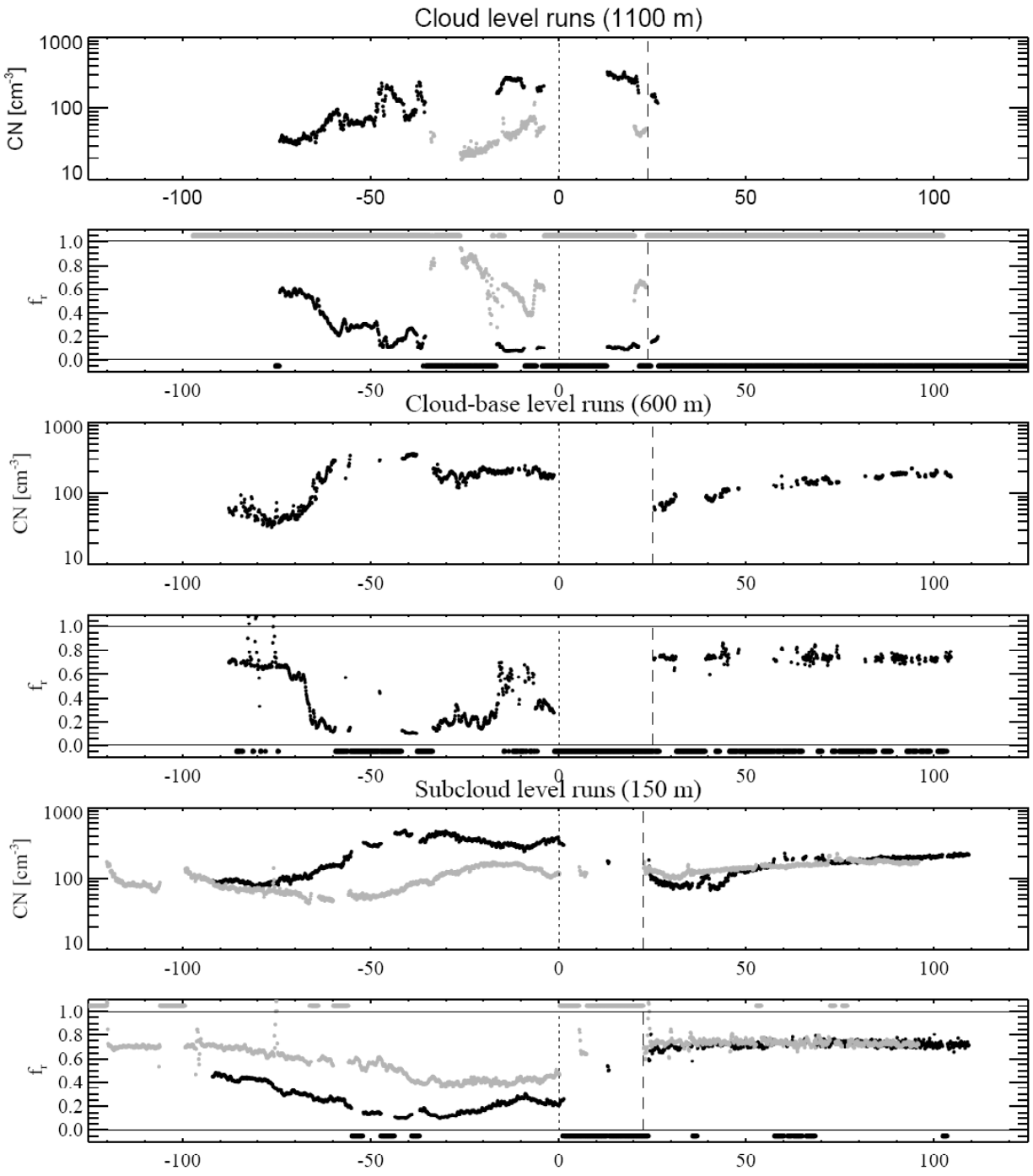

Figure 6:Distance series of total CN concentration (University of Hawaii CNCold) and the refractory CN fraction (f_r = CNHot/CNCold) as a function of distance from the leading edge, for runs in the cloud layer (C1, black; C2, gray, top two panels), in the cloud-base layer (CB1, black, middle two panels) and for the subcloud layer (SC1, black; SC2, gray, lower two panels). For the f_r panels, we also show, above and below the main panel for runs 1 and 2 respectively, locations where cloud or drizzle was observed in the runs. Only data screened to be free of cloud and drizzle are plotted (see text for screening criteria used). The dotted line shows the location of the leading edge, and the dashed line the location of the back edge (mean value if for those plots with two runs)

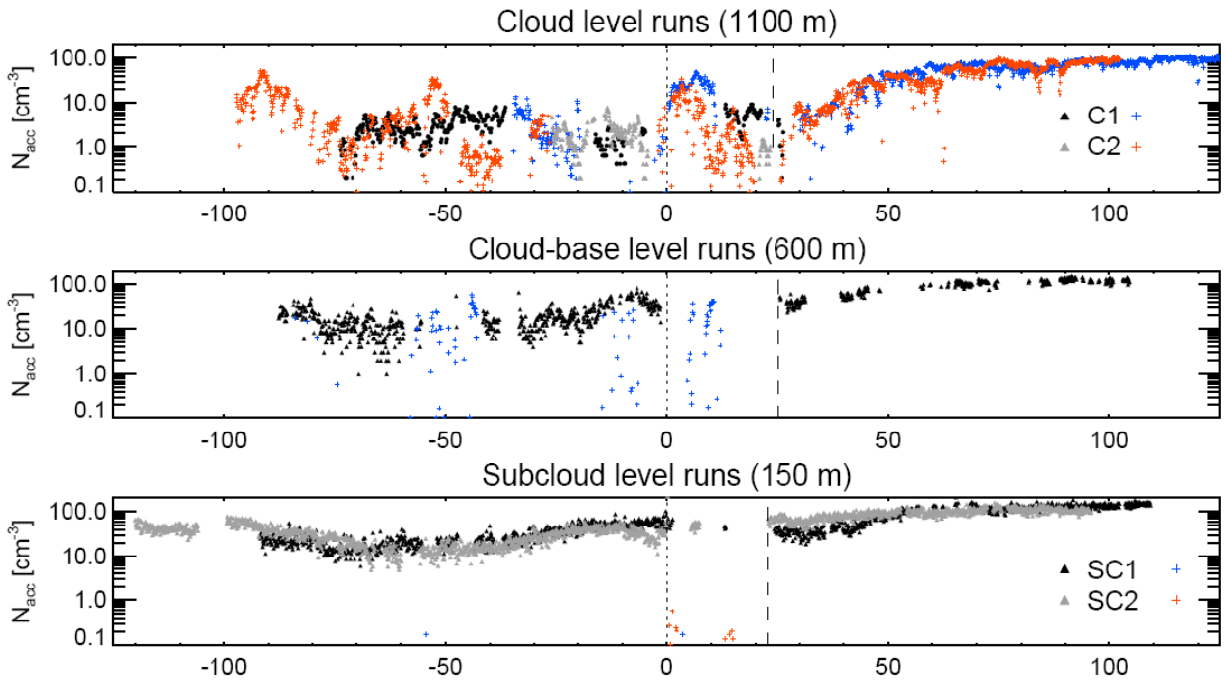

Figure 7:Distance series of accumulation mode aerosol concentration (PCASP, black and gray), and in-cloud droplet concentration (CDP, blue and red, conditioned on PVM cloud liquid water content > 0.02 g m^{-3}) as a function of distance from the leading edge, for runs in the cloud layer (C1, black; C2, gray, top two panels), in the cloud-base layer (CB1, black, middle two panels) and for the subcloud layer (SC1, black; SC2, gray, lower two panels). For the f, panels, we also show, above and below the main panel for runs 1 and 2 respectively, locations where cloud or drizzle was observed in the runs. Only data screened to be free of cloud and drizzle are plotted (see text for screening criteria used). The dotted line shows the location of the leading edge, and the dashed line the location of the back edge (mean value if for those plots with two runs)

Layer mean values of various parameters for inside POC, overcast region, boundary cell

Filled circle: overcast; open circle: POC; triangle: boundary cell

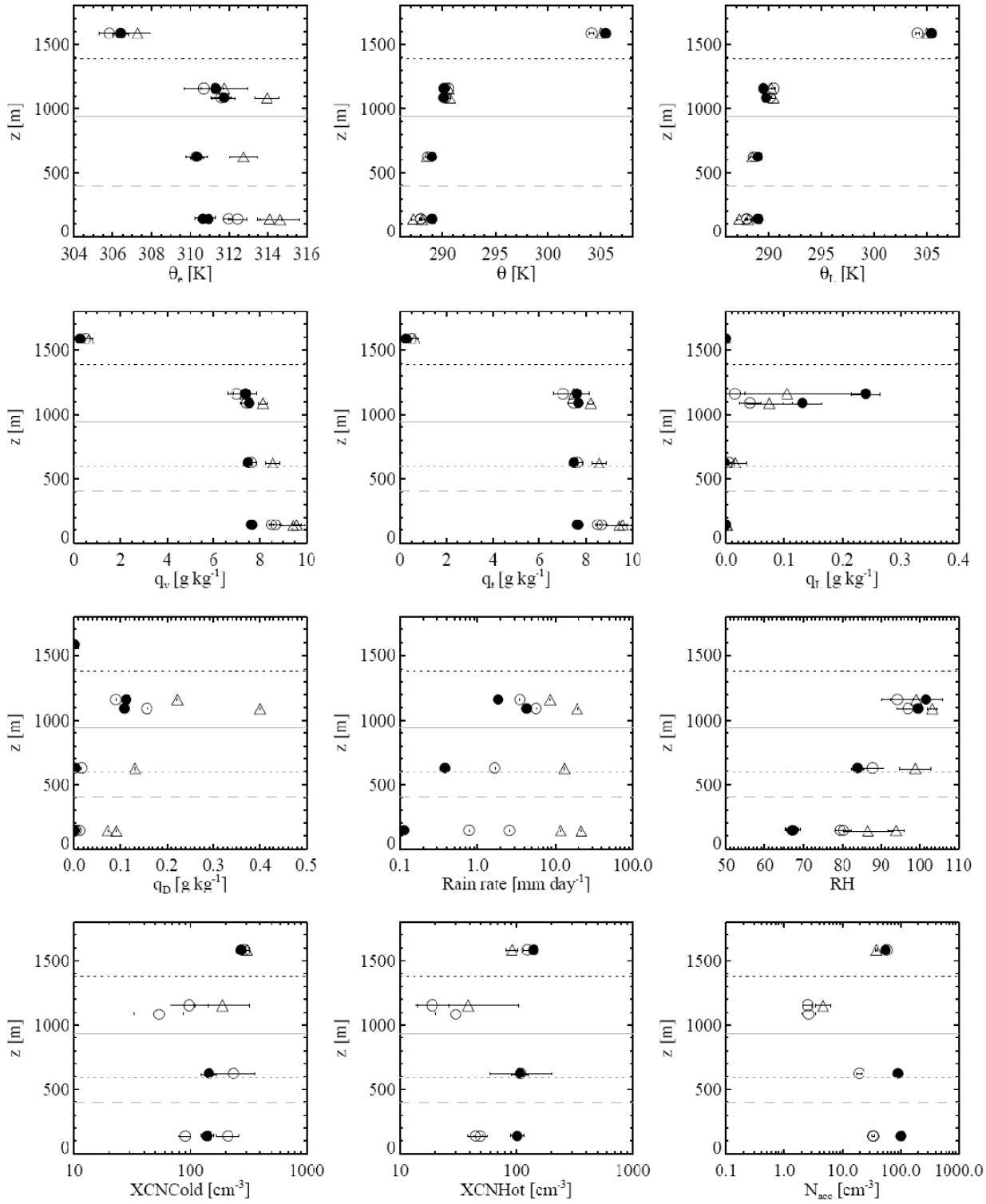

Profiles of aerosols ordered as a function of distance from leading edge

Dot: PCASP; dotted line: XCNHot; solid line: XCNcold. Distance from leading edge (km, negative=inside POC) shown in upper left of panels. Cloudy/drizzly regions screened out.

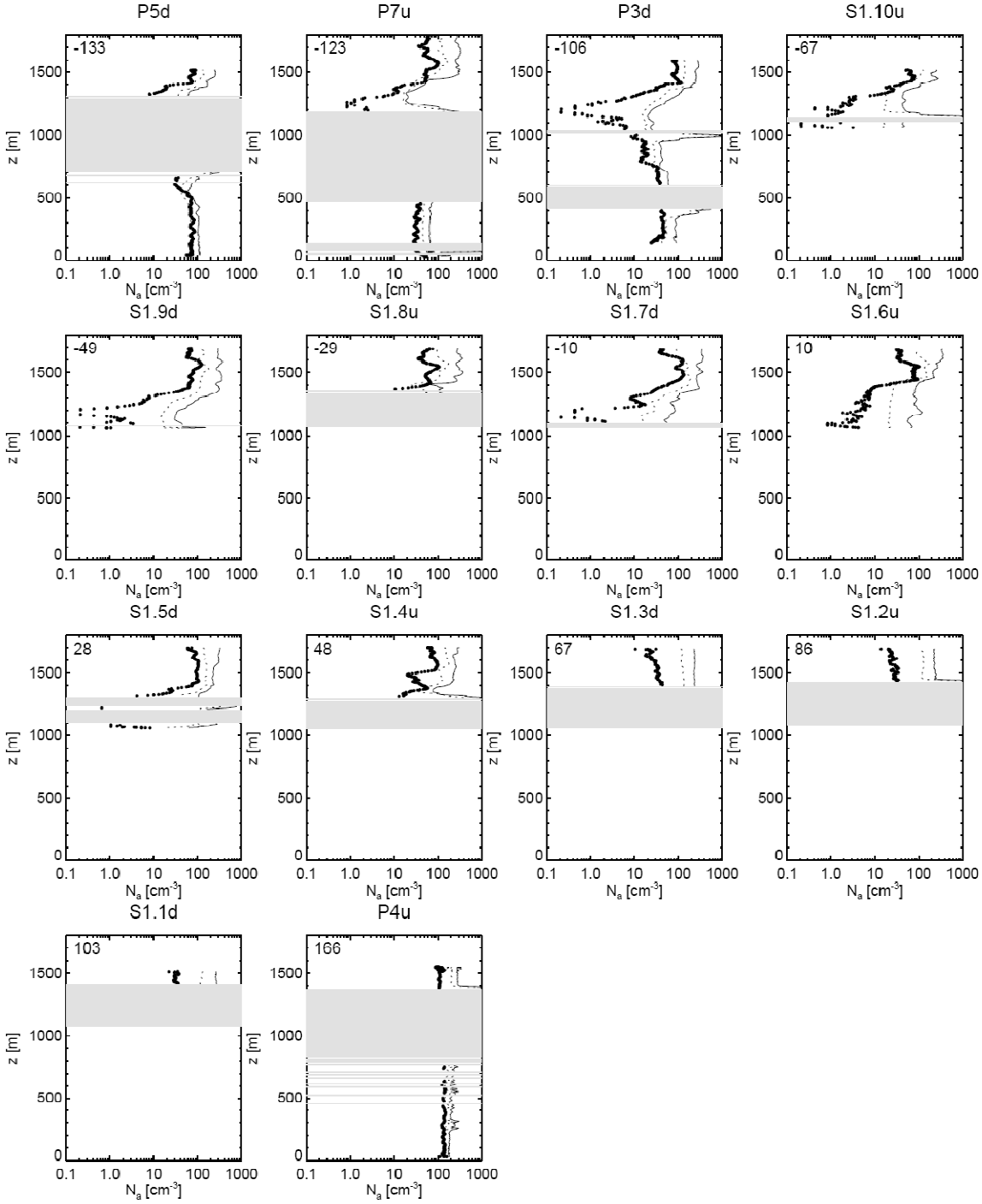

Structure of the boundary cell as seen by the WCR and WCL from the two subcloud runs (SC1 and SC2) is shown below. Images are from David Leon at the University of Wyoming.

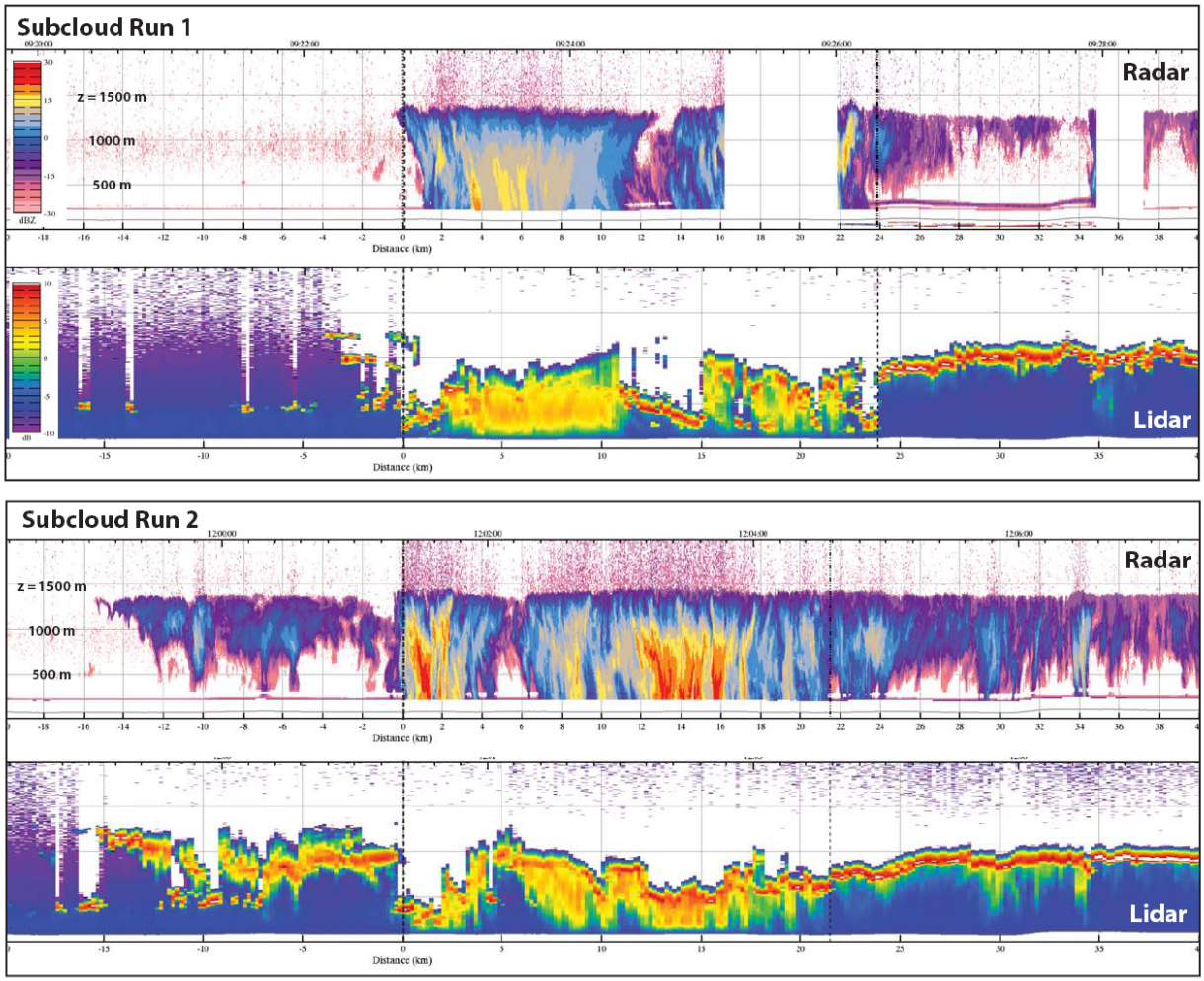

The POC sampled on RF06 was sampled approximately 12 hours earlier by the BAe-146:

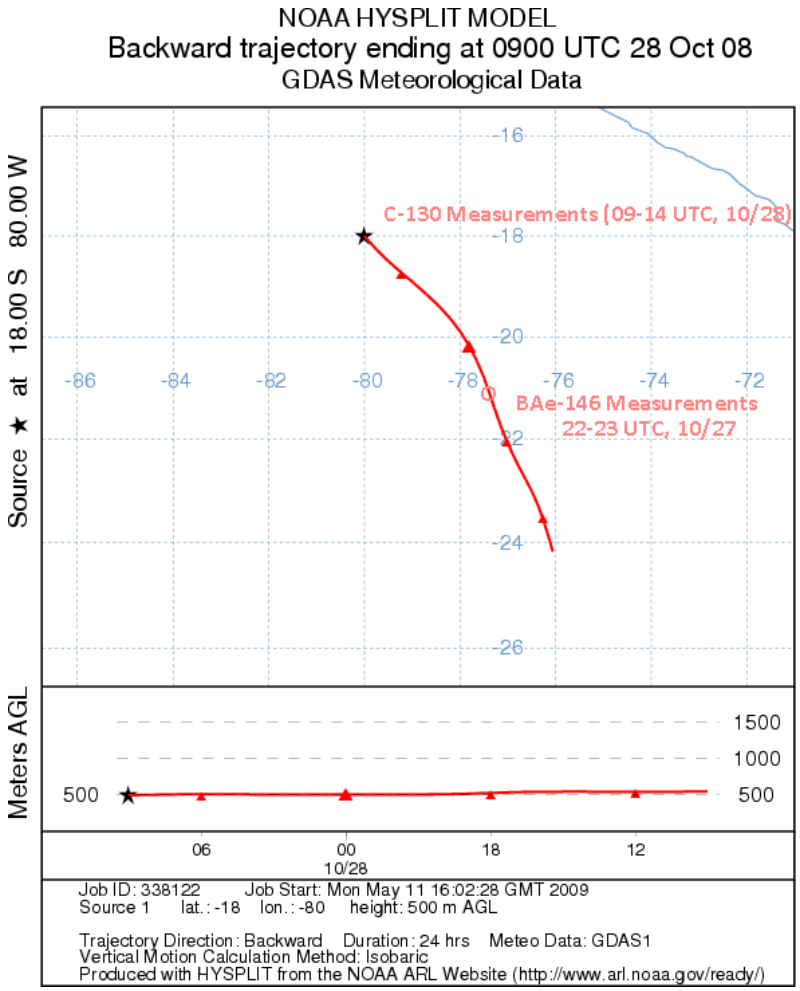

VOCALS RF06 – 10/28/08 – POC Mission

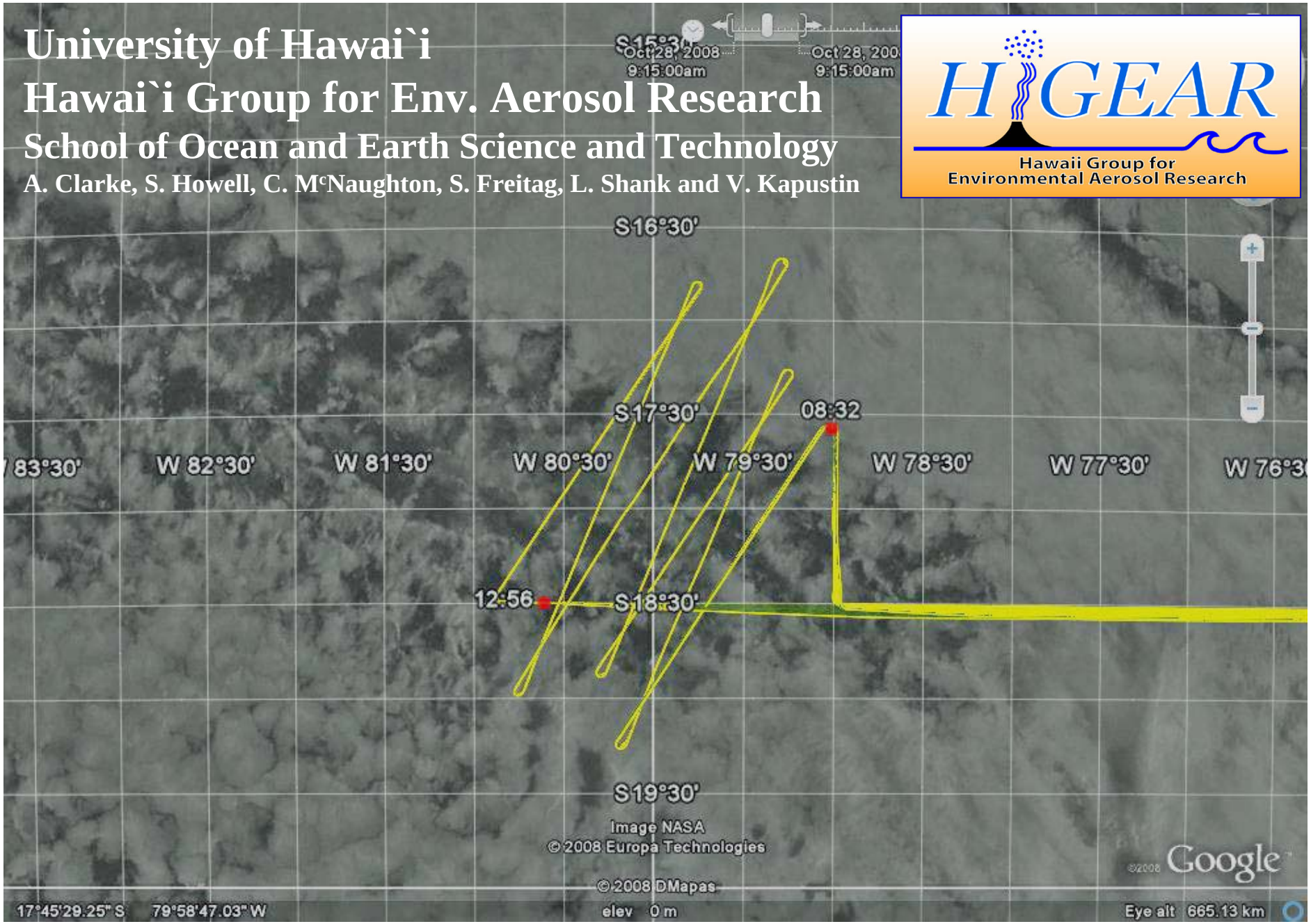

VOCALS RF06 – 10/28/08 – POC Mission

Mixing Ratio g/kg color code to right

Wind barbs show directional shear (more easterly) for above cloud leg - black

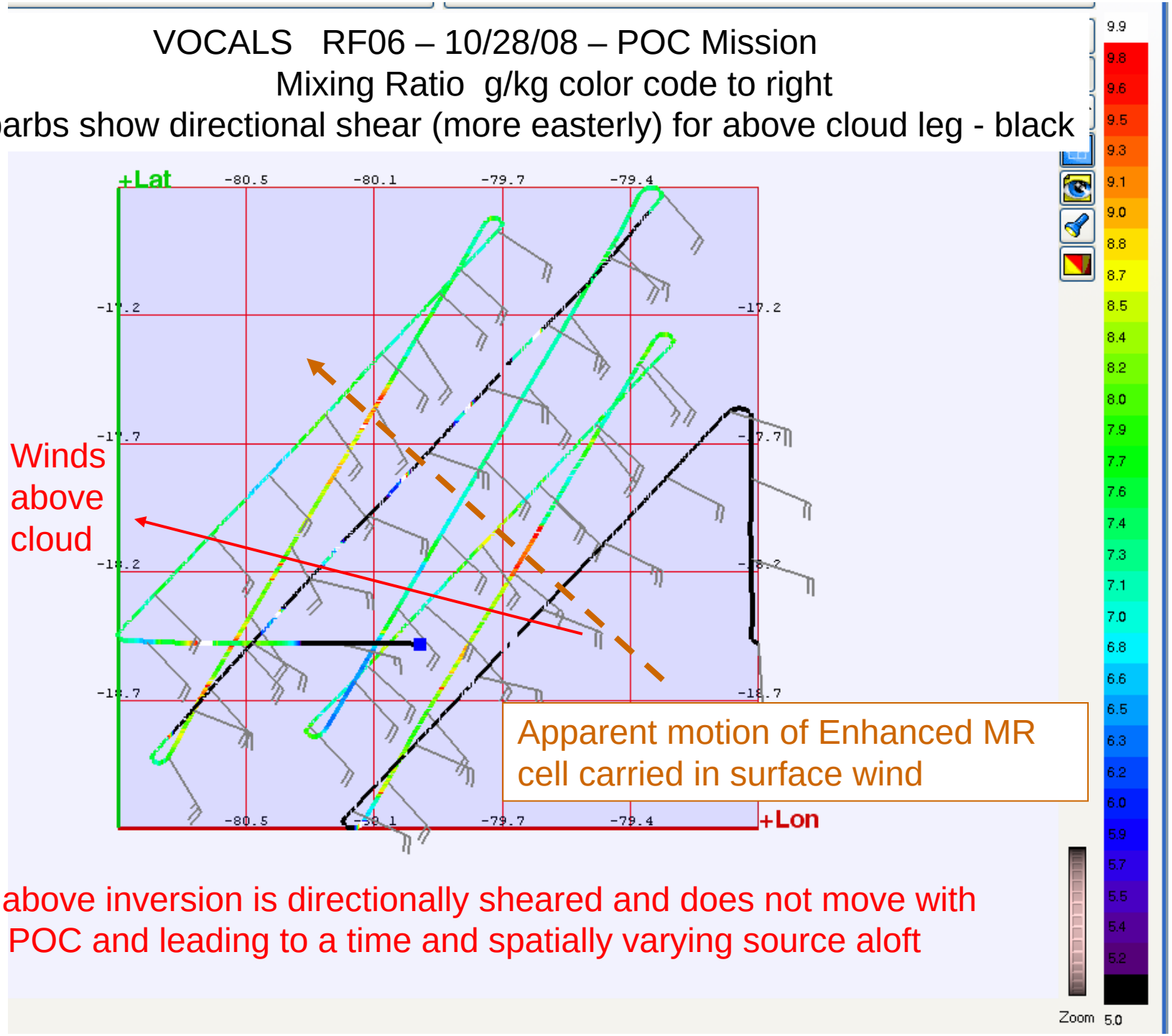

Air above inversion is directionally sheared and does not move with the POC and leading to a time and spatially varying source aloft

VOCALS RF06 – 10/28/2008 CN, CNhot,PCASP POC profiles

Notes:

PCASP and CNhot are *correlated* – PCASP are the largest sizes of the accumulation mode present as CNhot and where many are effective as "CCN" at low supersaturation.

CNhot and CN are *anti-correlated* – their difference (CN-CNhot) is the smaller volatile mode generally independent of the "CCN" mode (except at high supersaturations) and usually too small to be "CCN"

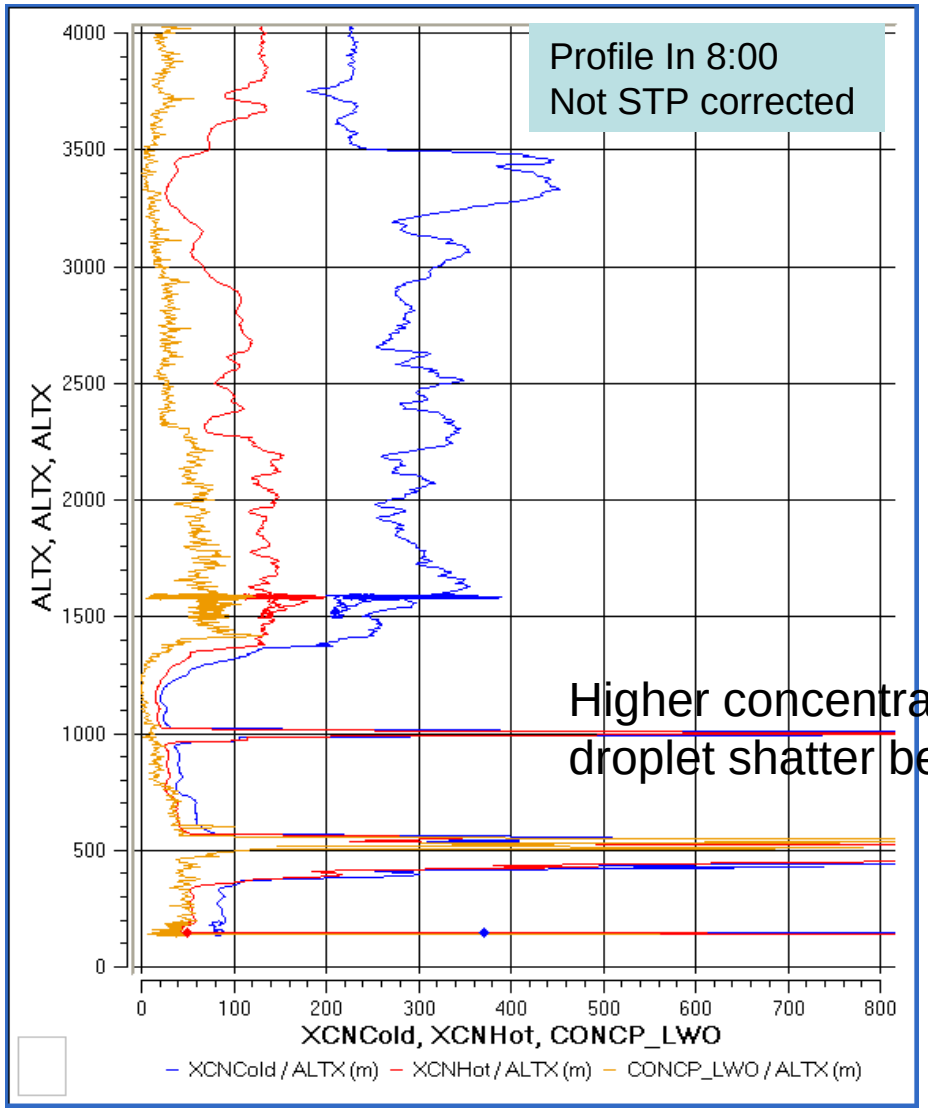

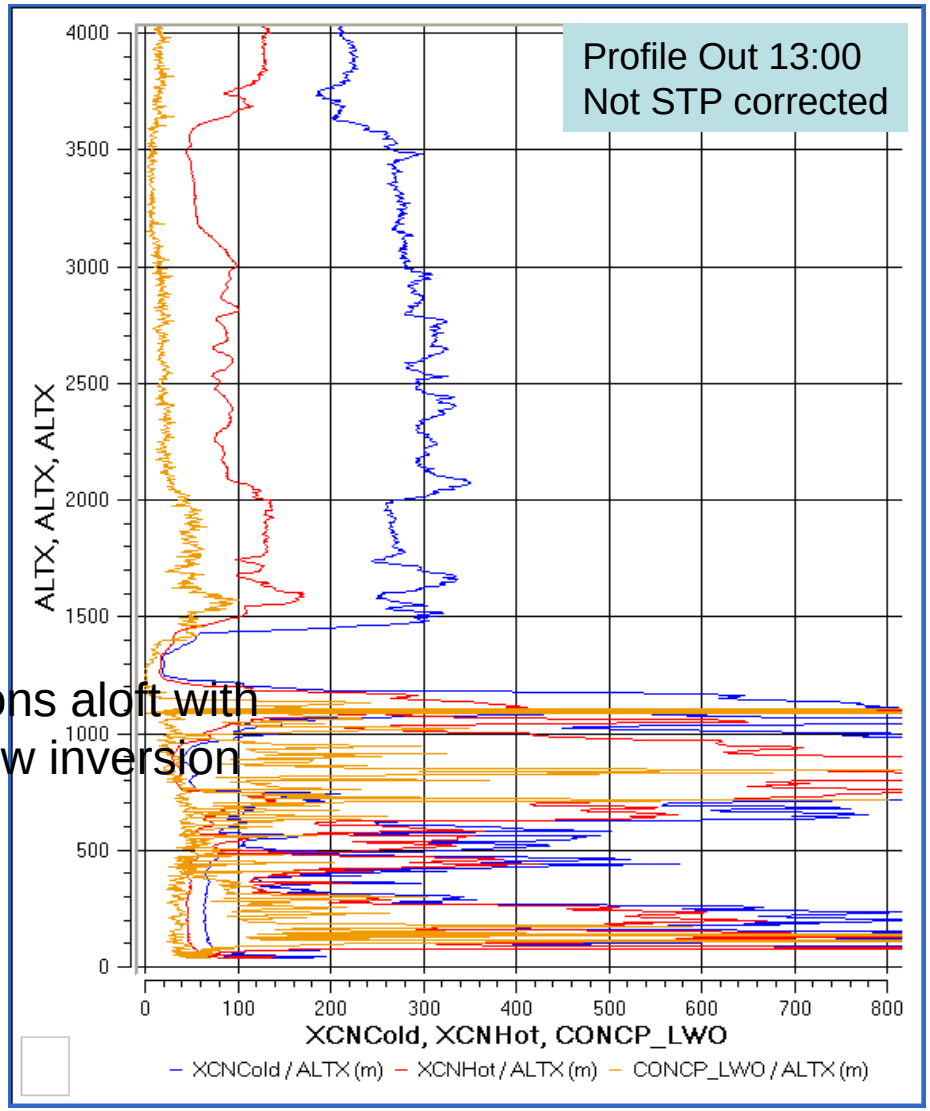

Higher concentrations aloft with droplet shatter below inversion

VOCALS RF06 – 10/28/2008 CN, CNhot,PCASP POC series

Note: Below cloud CNhot and PCASP also ***correlated*** but are virtually the same concentration. This reflects the larger sizes of CNhot in the MBL [possibly associated with uptake of sulfate etc.], also preferentially scavenged. Volatile CN (CN-CNhot) are max ~300/cc near 9:20 but similar values (~250) are evident above cloud 8:45).

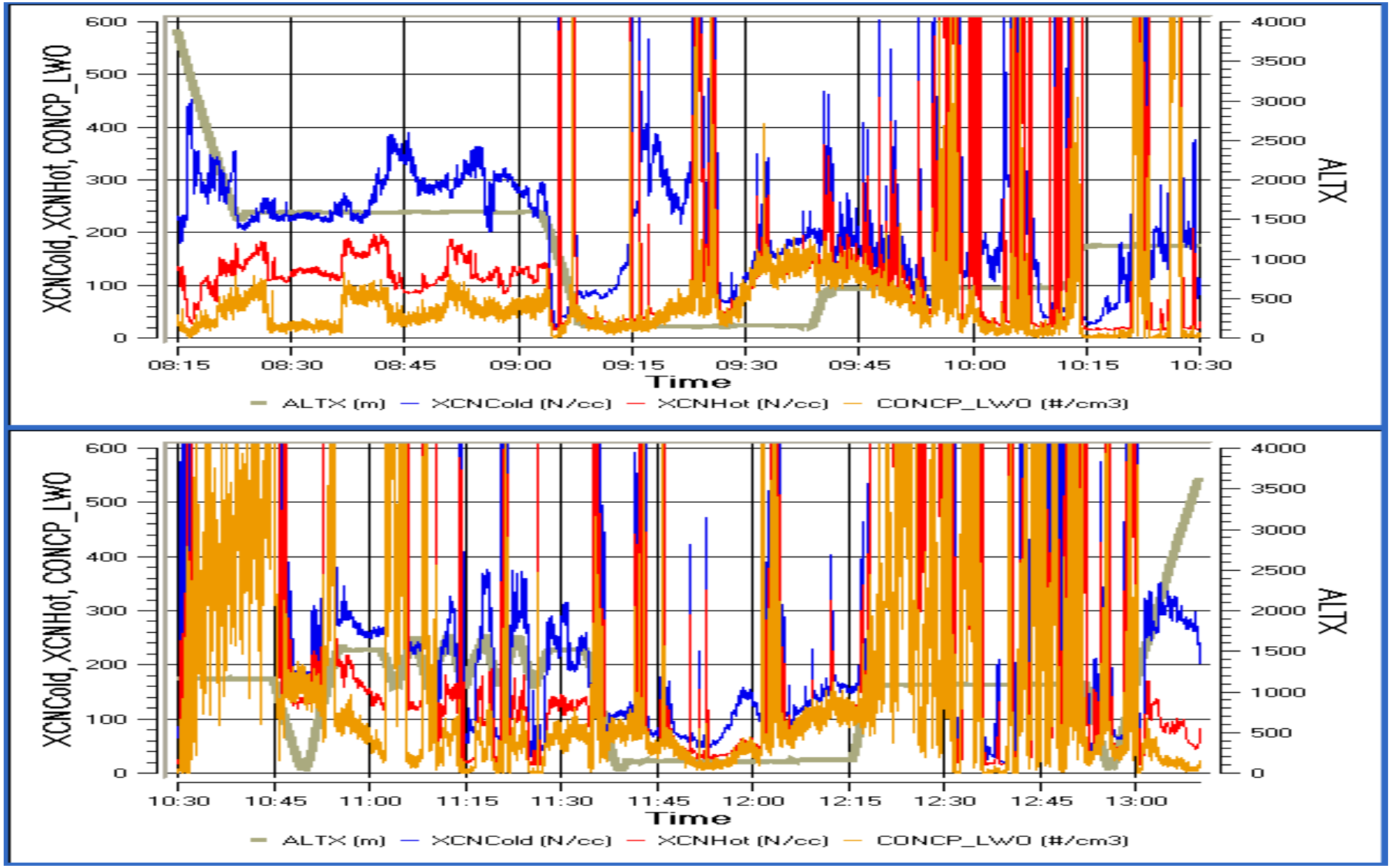

VOCALS RF06 – 10/28/2008 CN, CNhot,PCASP Sawtooth series

Note: When there is droplet shatter in the Boundary layer then CNhot dominate total CN and they correlate. This is characteristic of saline droplet shatter leaving refractory residuals (eg. Eg. 11:20-11:25 at low conc. As well as other pronounced shattering)

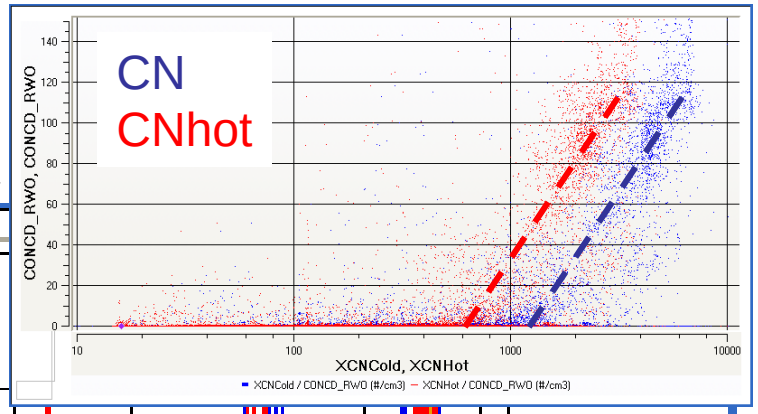

VOCALS RF06 – 10/28/2008 CN, CNhot,PCASP Sawtooth series

Note how variations in PCASP, CHhot and CO are closely coupled on above cloud leg indicating combustion derived aerosol linked to CCN sizes is patchy in space (and time) over clouds. CO more well mixed in MBL and unaffected by aerosol scavenging.

Variations in CO above cloud linked to changes in PCASP and CNhot and CN

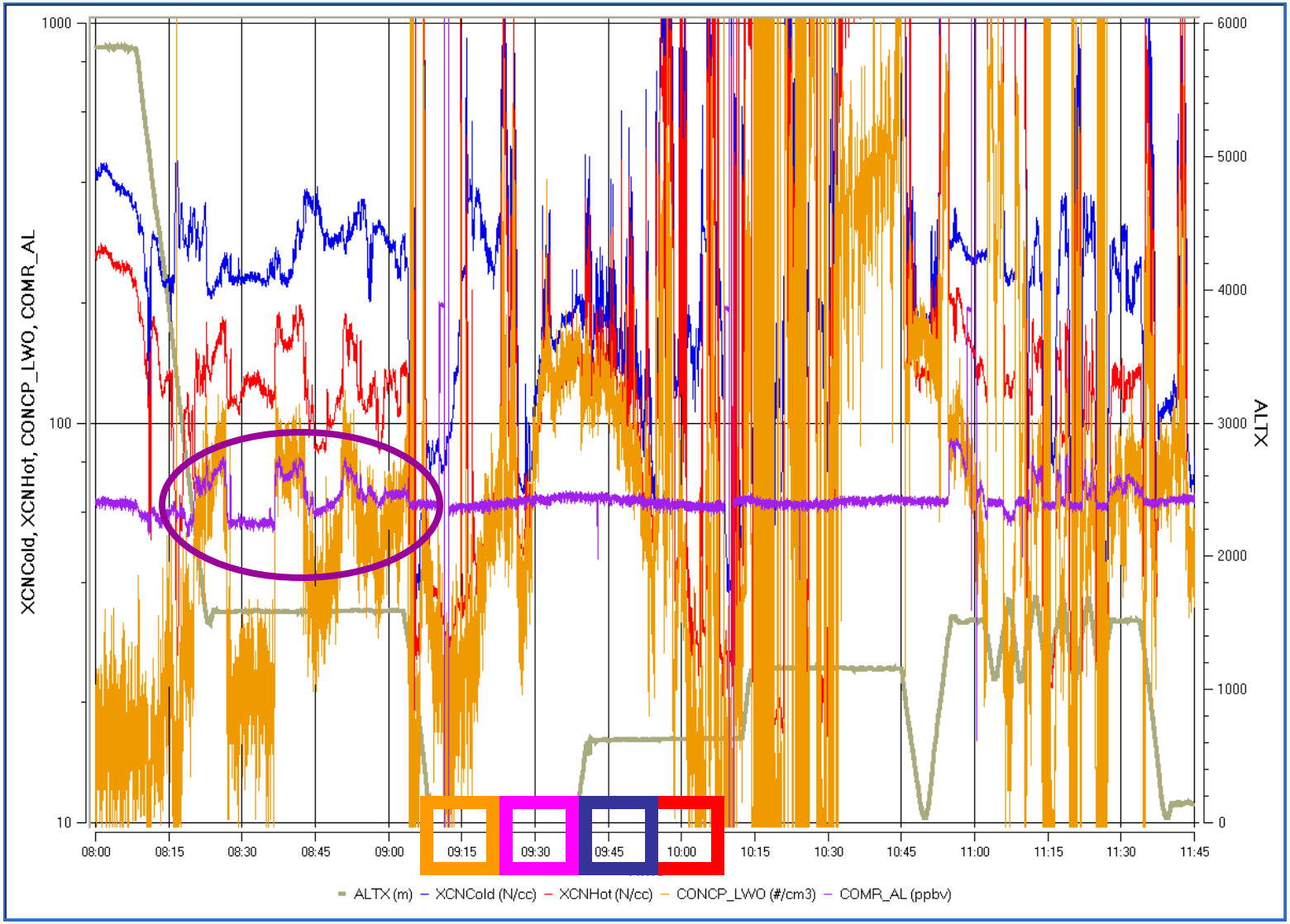

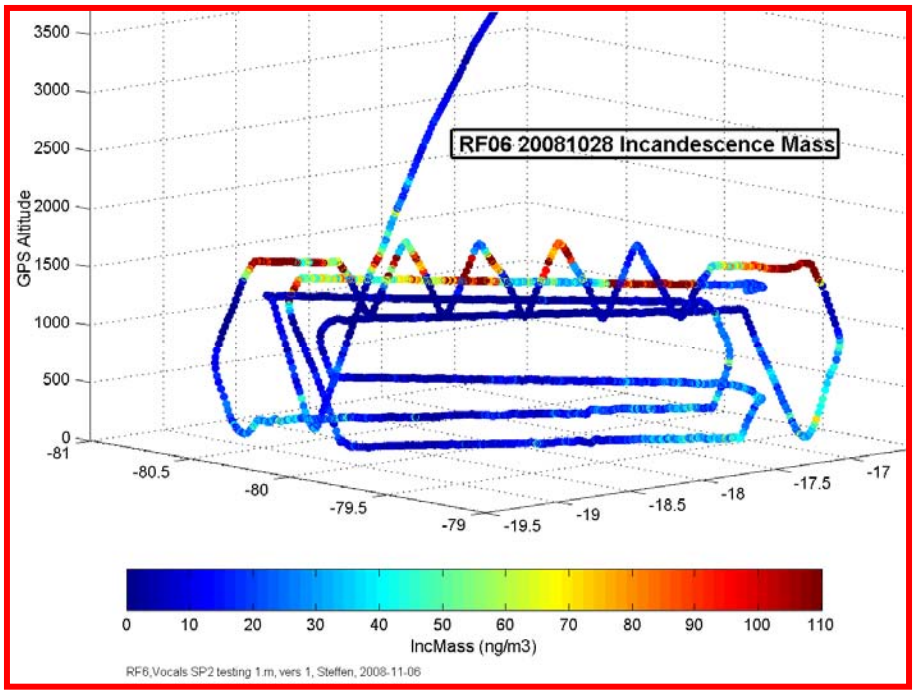

HIGEAR
Hawaii Group for Environmental Aerosol Research

SP2 Black Carbon on Flight RF06

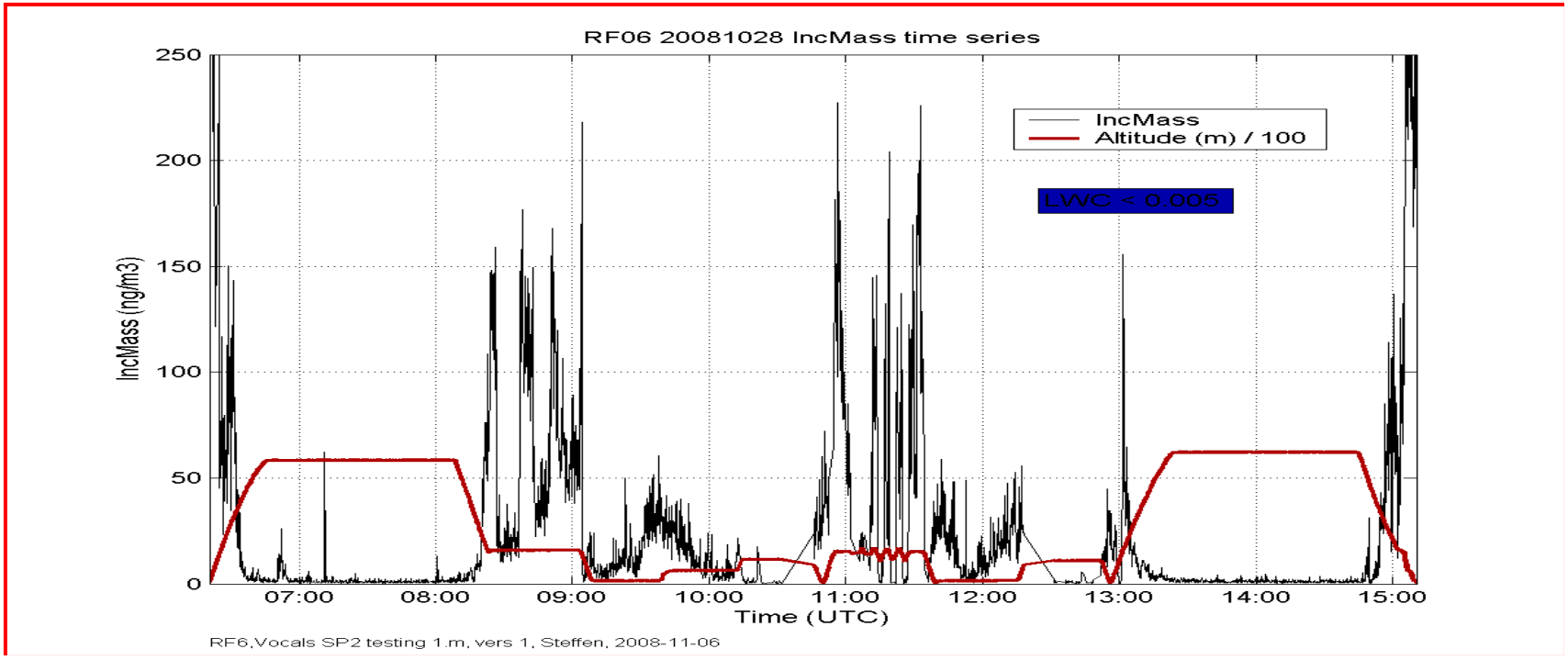

VOCALS RF06 – 10/28/2008 Below Cloud Size Distributions for previous Fig.

Green – total CN
Black - CNhot

POC

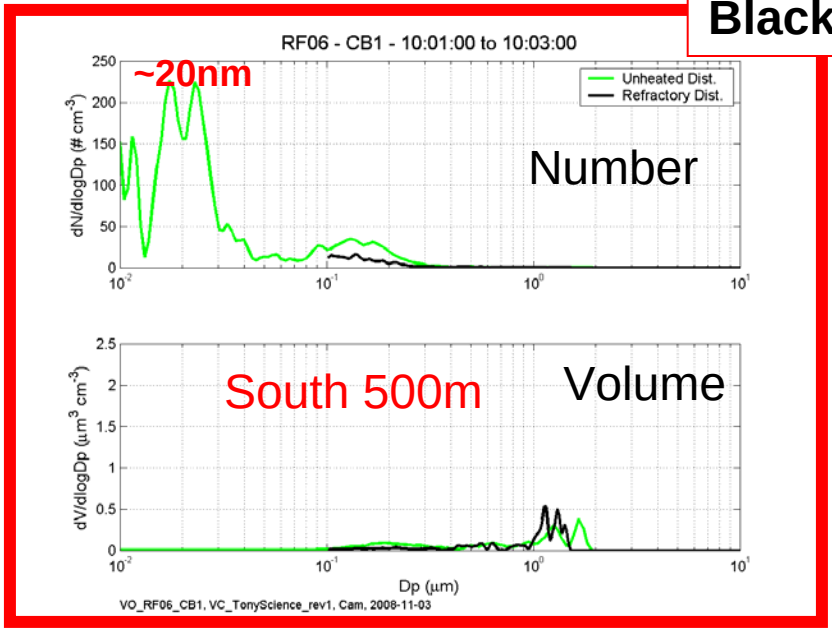

Cloud Region

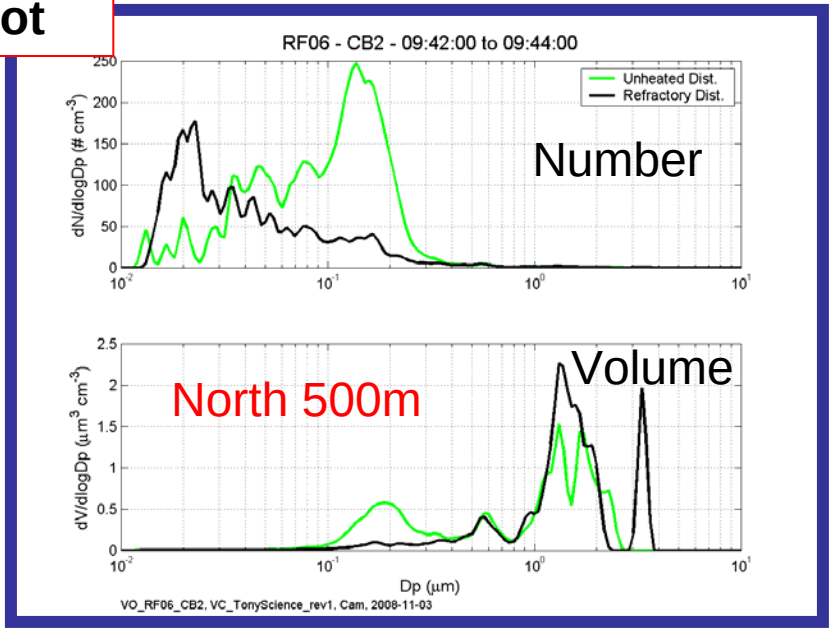

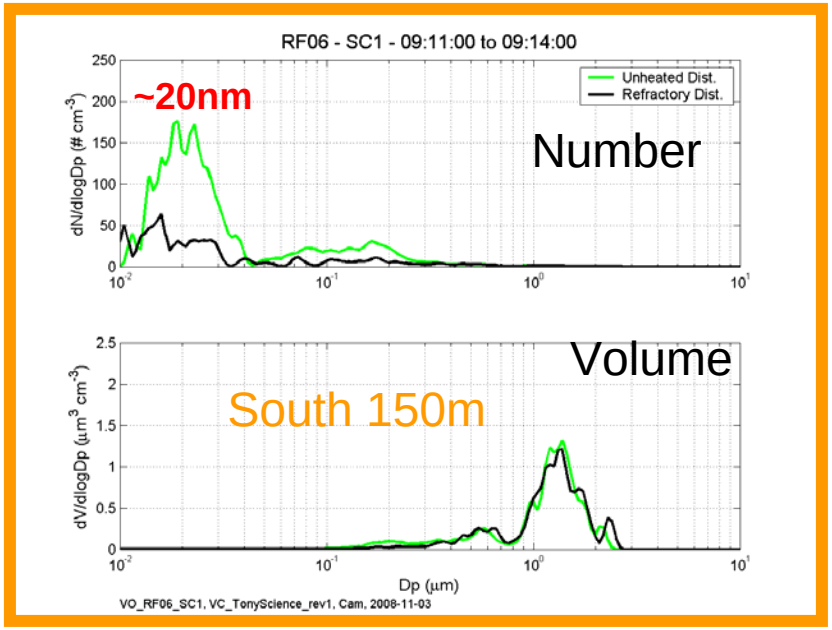

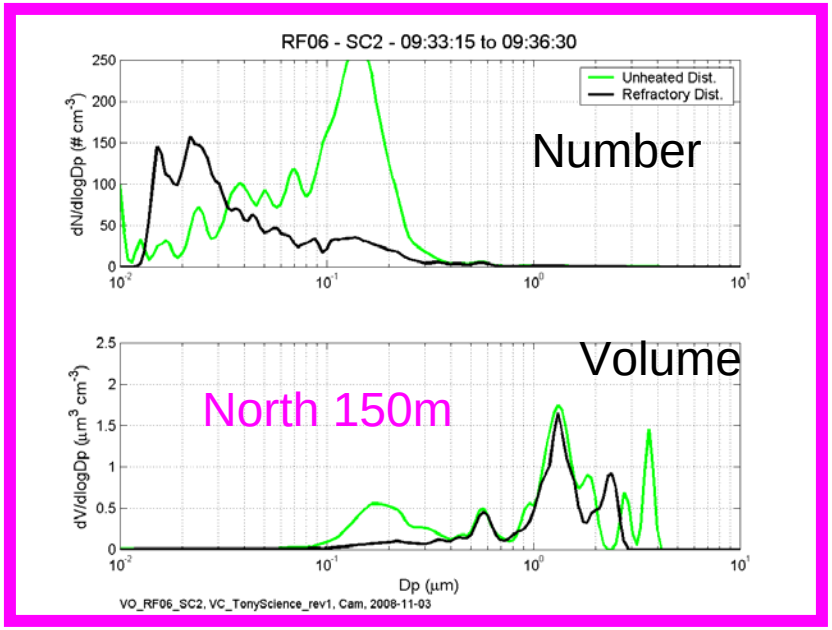

VOCALS RF06–10/28/2008 Above cloud leg number distributions variable

Green – total CN
Black - CNhot

Above cloud leg shows particle number peak diameter vary from about 25 to 75 nm

Larger sizes tend to have more refractory aerosol, CNhot, also linked to combustion sources.

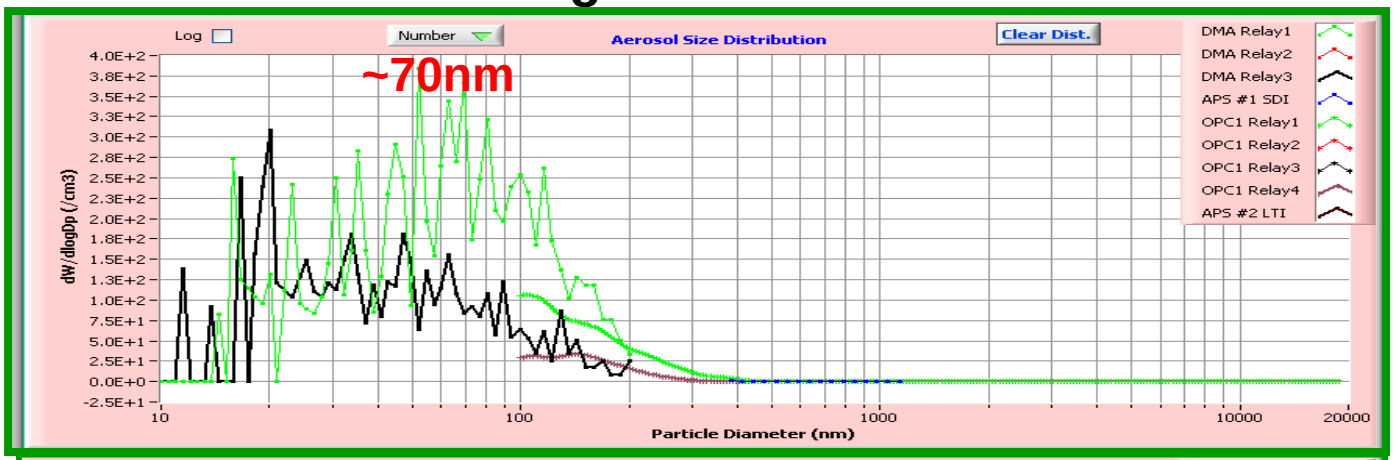

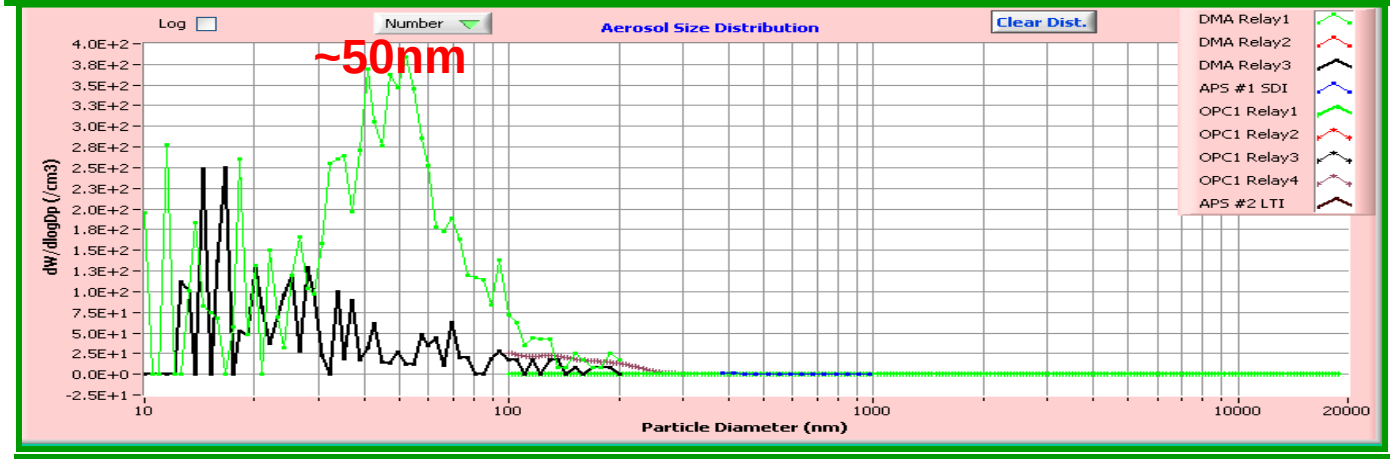

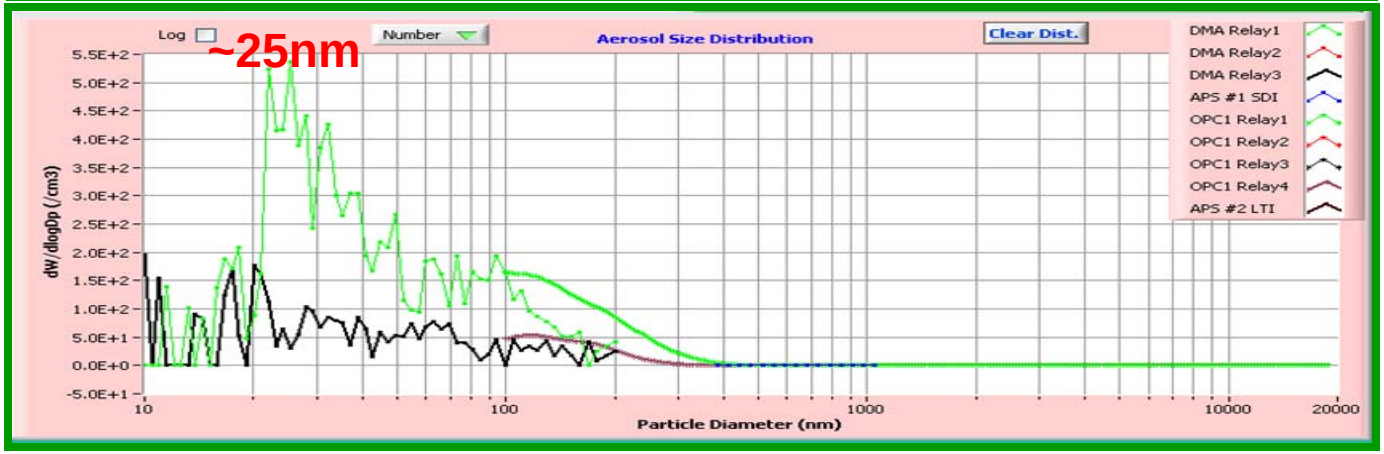

VOCALS RF06 Preliminary POC Observations

- Most CCN size aerosol are linked to CNhot (300C) indicative of accumulation mode that includes the larger PCASP sizes. When these are entrained into MBL and can grow even larger making PCASP (Dp>100nm) and CNhot numerically similar in MBL

- These are also scavenged in MBL where both PCASP and CNhot vary together.

- Smaller and more volatile CN vary above cloud from near peak diameters near 25nm to 75 nm diameter. While it is not clear if or what may have been entrained into MBL a day earlier these smaller sizes are all that remain in scavenged MBL air to the south.

- While some additional smaller sizes may also have nucleated in MBL, it is not certain. Even so, it is unlikely these will age in MBL to effective CCN sizes relative to larger aerosol entrained.

- These larger sizes often linked to elevated CO and black carbon aerosol

VOCALS RF07 – 10/31/2008 GOES Image and Photo over POC

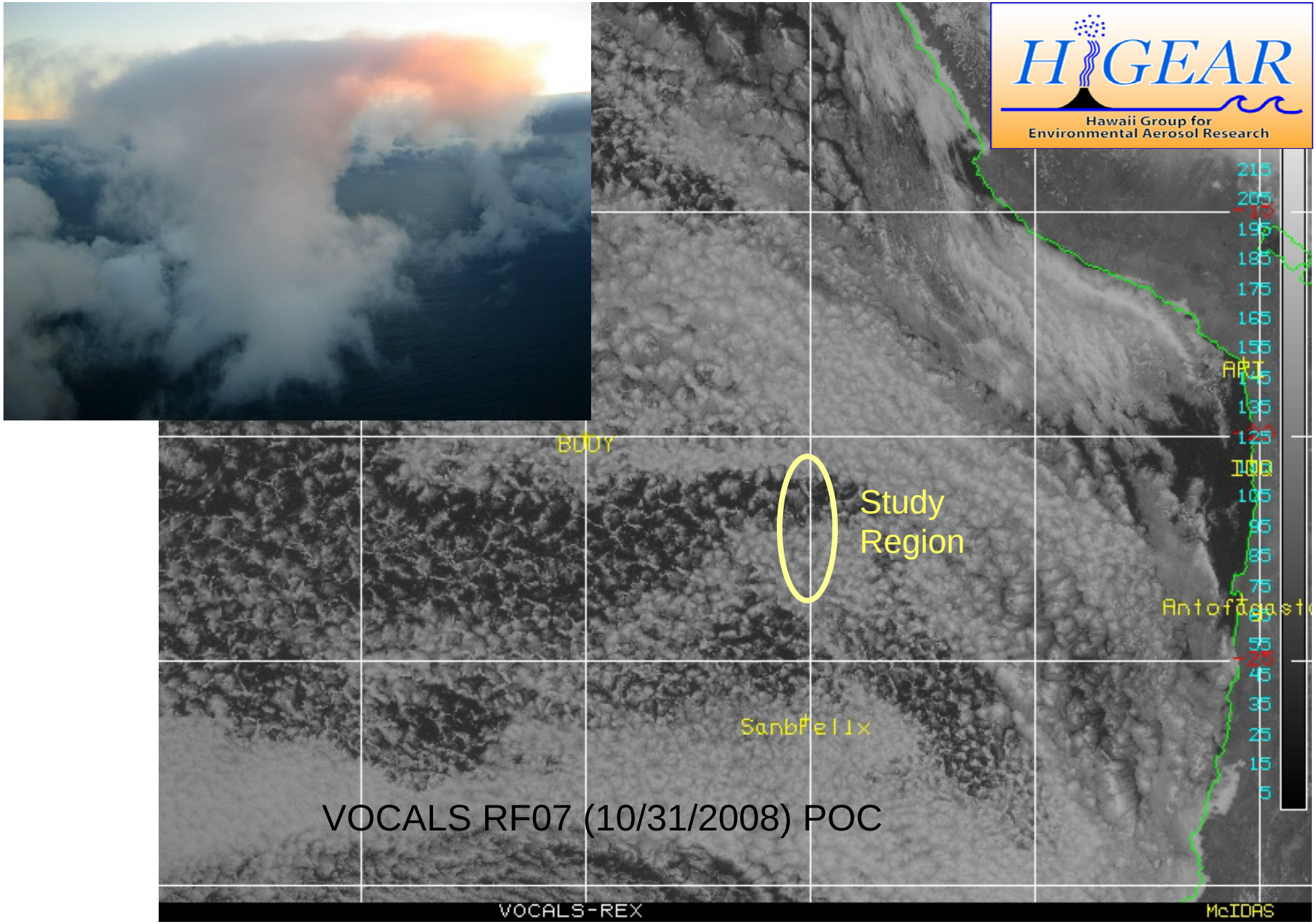

VOCALS RF07 (10/31/2008) POC

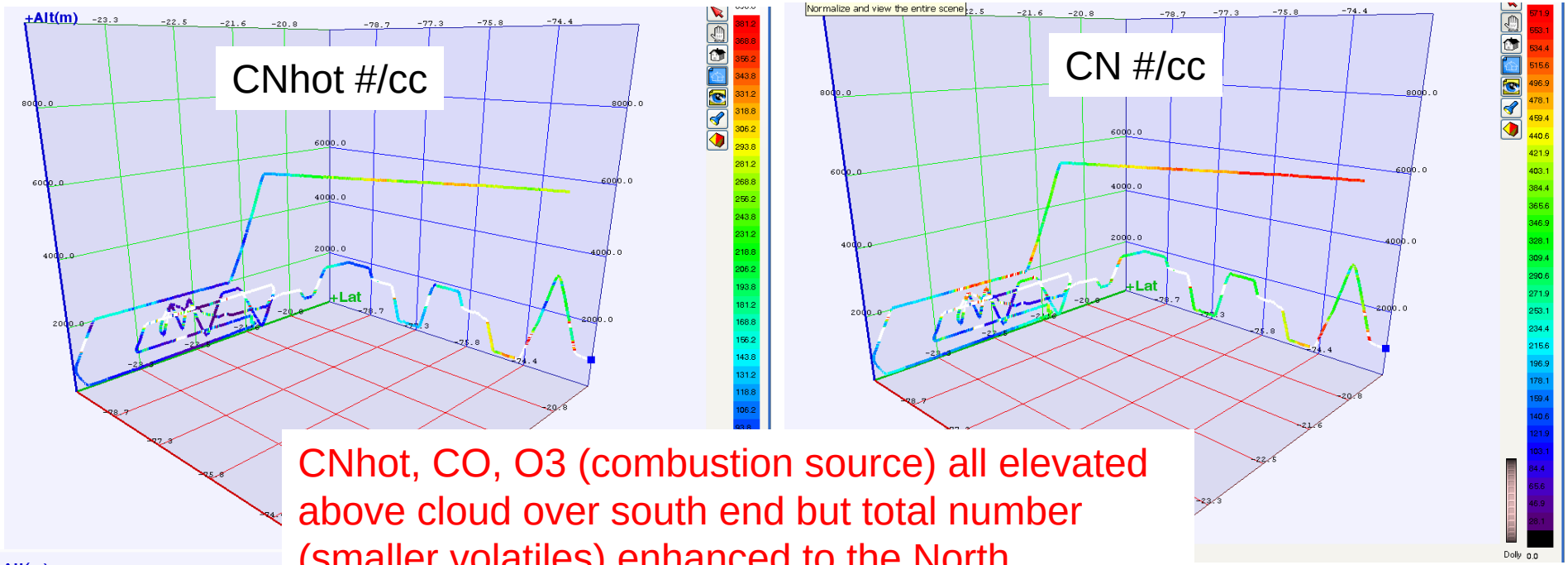

CNhot, CO, O3 (combustion source) all elevated above cloud over south end but total number (smaller volatiles) enhanced to the North

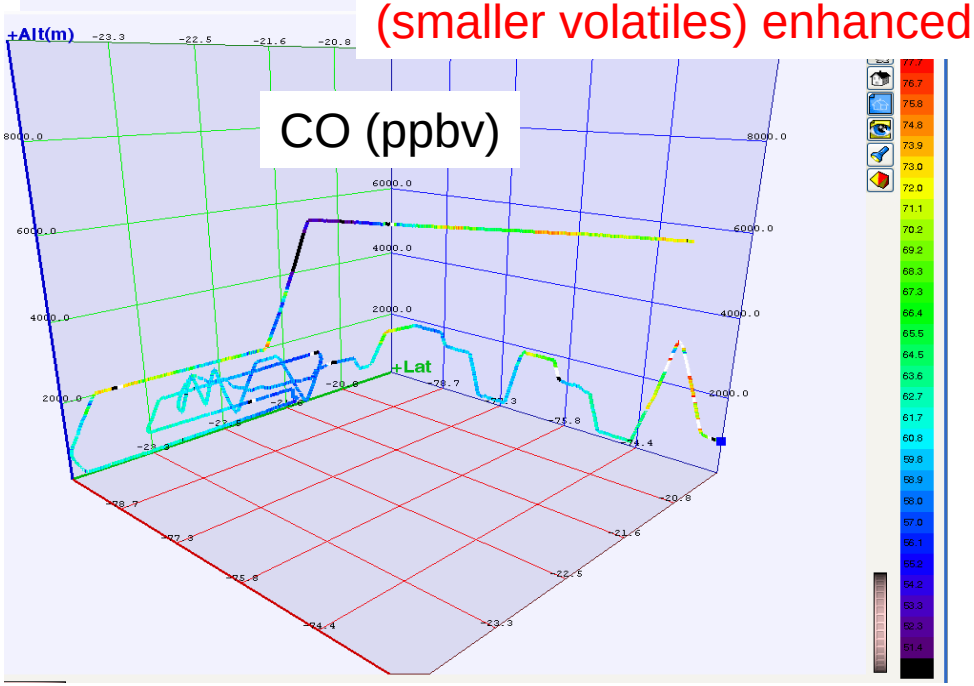

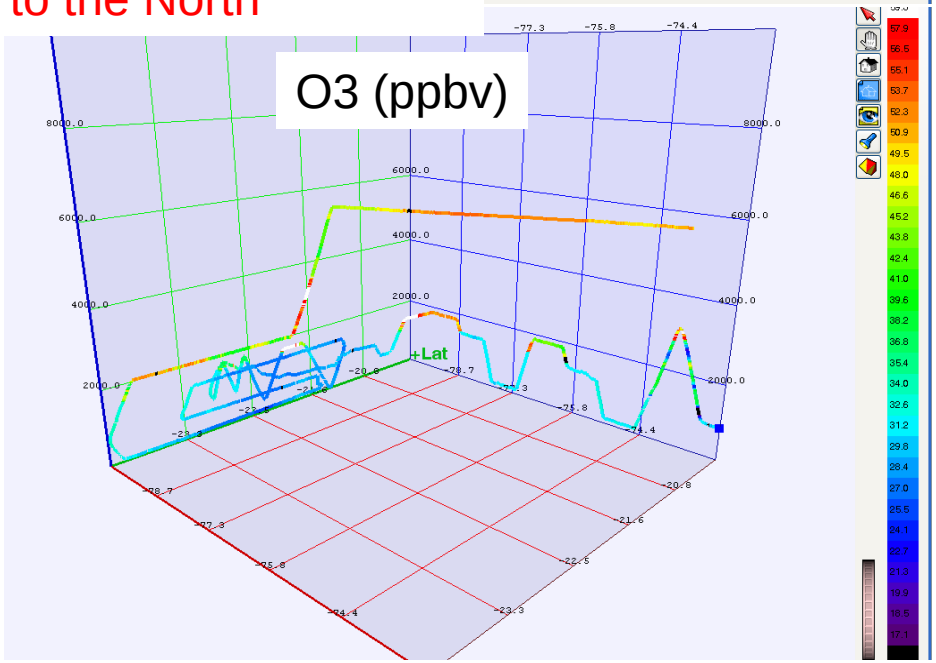

VOCALS RF07 – 10/31/2008 RF07 LDMA distributions

Above cloud – Number increases but mass decreases from South (Cloud) to North (POC)
Cloud Base – Number similar (~30nm Dp) both South and North
Below Cloud – Number increases and mass similar from South to North

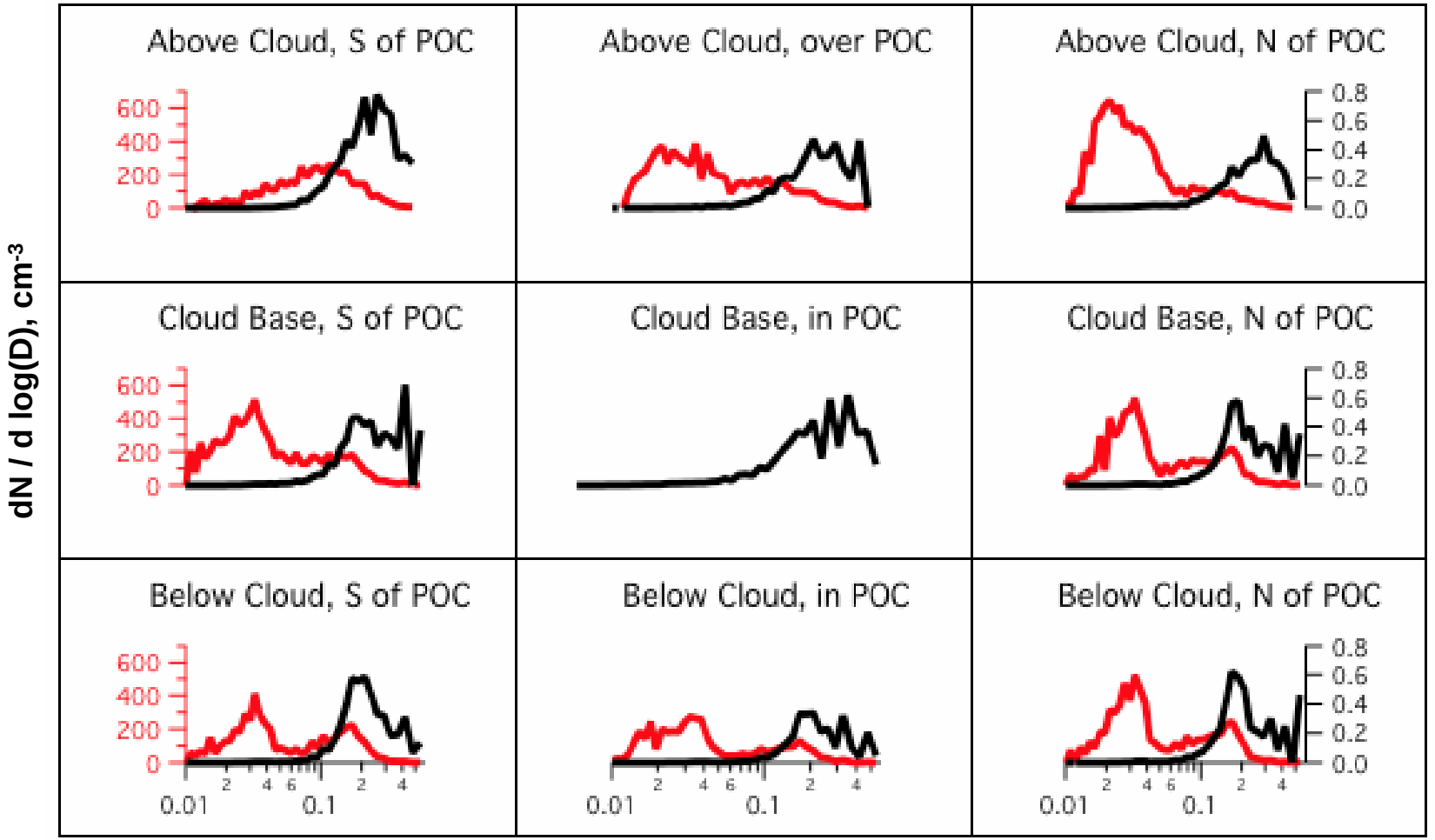

VOCALS RF07 – 10/31/2008 AMS Org/SO4 - Sawtooth series

Organic to Sulfate ratio higher in cloud and aloft than MBL but lowest below cloud

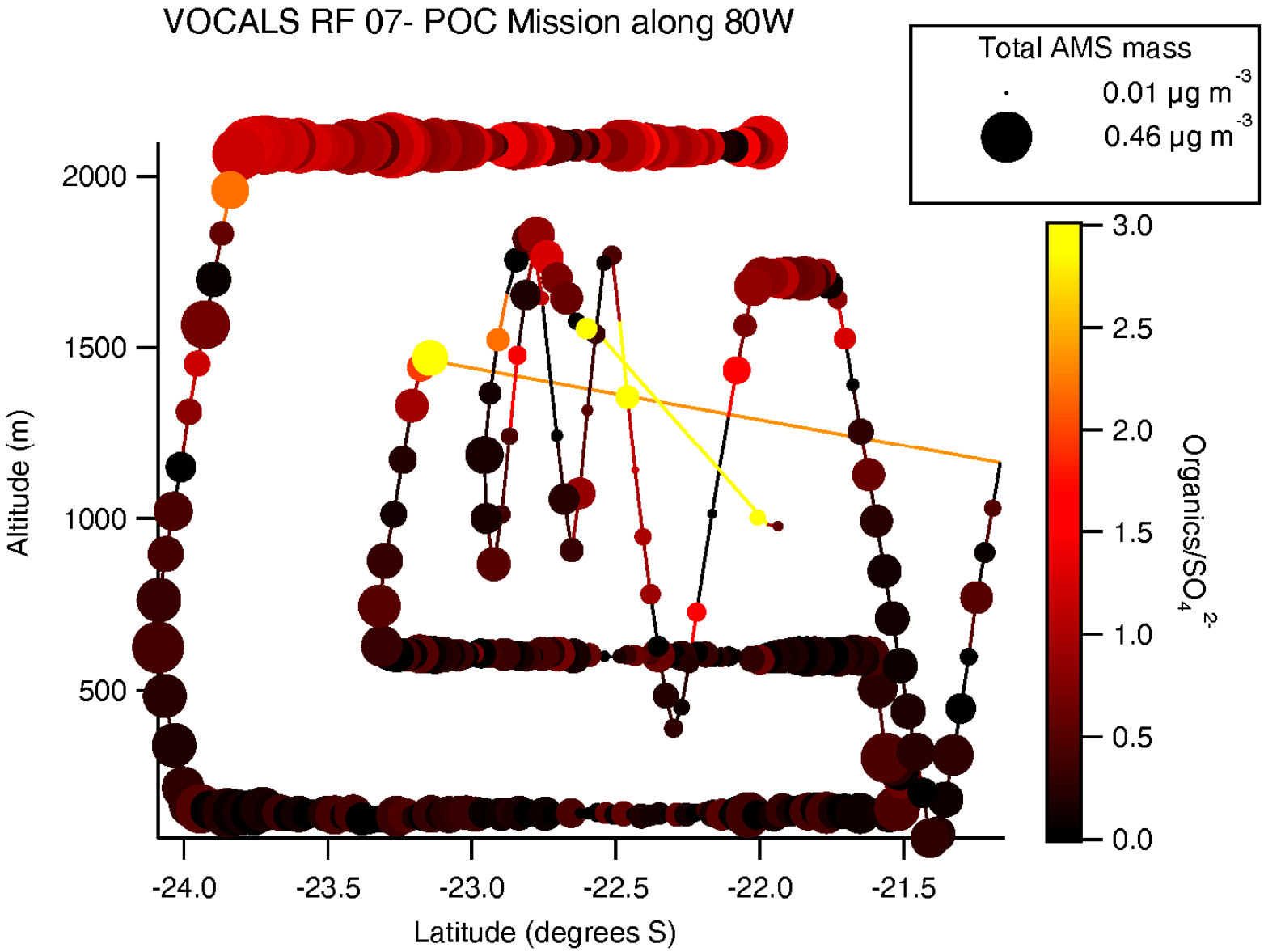

VOCALS RF07 – 10/31/2008 AMS Organics and SO4 - Profiles in POC

Organic and Sulfate concentration higher aloft than MBL and both are lower below cloud and but sulfate higher in the surface mixed layer

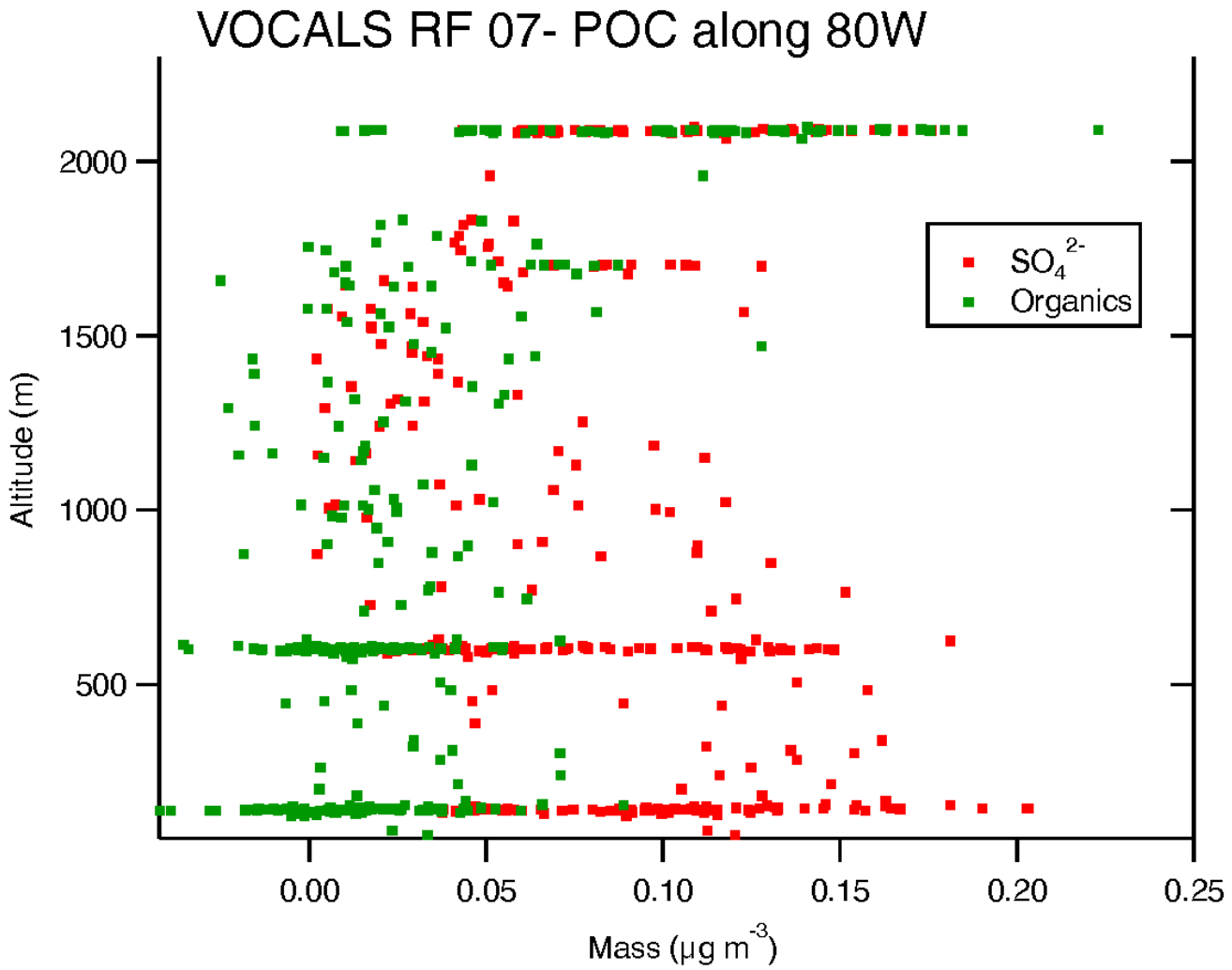

Work in Progress

- Can patchy layers of larger aerosol (potential CCN) associated with elevated CO, O3 stabilize clouds through entrainment?
- Is entrainment of aerosol from regions aloft with smaller sizes (and poor CCN) related to POC development?
- How is partitioning of Organic and Sulfate aerosol linked to boundary layer processes and CCN?
- How important is Black Carbon aerosol in establishing accumulation mode number and sizes effective as CCN?

Dynamics of a POCS and its surroundings

Jorgen Jensen and David Leon

Objective:

To use measurements of pressure perturbations to calculate the across-track component of the geostrophic wind.

Caveat:

Further calculations are necessary to estimate the effect of friction and rotation in predicting the across-track component of the wind.

Case study:

VOCALS RF06, 09:10:00 – 09:38:00

Method

LeMone and Tarleton (1986, JAS) define the D-value as:

$$D = z_{ac} - z_{pres}$$

Thus the pressure perturbation along the flight track is:

$$p' = (D - D_{bar}) \times \rho_{air} \times g$$

The geostrophic wind component, V_g, across the flight track is then:

$$V_g = - 1 / (f \times \rho_{air}) \times \Delta p' / \Delta x$$

This can be compared to the across-track component of the observed wind, VYC.

The POC is SSW of the main cloud band (85-110 km), the so-called Albrecht Machine.

UXC is the along-track component of the measured wind, and C_t is the along-track convergence.

VYC is the across-track component of the measured wind, and V_g is the component of the geostrophic wind across the flight track.

V_g is about 13 m/s, whereas VYC is only 10.5 m/s.

The hypothesis (yet to be tested) is that the high-pressure in the POC is so strong that it creates a pressure gradient with a geostrophic wind exceeding the observed wind; i.e. the POC is forcing a system that is not in balance with the POC forcing.

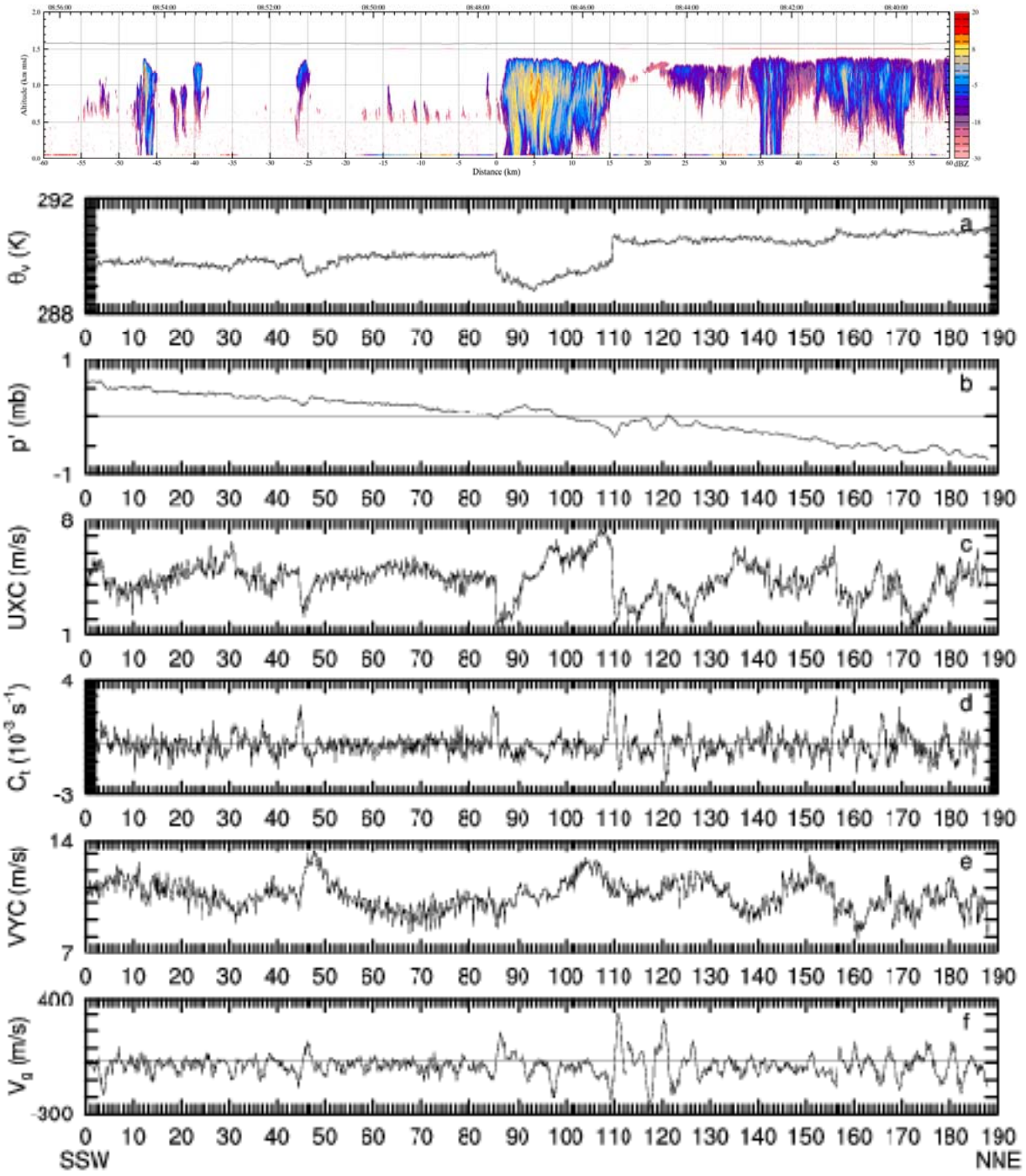

J. Anderson
SEM generated size distributions for Giant Nuclei Impactor Slides from RF7, a POC mission.

Comments: These are raw size distributions from a subset of the GNI samples collected by Jorgen Jensen. I will later calculate the absolute concentrations for these samples, but have not yet done so. The lower size cut on the GNI is determined by the aircraft air speed and is around 1 micron diameter. Roughly 1000 particles were analyzed in each sample, filtered so that the minimum size analyzed was 1 micron.

The sizes reported are average diameters (average of maximum and minimum diameters), reported in microns for dry particles. While most of these are sea salt, some of the large ones are biogenic. My X-ray detector failed a couple of months back and I'm waiting for a new one to be delivered and installed. When the new X-ray detector is in place I will redo all of these, so please don't use these preliminary data for anything other than to get an idea about supermicron particle size distributions. There is no lack of large particles in the subcloud runs at 500'. The one surprise is the presence of similar large particles in a clear patch during a cloud run at 4800' (but not necessarily at the same absolute concentrations for the 500' samples).

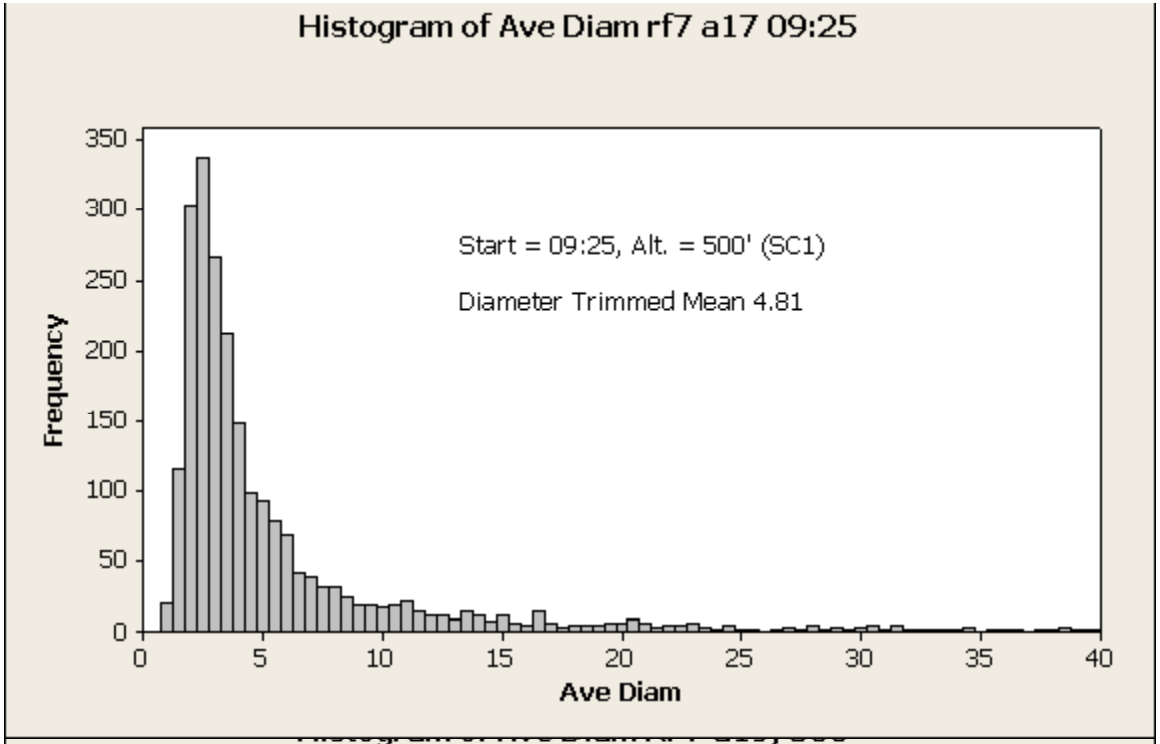

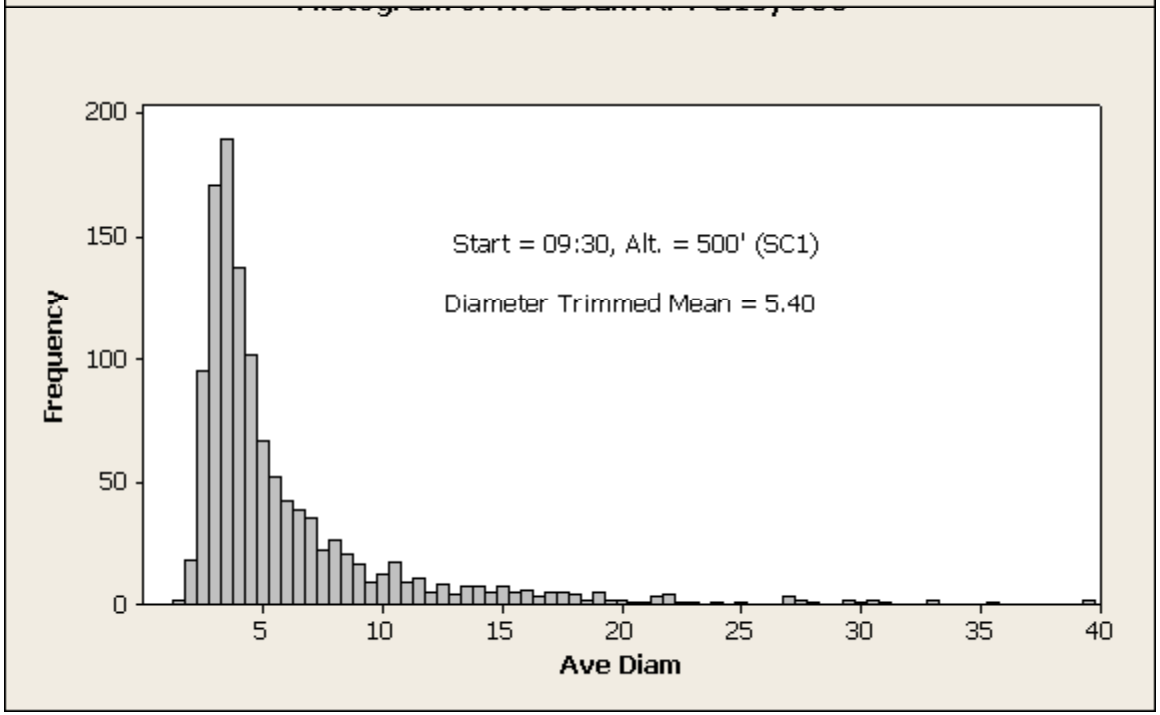

RF07, subcloud run 1

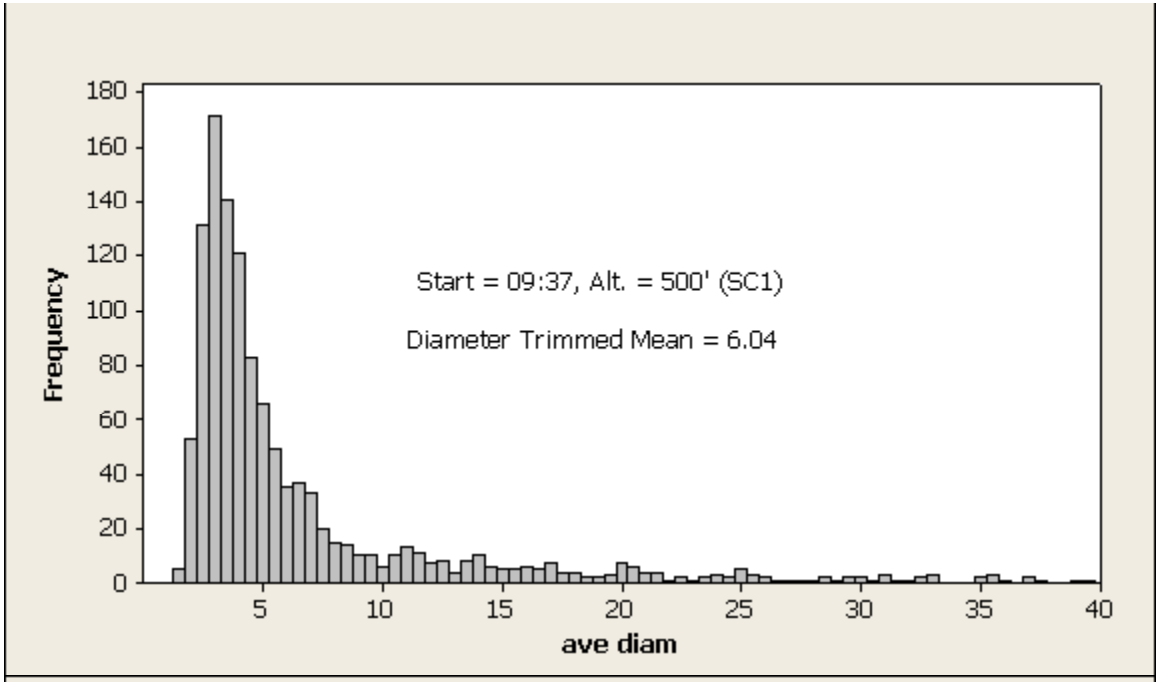

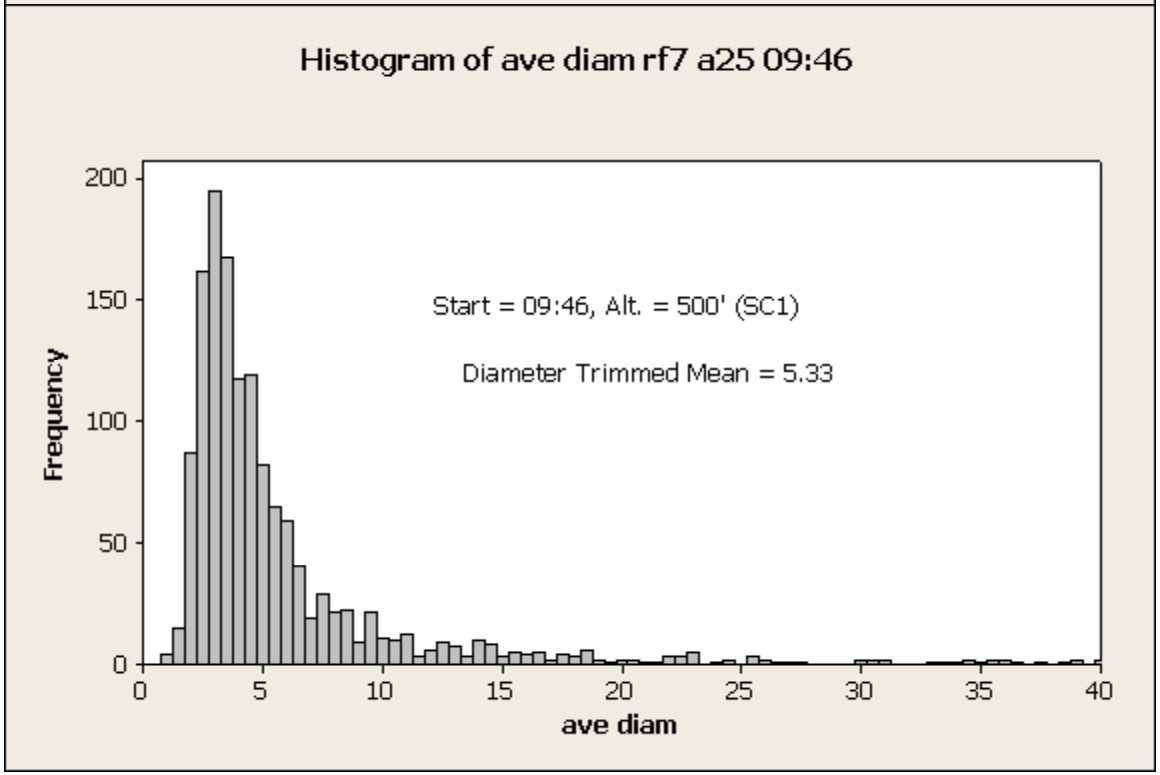

RF07, subcloud run 1, continued

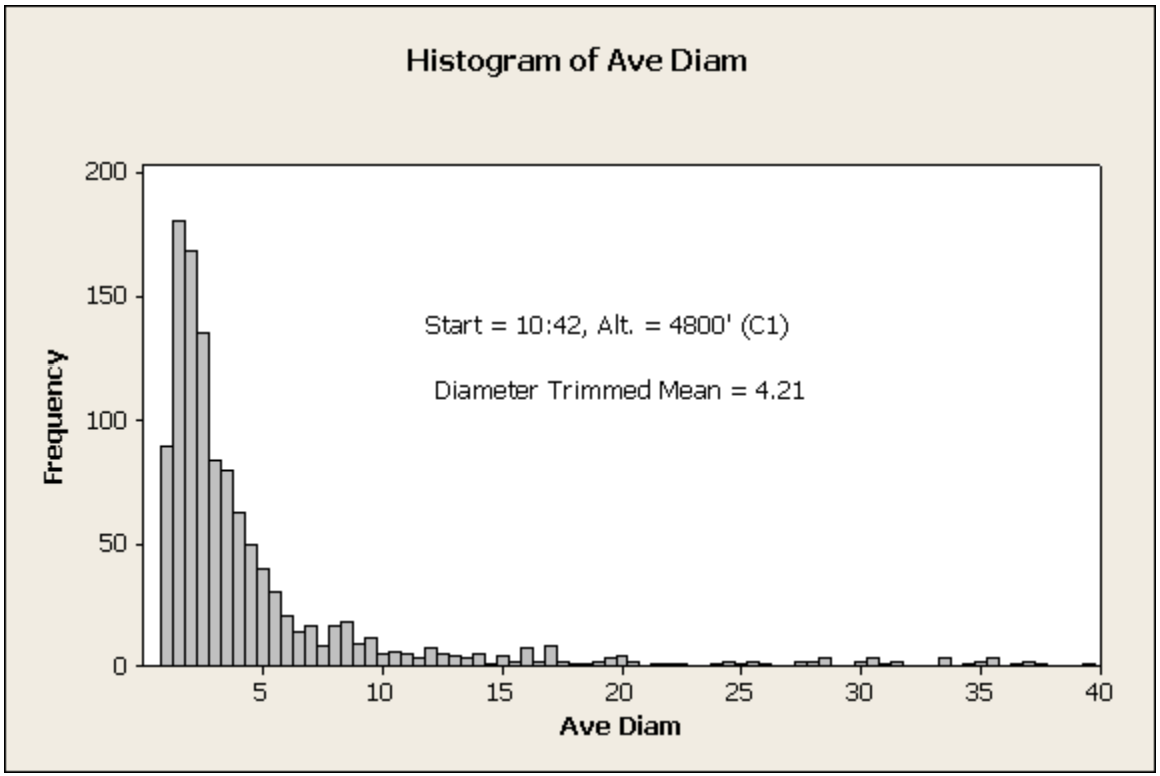

RF07, cloud run 1 (open area)

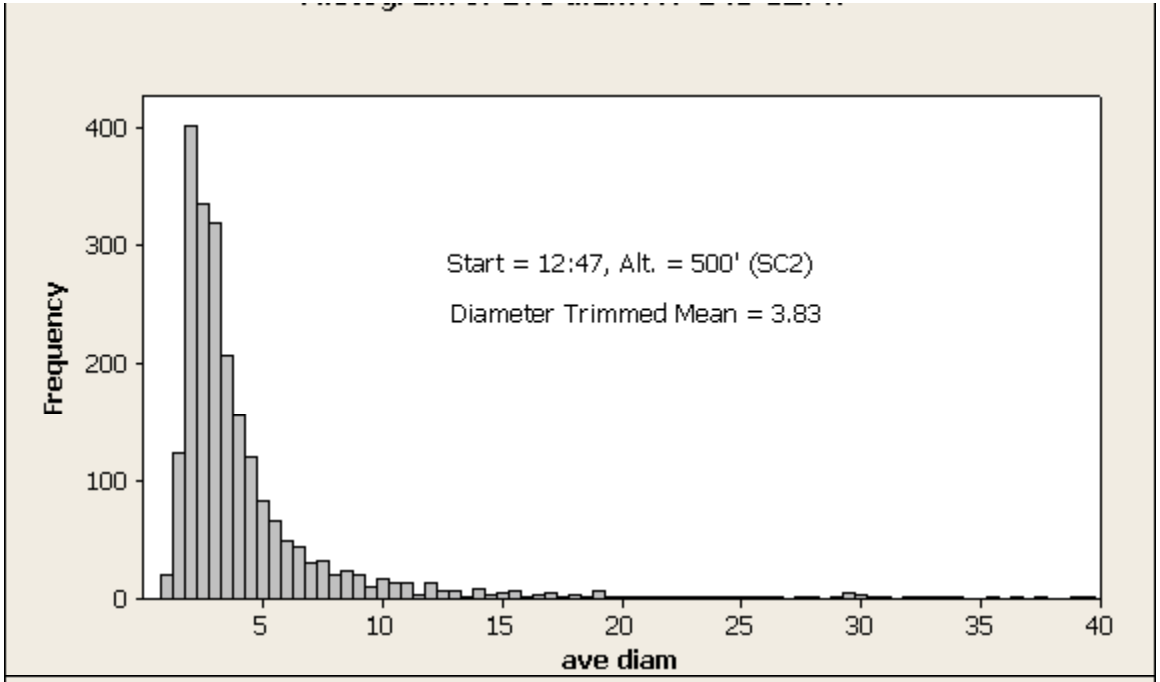

Subcloud run 2

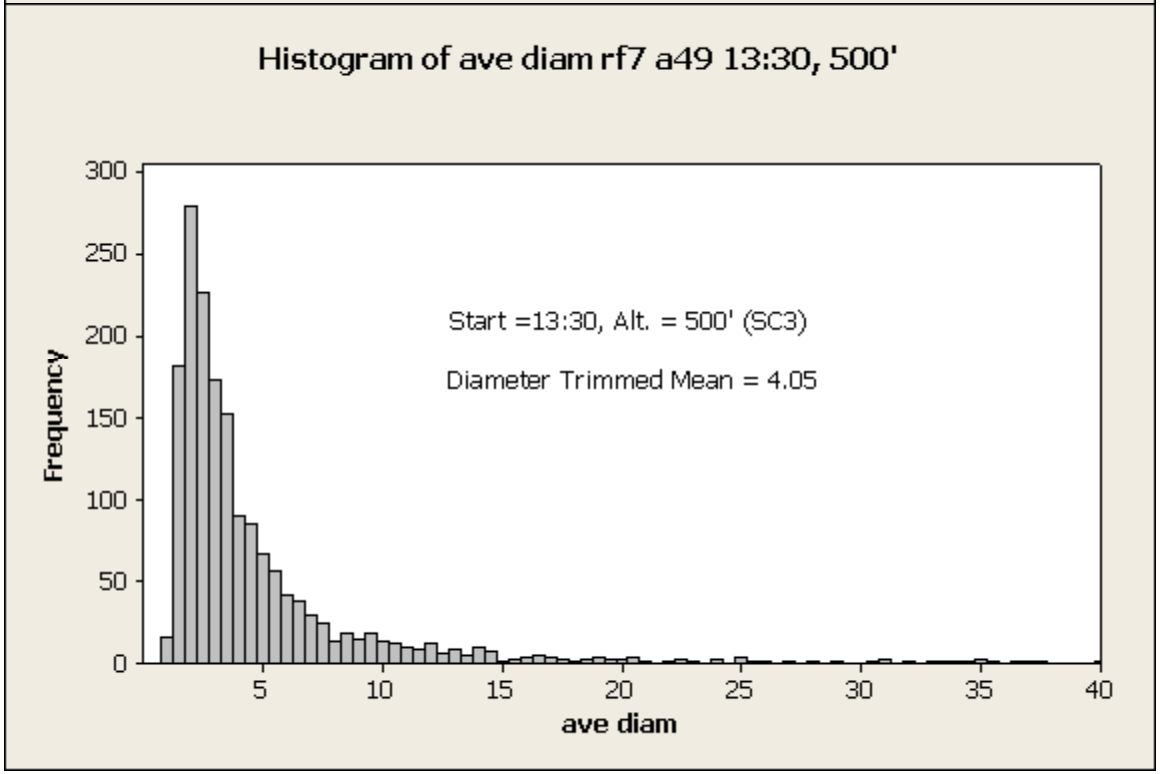

Subcloud run 3

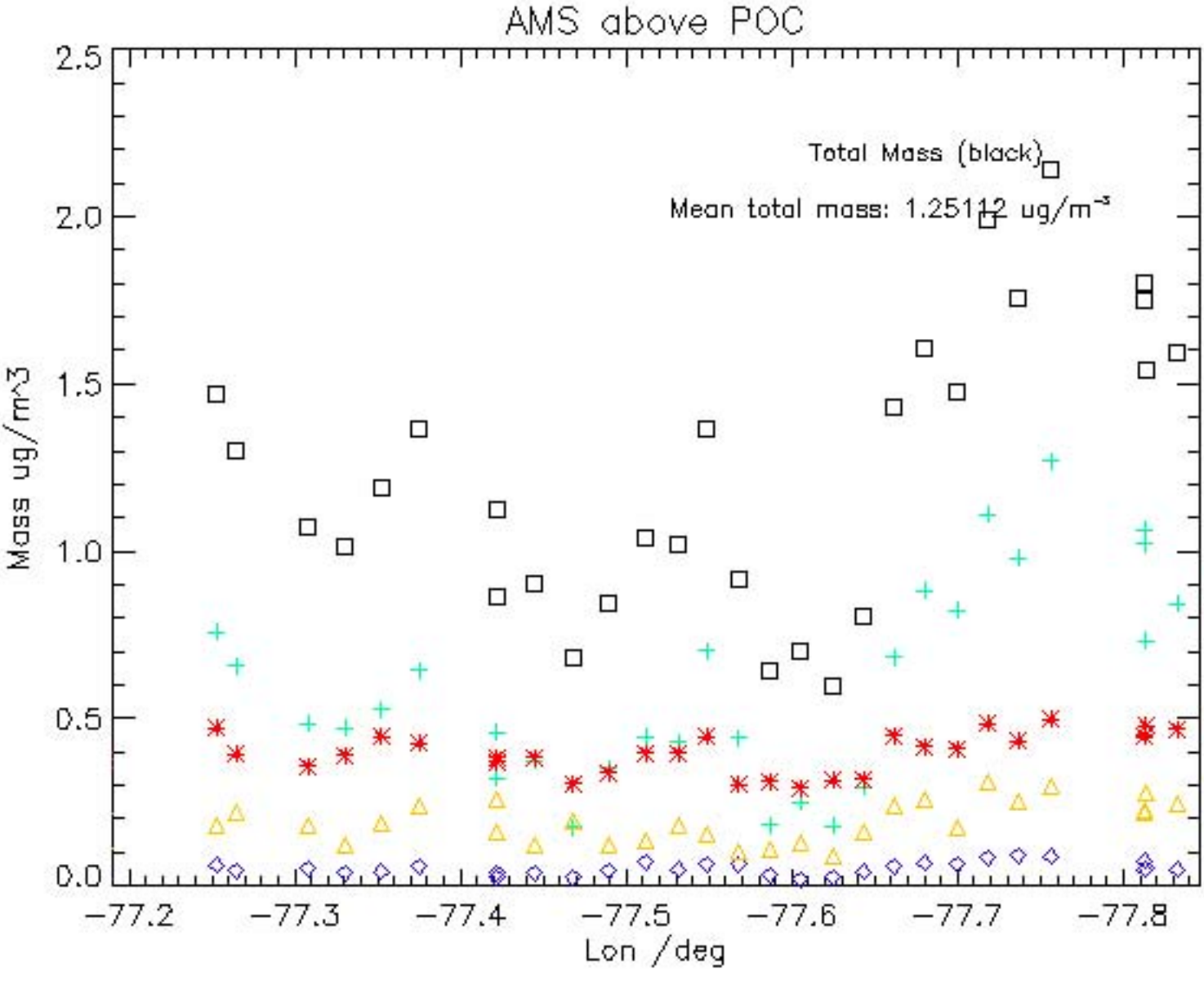
AMS above POC
Total Mass (black)
Mean total mass: 1.25112 ug/m^-3
Mass ug/m^3
Lon /deg
2.5
2.0
1.5
1.0
0.5
0.0
-77.2
-77.3
-77.4
-77.5
-77.6
-77.7
-77.8

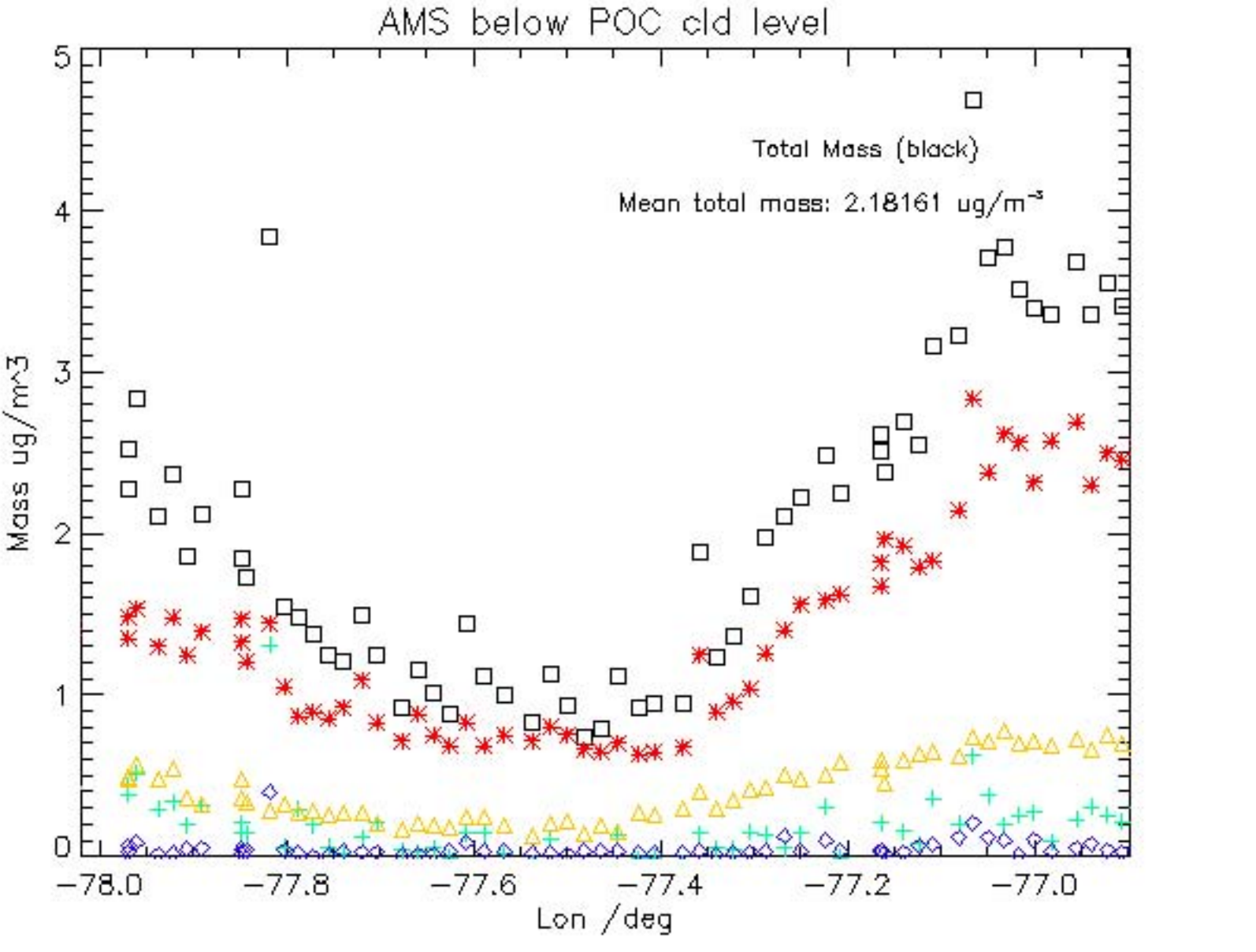
AMS below POC cld level
Total Mass (black)
Mean total mass: 2.18161 ug/m-3
Mass ug/m^3
Lon /deg
0
1
2
3
4
5
−78.0
−77.8
−77.6
−77.4
−77.2
−77.0

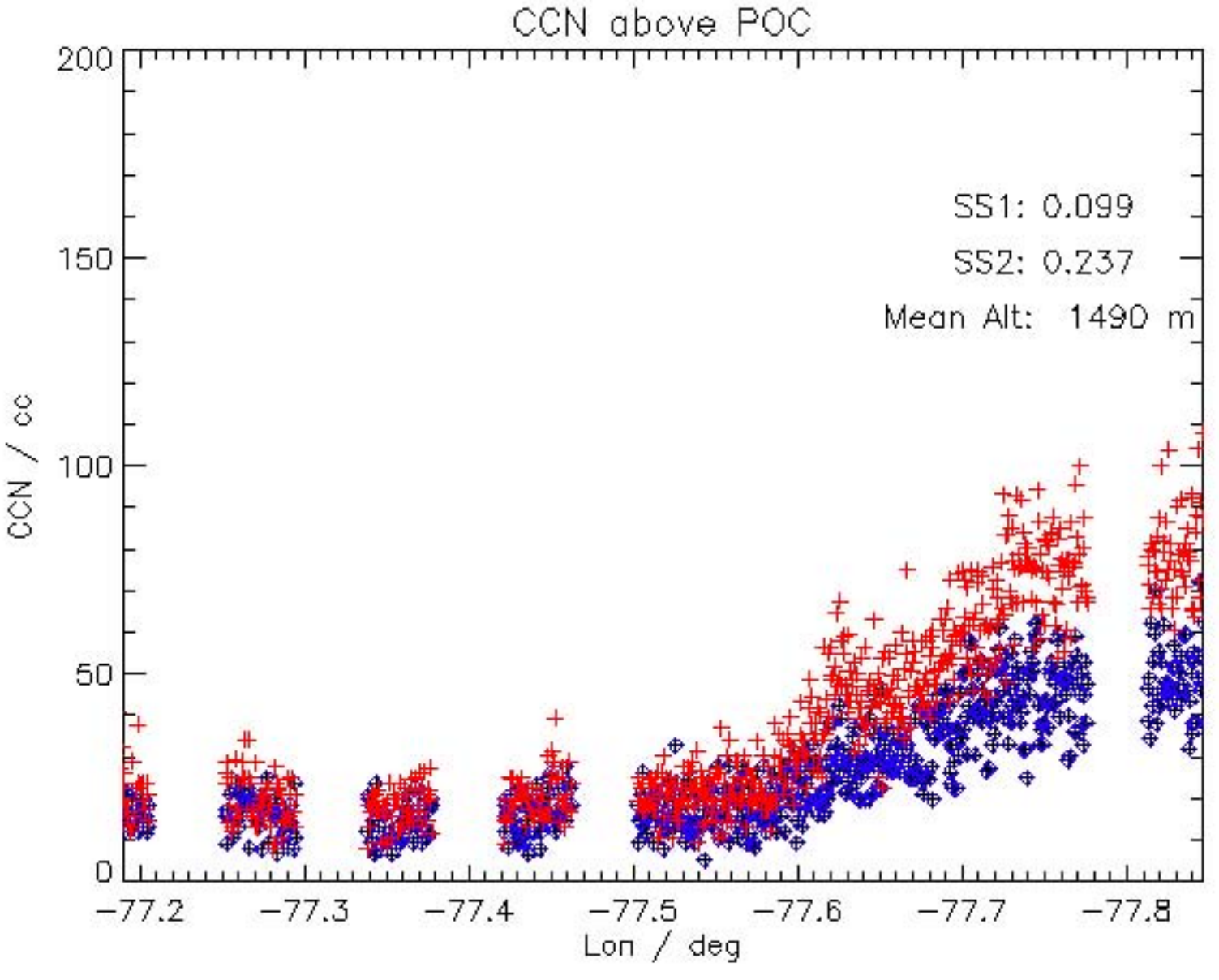
CCN above POC
SS1: 0.099
SS2: 0.237
Mean Alt: 1490 m
CCN / cc
200
150
100
50
0
−77.2
−77.3
−77.4
−77.5
−77.6
−77.7
−77.8
Lon / deg

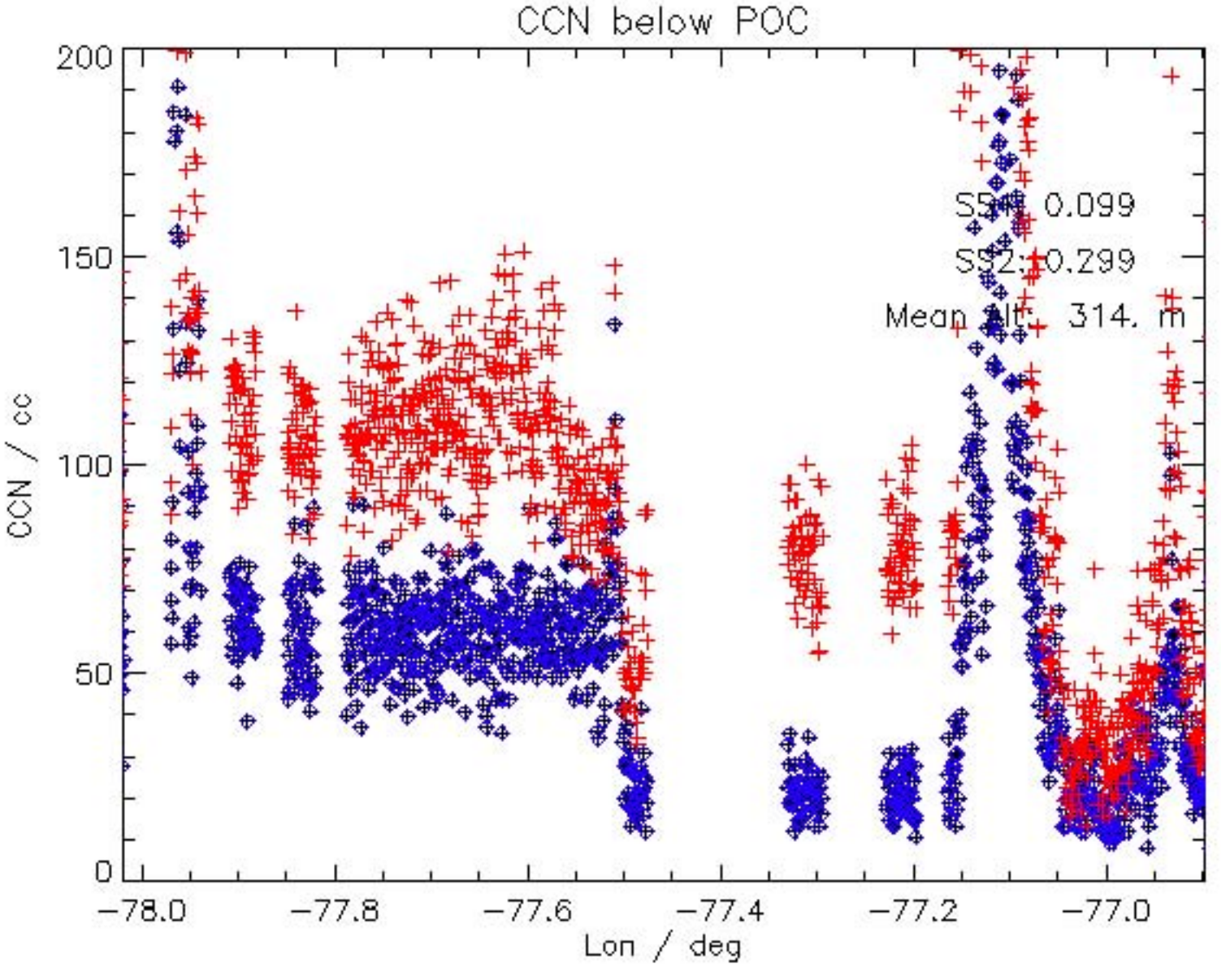
CCN below POC
SS1: 0.099
SS2: 0.299
Mean Alt: 314. m
CCN / cc
Lon / deg
200
150
100
50
0
−78.0
−77.8
−77.6
−77.4
−77.2
−77.0

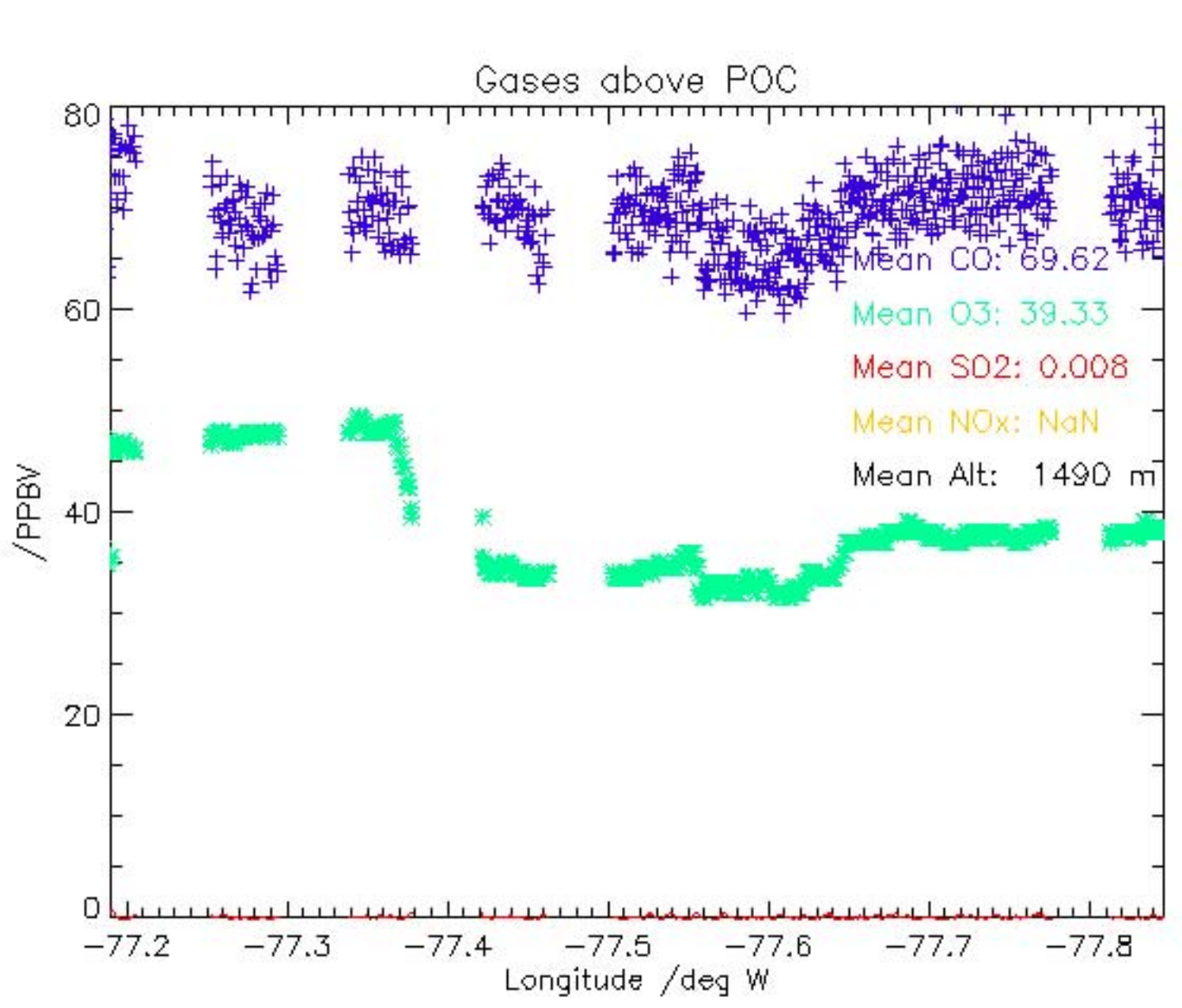
Gases above POC
Mean CO: 69.62
Mean O3: 39.33
Mean SO2: 0.008
Mean NOx: NaN
Mean Alt: 1490 m
/PPBV
80
60
40
20
0
−77.2
−77.3
−77.4
−77.5
−77.6
−77.7
−77.8
Longitude /deg W

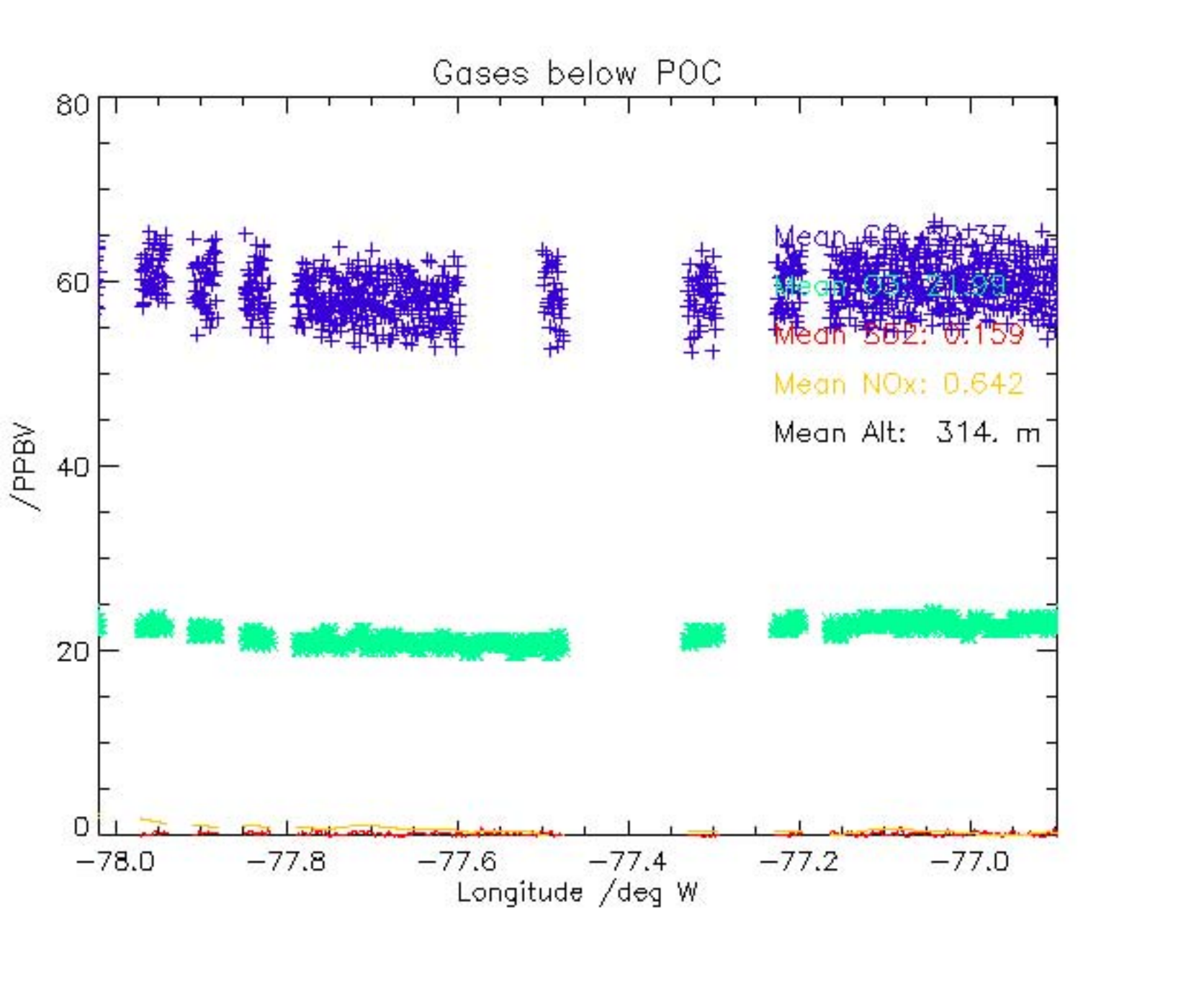
Gases below POC
80
60
40
20
0
/PPBV
Mean CO: 64.37
Mean O3: 21.98
Mean SO2: 0.159
Mean NOx: 0.642
Mean Alt: 314. m
−78.0
−77.8
−77.6
−77.4
−77.2
−77.0
Longitude /deg W

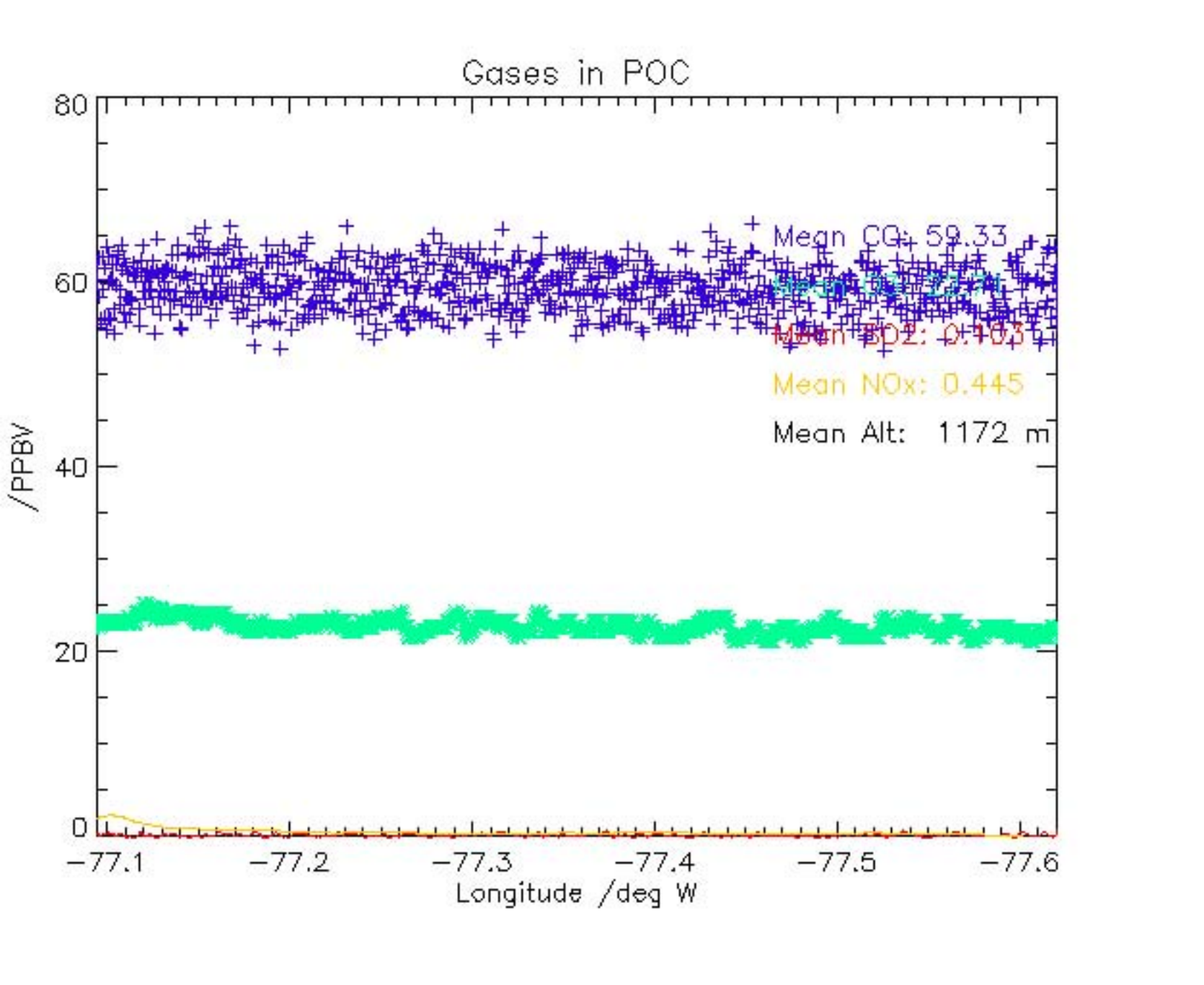
Gases in POC
80
60
40
20
0
/PPBV
Mean CO: 59.33
Mean SO2: 0.103
Mean NOx: 0.445
Mean Alt: 1172 m
−77.1
−77.2
−77.3
−77.4
−77.5
−77.6
Longitude /deg W

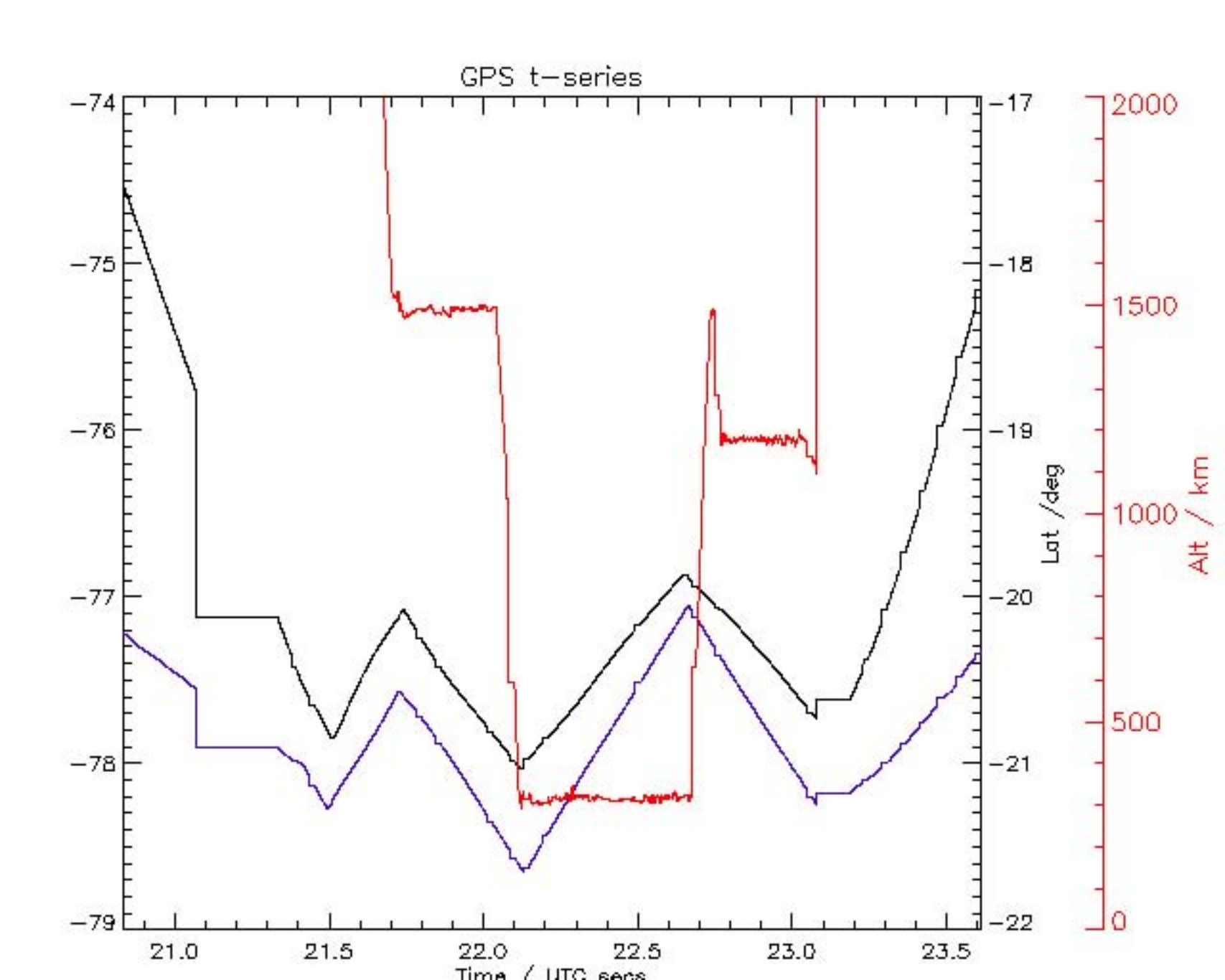
GPS t−series
−74
−75
−76
−77
−78
−79
−17
−18
−19
−20
−21
−22
2000
1500
1000
500
0
Lat /deg
Alt / km
21.0
21.5
22.0
22.5
23.0
23.5
Time / UTC secs

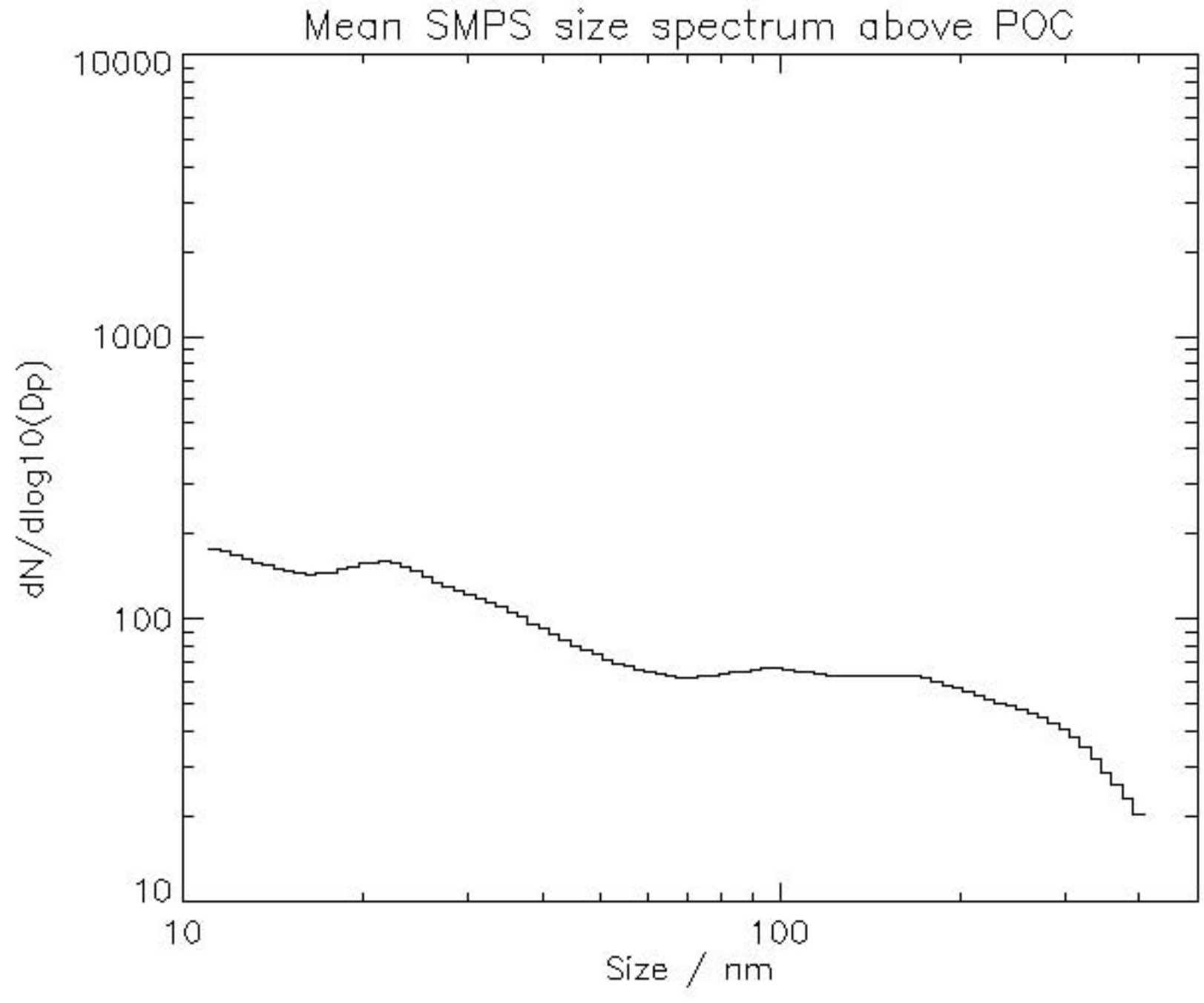
Mean SMPS size spectrum above POC
10000
1000
100
10
dN/dlog10(Dp)
10
100
Size / nm

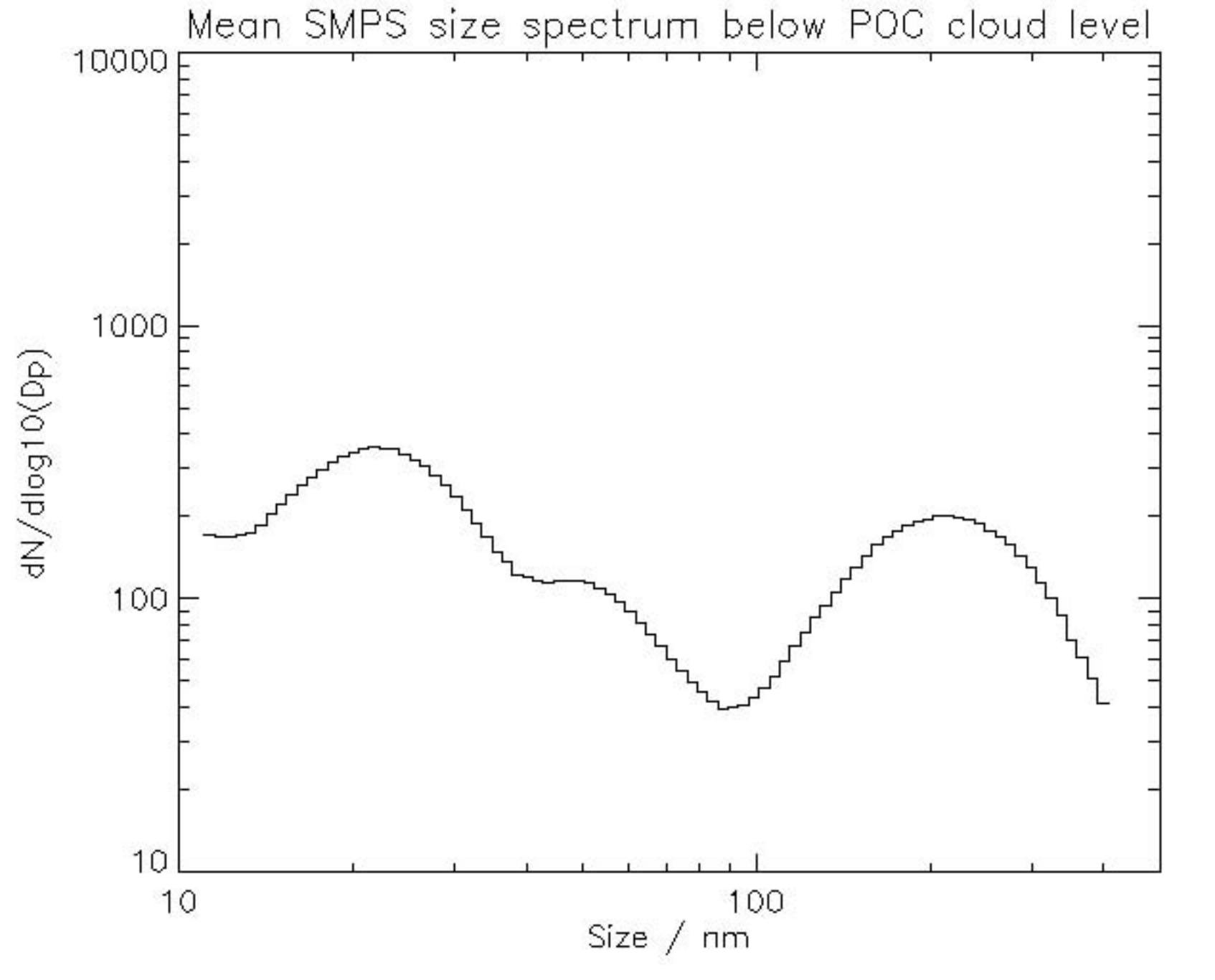
Mean SMPS size spectrum below POC cloud level
10000
1000
100
10
dN/dlog10(Dp)
10
100
Size / nm

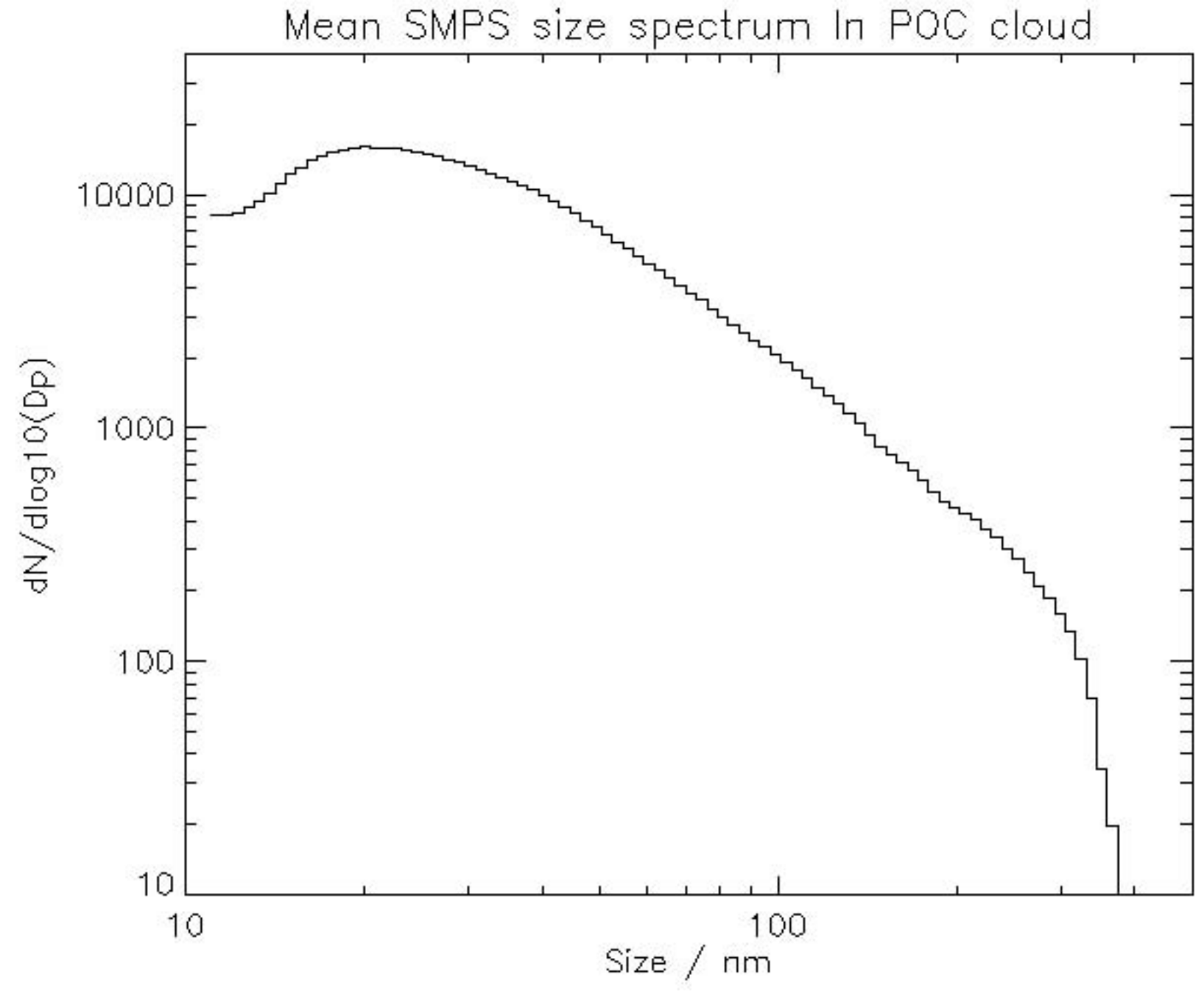
Mean SMPS size spectrum In POC cloud
10000
1000
100
10
dN/dlog10(Dp)
10
100
Size / nm

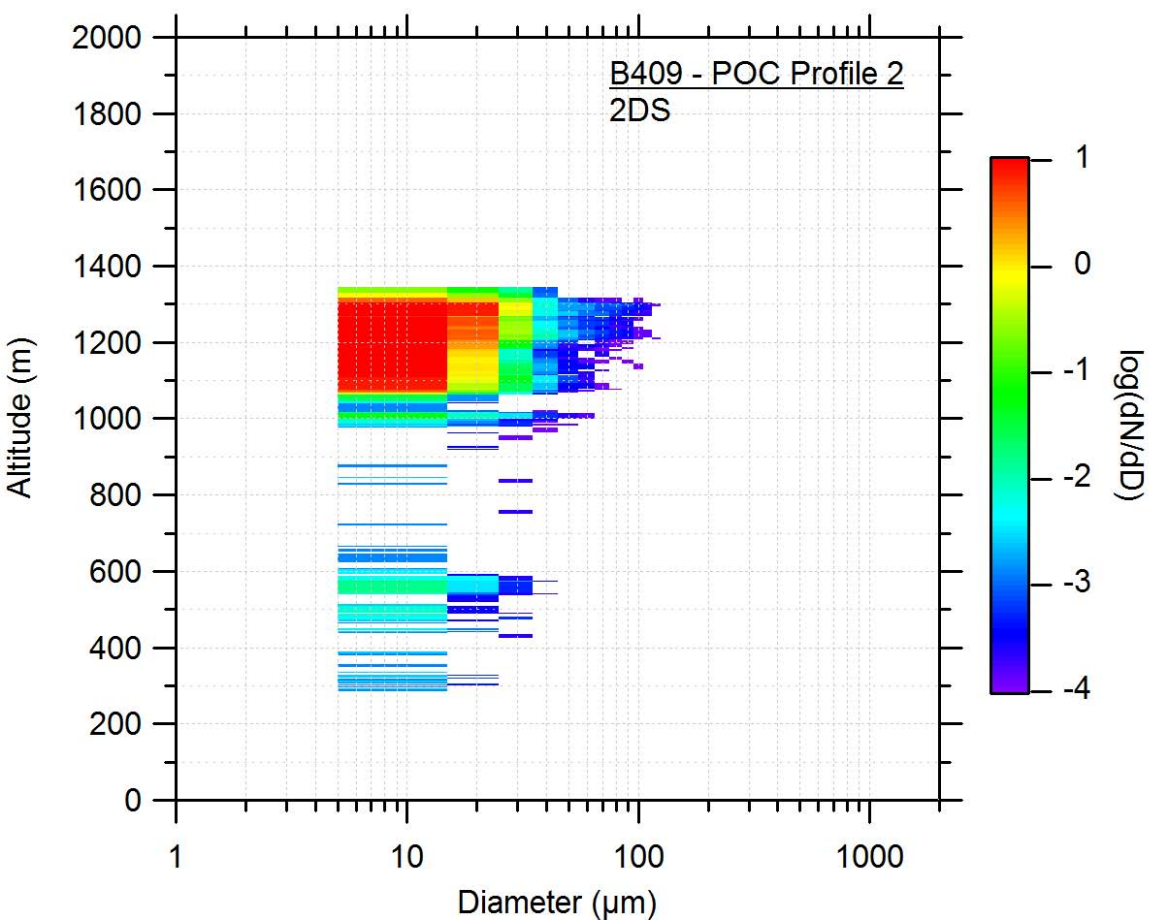
B409 - POC Profile 2
2DS
Altitude (m)
2000
1800
1600
1400
1200
1000
800
600
400
200
0
1
10
100
1000
Diameter (µm)
log(dN/dD)
1
0
-1
-2
-3
-4

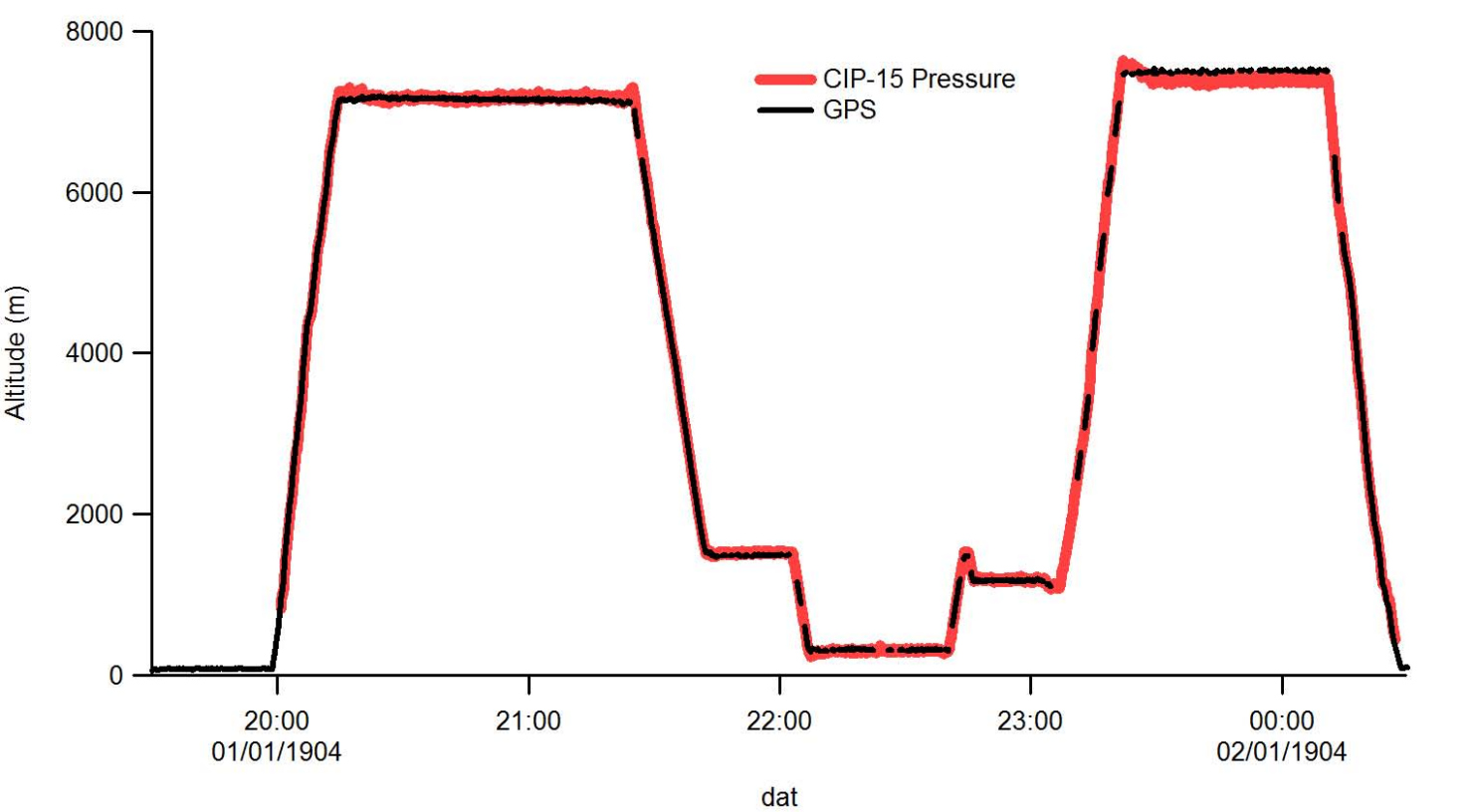
8000
6000
4000
2000
0
Altitude (m)
CIP-15 Pressure
GPS
20:00
01/01/1904
21:00
22:00
23:00
00:00
02/01/1904
dat

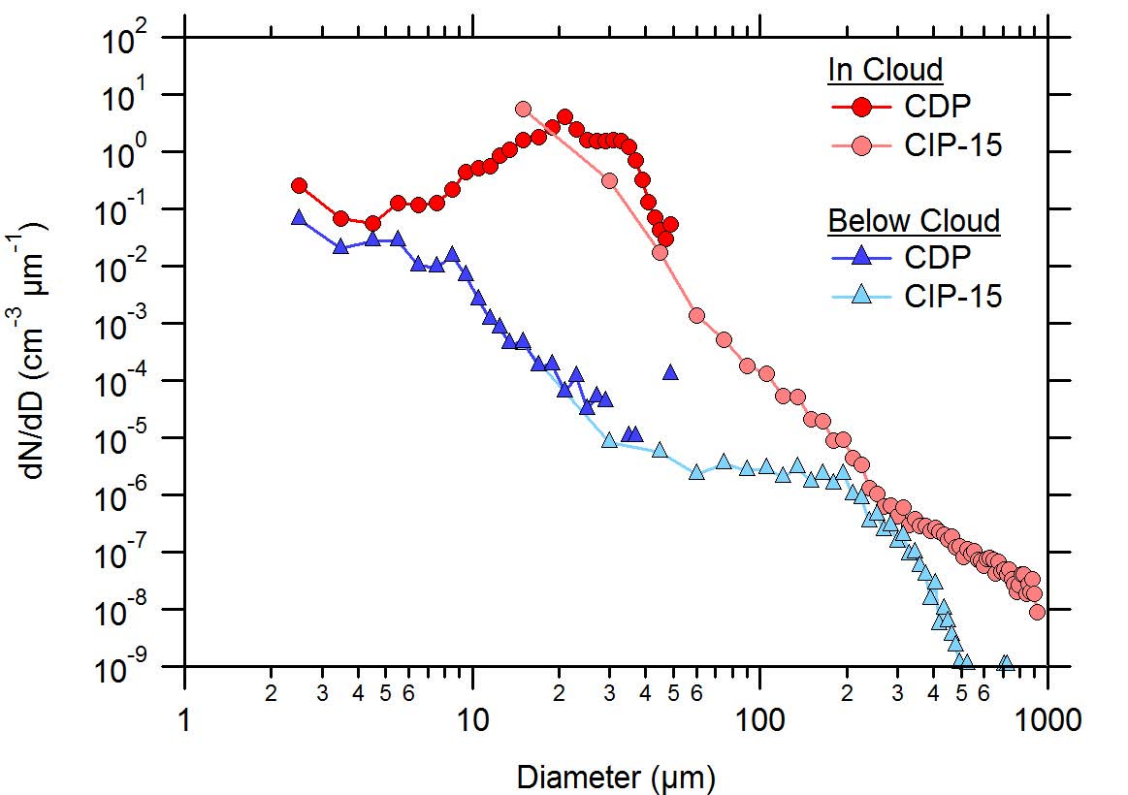
In Cloud
CDP
CIP-15
Below Cloud
CDP
CIP-15
dN/dD (cm-3 µm-1)
Diameter (µm)
10^2
10^1
10^0
10^-1
10^-2
10^-3
10^-4
10^-5
10^-6
10^-7
10^-8
10^-9
1
2
3
4
5
6
10
2
3
4
5
6
100
2
3
4
5
6
1000

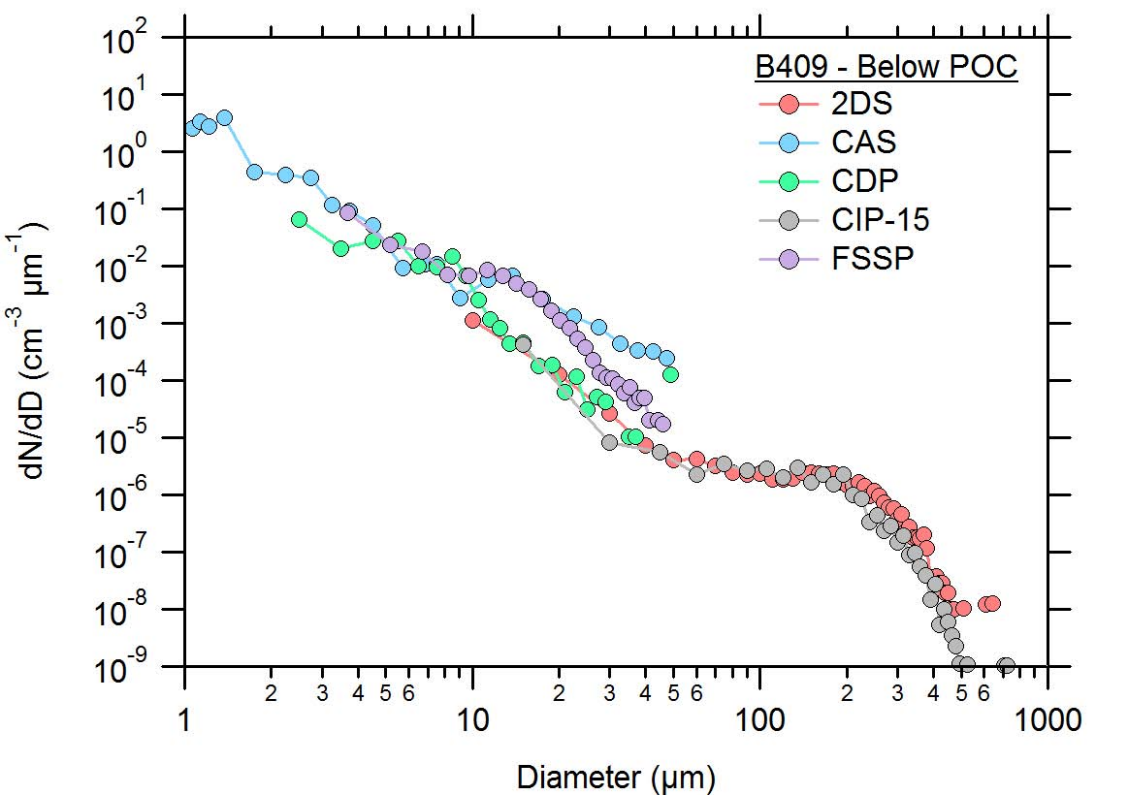
B409 - Below POC
2DS
CAS
CDP
CIP-15
FSSP
dN/dD (cm-3 µm-1)
Diameter (µm)
10^2
10^1
10^0
10^-1
10^-2
10^-3
10^-4
10^-5
10^-6
10^-7
10^-8
10^-9
1
2
3
4
5
6
10
2
3
4
5
6
100
2
3
4
5
6
1000

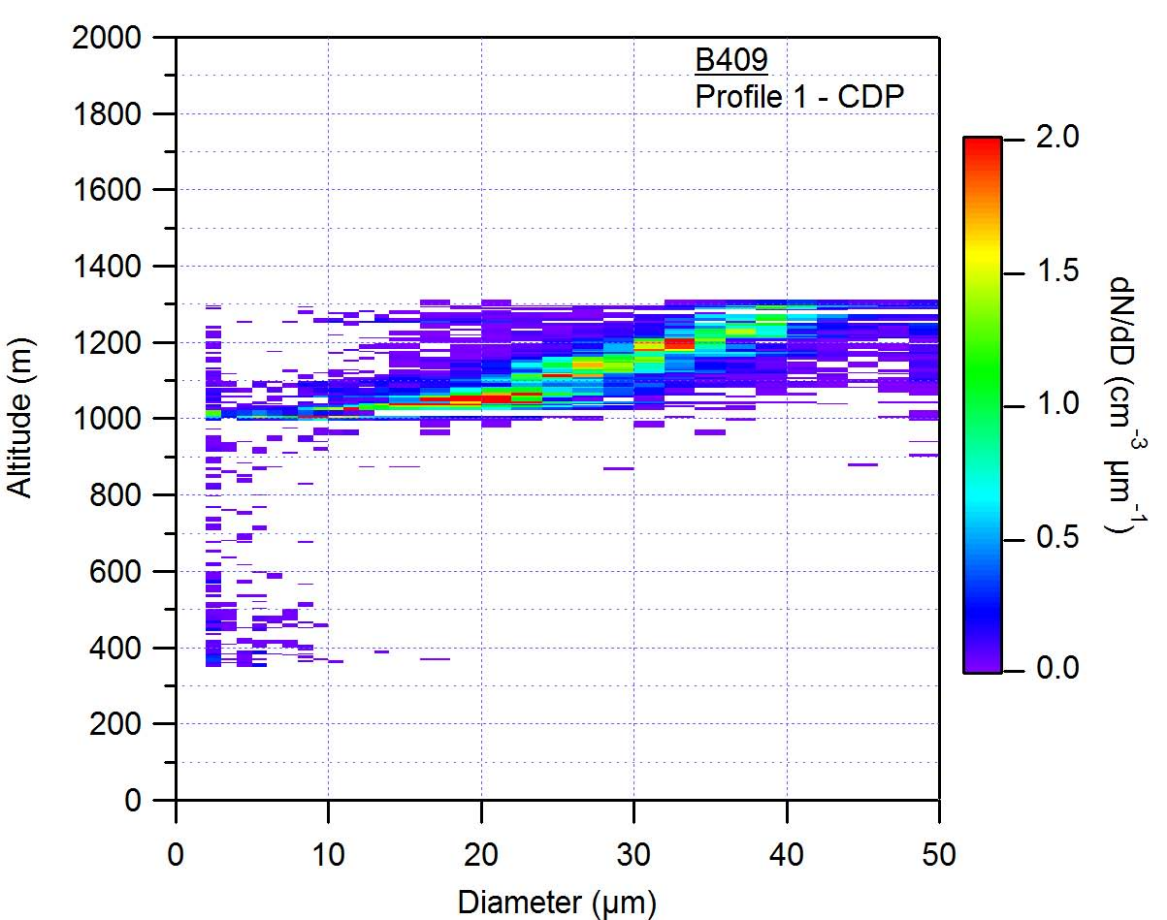
B409
Profile 1 - CDP
Altitude (m)
2000
1800
1600
1400
1200
1000
800
600
400
200
0
0
10
20
30
40
50
Diameter (µm)
2.0
1.5
1.0
0.5
0.0
dN/dD (cm-3 µm-1)

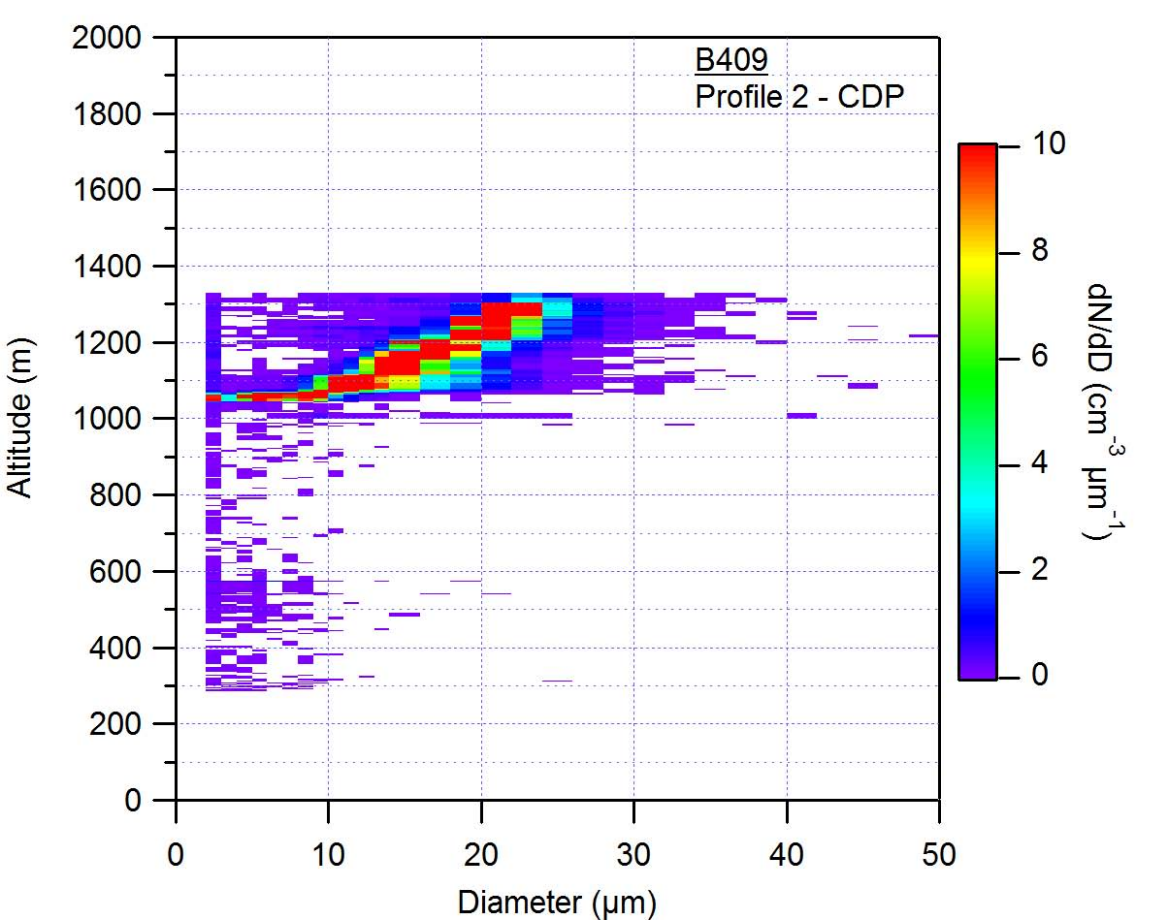
B409
Profile 2 - CDP
Altitude (m)
2000
1800
1600
1400
1200
1000
800
600
400
200
0
0
10
20
30
40
50
Diameter (µm)
dN/dD (cm-3 µm-1)
10
8
6
4
2
0

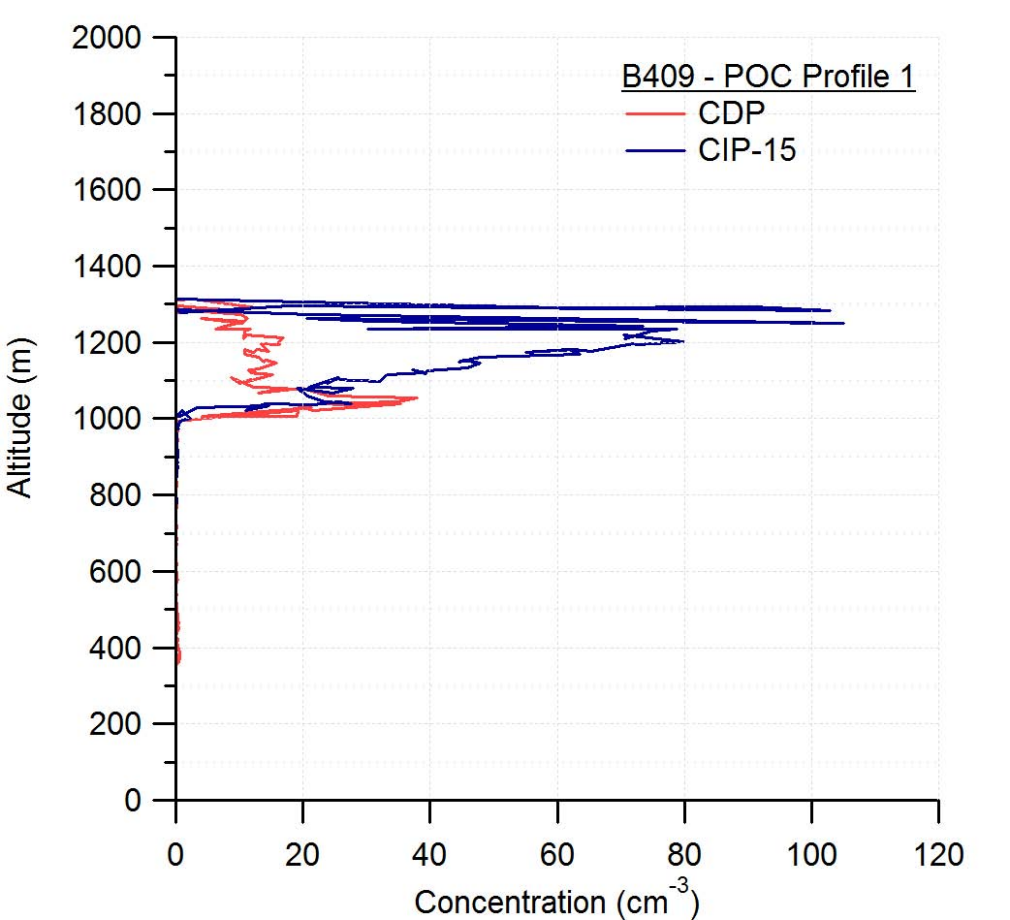
B409 - POC Profile 1
CDP
CIP-15
Altitude (m)
2000
1800
1600
1400
1200
1000
800
600
400
200
0
0
20
40
60
80
100
120
Concentration (cm-3)

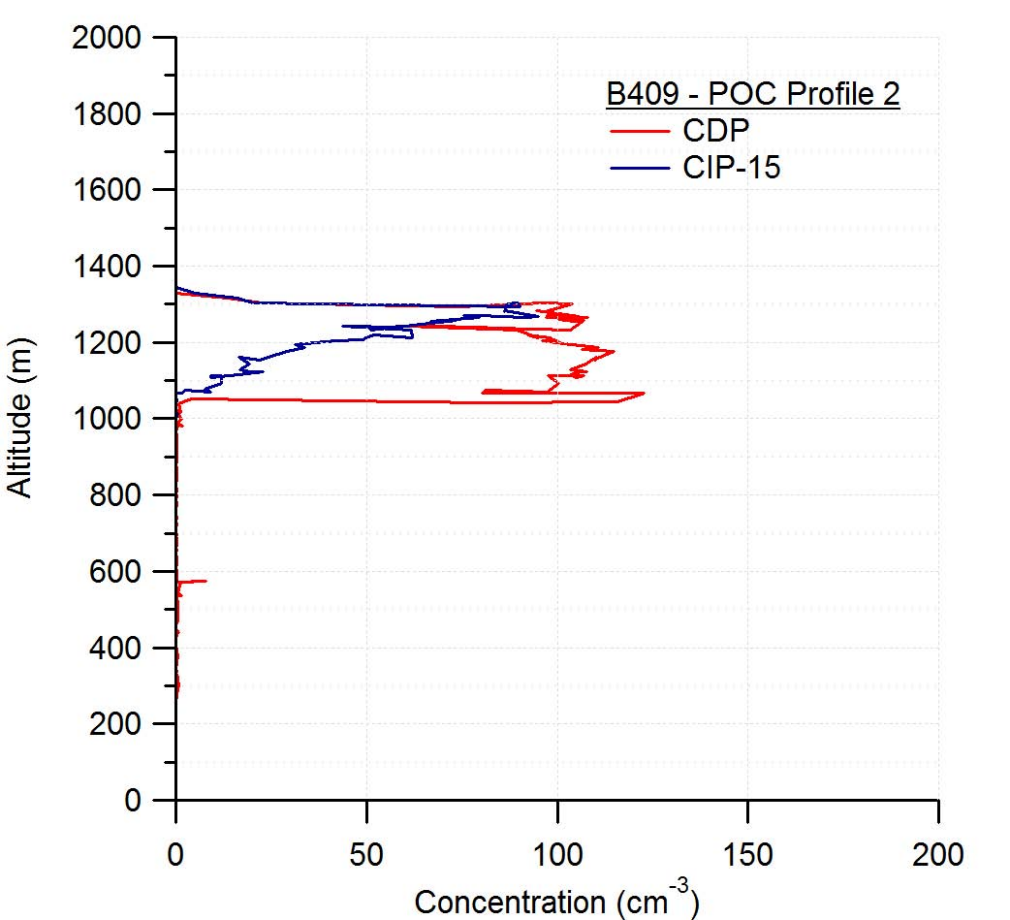
B409 - POC Profile 2
CDP
CIP-15
Altitude (m)
2000
1800
1600
1400
1200
1000
800
600
400
200
0
0
50
100
150
200
Concentration (cm-3)

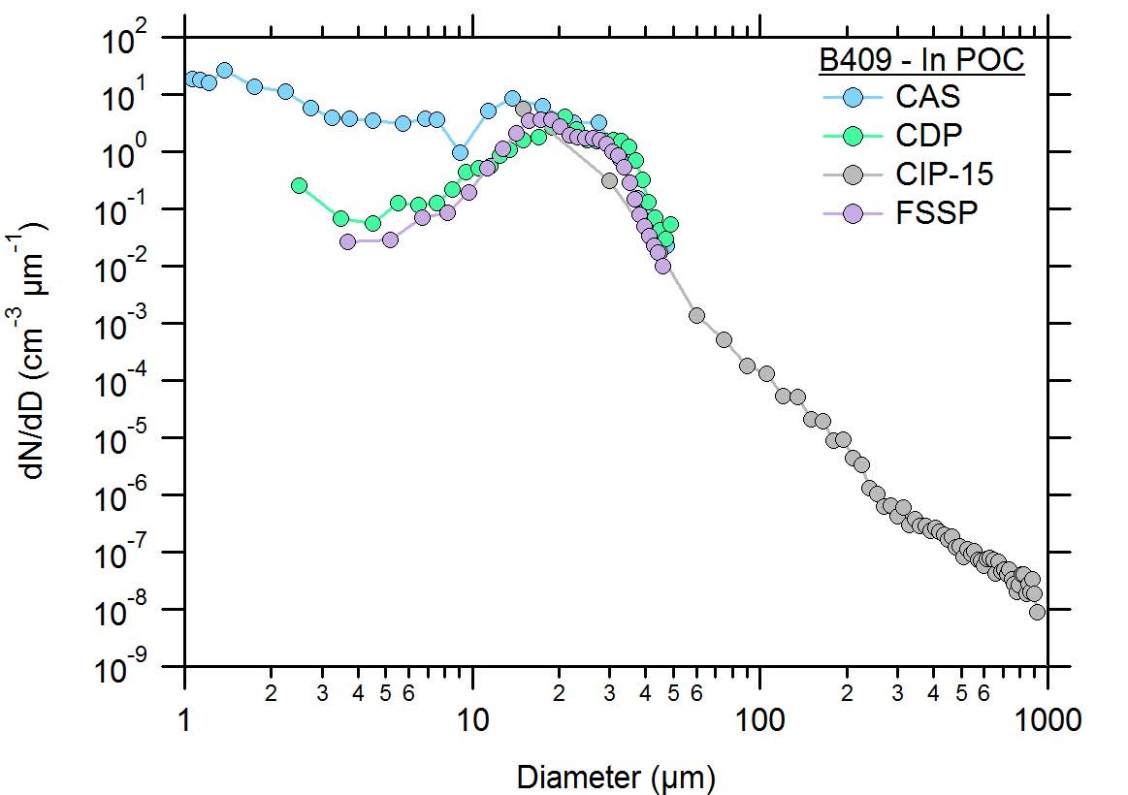
B409 - In POC
CAS
CDP
CIP-15
FSSP
dN/dD (cm-3 µm-1)
Diameter (µm)
10^2
10^1
10^0
10^-1
10^-2
10^-3
10^-4
10^-5
10^-6
10^-7
10^-8
10^-9
1
2
3
4
5
6
10
2
3
4
5
6
100
2
3
4
5
6
1000

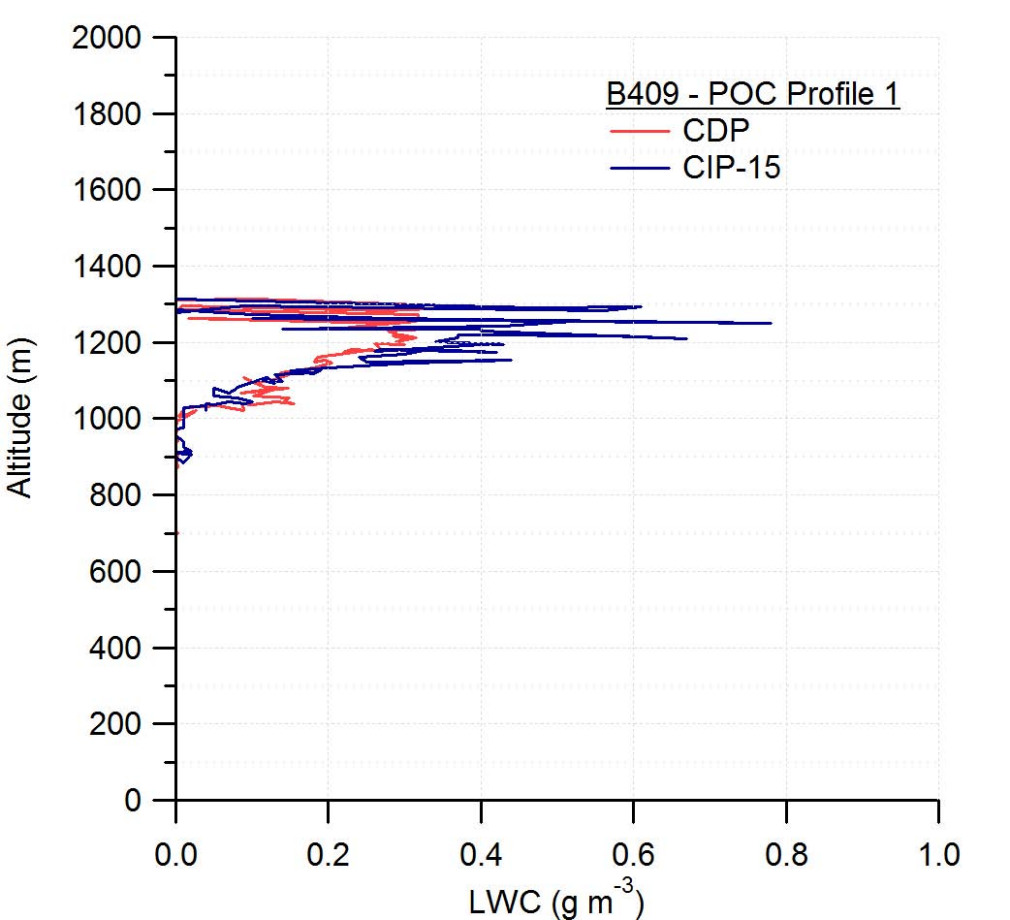
B409 - POC Profile 1
CDP
CIP-15
Altitude (m)
2000
1800
1600
1400
1200
1000
800
600
400
200
0
0.0
0.2
0.4
0.6
0.8
1.0
LWC (g m-3)

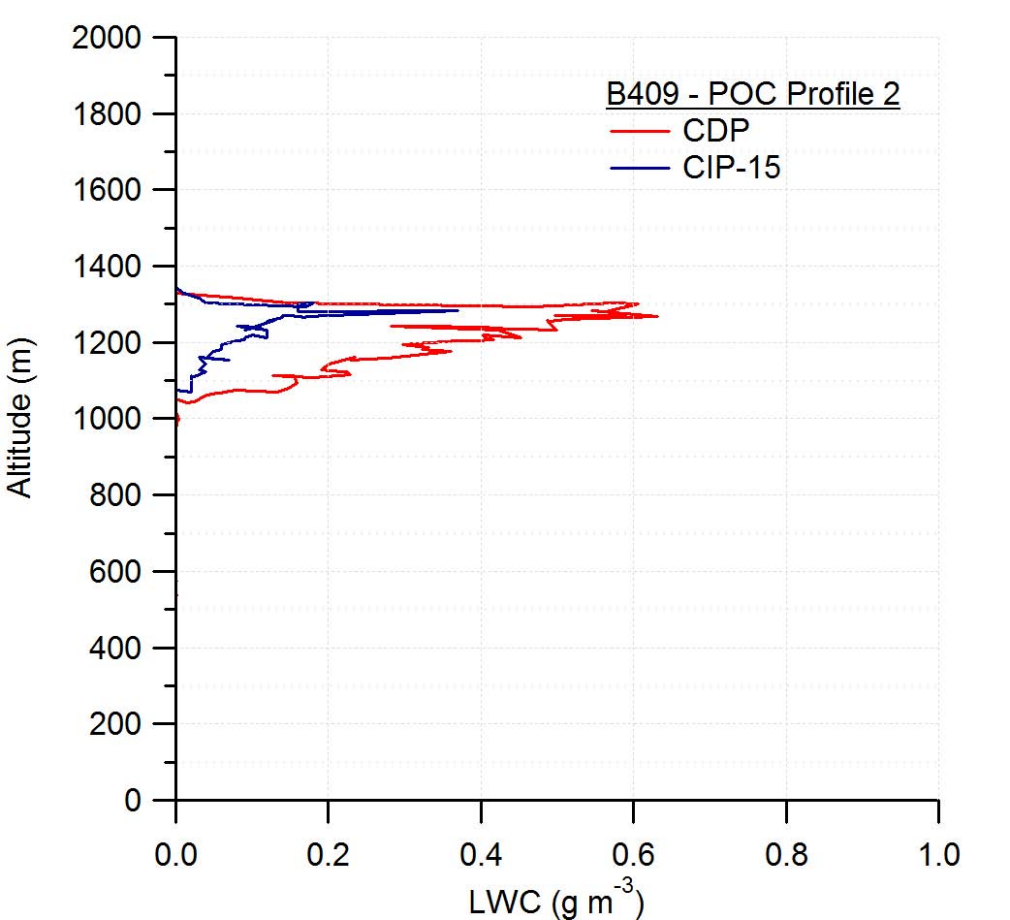
B409 - POC Profile 2
CDP
CIP-15
Altitude (m)
2000
1800
1600
1400
1200
1000
800
600
400
200
0
0.0
0.2
0.4
0.6
0.8
1.0
LWC (g m-3)

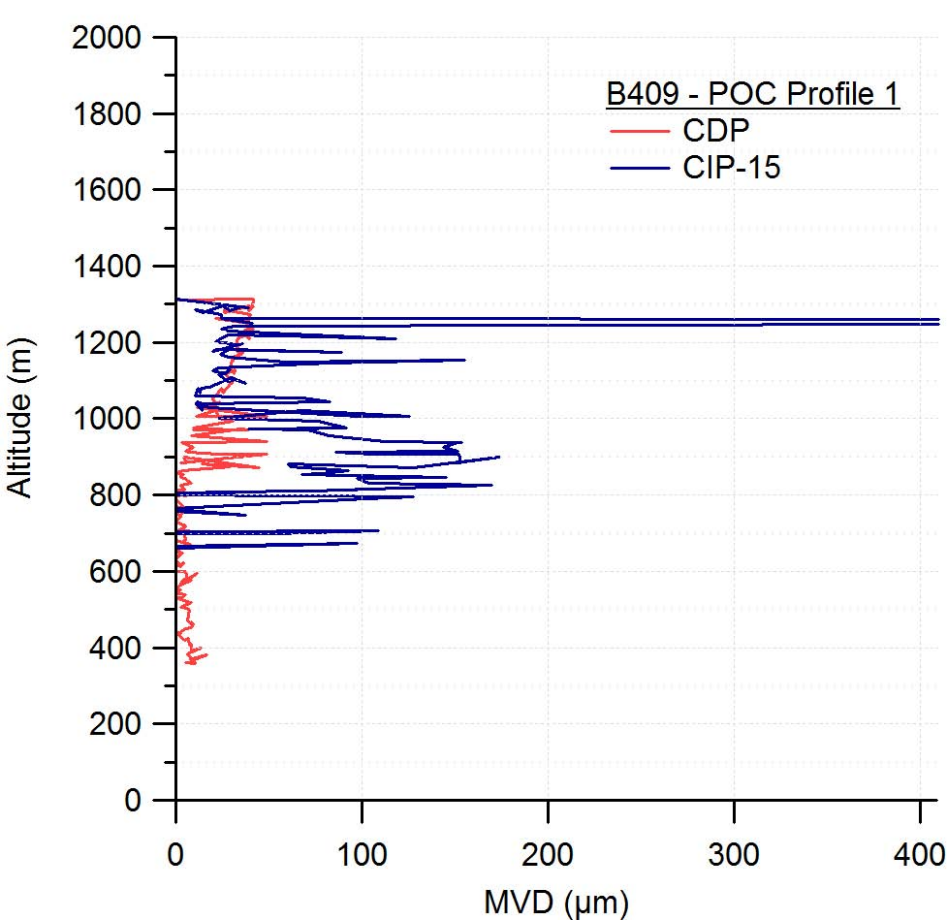
B409 - POC Profile 1
CDP
CIP-15
Altitude (m)
2000
1800
1600
1400
1200
1000
800
600
400
200
0
0
100
200
300
400
MVD (µm)

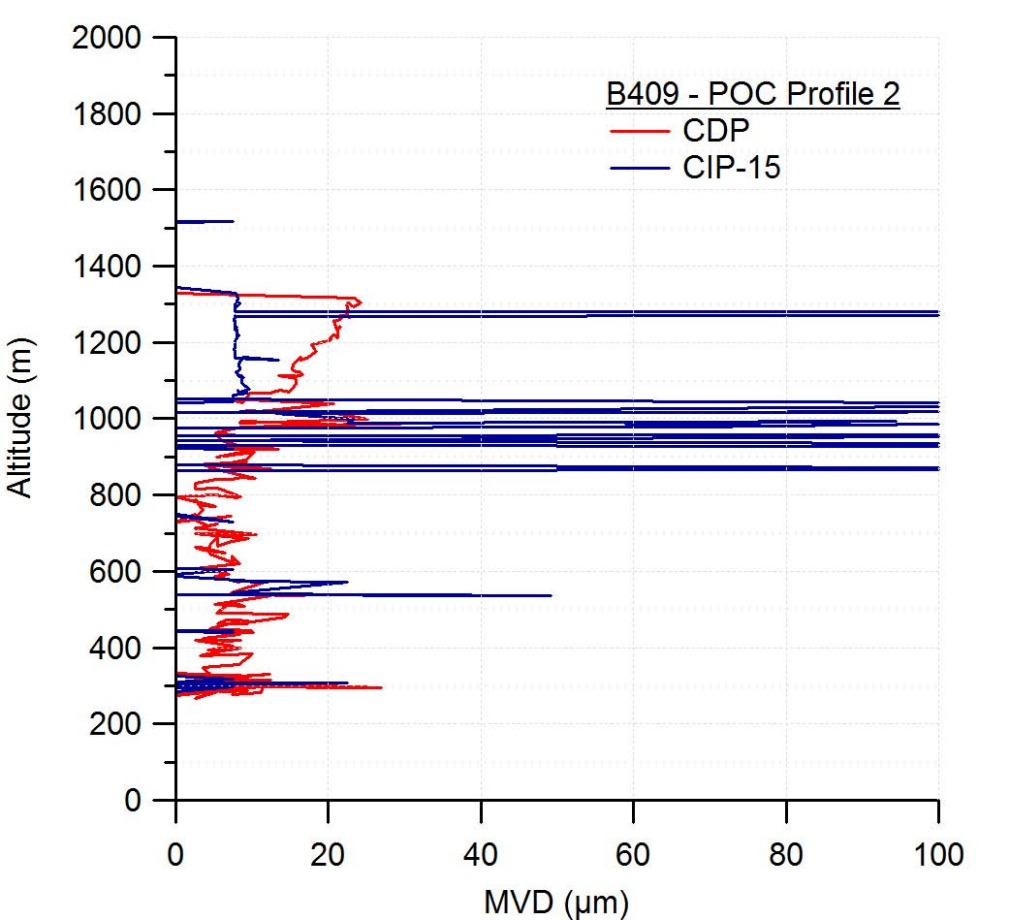
B409 - POC Profile 2
CDP
CIP-15
Altitude (m)
2000
1800
1600
1400
1200
1000
800
600
400
200
0
0
20
40
60
80
100
MVD (µm)